R-TR-75-010

THEORY AND APPLICATION OF MATHEMATICAL MODELING OF SHOULDER-FIRED WEAPONS

PART I: M16A1 RIFLE

BY

PAUL E. EHLE

ALBERT E. RAHE

1 NOVEMBER 1972

FINAL REPORT

RESEARCH DIRECTORATE

GENERAL THOMAS J. RODMAN LABORATORY
ROCK ISLAND ARSENAL
ROCK ISLAND, ILLINOIS 61201

DISCLAIMER

The findings of this report are not to be construed as an official Department of the Army position unless so designated by other authorized documents.

DISPOSITION INSTRUCTIONS

Destroy this report when it is no longer needed. Do not return it to the originator.

REPORT DOCUMENTATION PAGE

READ INSTRUCTIONS BEFORE COMPLETING FORM

1. REPORT NUMBER: R-TR-75-010	2. GOVT ACCESSION NO.
3. RECIPIENT'S CATALOG NUMBER	
4. TITLE *(and Subtitle)*: Theory and Application of Mathematical Modeling of Shoulder-Fired Weapons Part I: M16A1 Rifle	5. TYPE OF REPORT & PERIOD COVERED: Final Report Oct 1970 - Oct 1972
6. PERFORMING ORG. REPORT NUMBER	
7. AUTHOR(s): Paul E. Ehle, Albert E. Rahe	8. CONTRACT OR GRANT NUMBER(s)
9. PERFORMING ORGANIZATION NAME AND ADDRESS: Research Directorate, SARRI-LR-S, GEN Thomas J. Rodman Laboratory, Rock Island Arsenal, Rock Island, IL 61201	10. PROGRAM ELEMENT, PROJECT, TASK AREA & WORK UNIT NUMBERS: 62604A 1W562604A607 00 004 B21C116
11. CONTROLLING OFFICE NAME AND ADDRESS: Research Directorate, SARRI-LR-S, GEN Thomas J. Rodman Laboratory, Rock Island Arsenal, Rock Island, IL 61201	12. REPORT DATE: 1 Nov 1972
	13. NUMBER OF PAGES: 243
14. MONITORING AGENCY NAME & ADDRESS *(if different from Controlling Office)*	15. SECURITY CLASS. *(of this report)*: Unclassified
	15a. DECLASSIFICATION/DOWNGRADING SCHEDULE

16. DISTRIBUTION STATEMENT *(of this Report)*
Distribution limited to U.S. Government agencies only; Test and Evaluation; Nov 1972. Other requests for this document must be referred to GEN Thomas J. Rodman Laboratory, Rock Island Arsenal, Rock Island, Illinois 61201.

17. DISTRIBUTION STATEMENT *(of the abstract entered in Block 20, if different from Report)*

18. SUPPLEMENTARY NOTES

19. KEY WORDS *(Continue on reverse side if necessary and identify by block number)*

M16 Rifle	Simulation
Dynamics	Man Weapon
Mathematical Model	Kinematics

20. ABSTRACT *(Continue on reverse side if necessary and identify by block number)*
A mathematical model of the M16A1 Rifle was constructed by personnel of the Research Directorate to serve as (1) a vehicle to extend the state-of-the-art in weapon modeling, (2) a basis with which to compare performance characteristics of other weapons such as the XM19 Rifle, (3) an aid to troubleshoot the weapon, (4) a means to increase present knowledge of the M16A1, and (5) a way to explore and demonstrate the capabilities and limitations of mathematical models of weapons.

20. For each component mass, equations of motion are written. These allow a total of eleven degrees of freedom plus a nearly arbitrary number of degrees of freedom for the drive spring. To provide accuracy data, one rotational degree of freedom is allowed for weapon pitch motion. Expressions are derived for the many diverse forces acting on the masses. The resulting equations are solved on an IBM 360/65 digital computer. A sensitivity analysis is conducted, and the results are compared with those from a similar model of the XM19 Rifle. The greatest differences between the M16A1 and the XM19 sensitivities were found to be the effect of the ignition delay and the drive spring on cycle time and the mounting conditions on accuracy.

The methods developed during model construction are applicable to the modeling of many other weapons. Part II of this two-report series is an application of these techniques to the XM19 Rifle.

FOREWORD

Acknowledgement is made to a number of persons in the Research Directorate, Weapons Laboratory, Rock Island Arsenal, who contributed toward the completion of this project. Mr. Albert J. Patsche and Mr. Paul A. Cacari participated in the early explorations of dynamic spring and buffer behavior. Mr. Lanny D. Wells and Mr. Robert B. Long applied to several test cases the method to couple complex models (developed in Appendix G).

Mr. Timothy L. Brosseau, BRL, contributed much valuable information through telephone conversations.

Special thanks is due to Mrs. Louise C. Cruson, of the Research Directorate, for her fine editing, professional job of typing, and assembly of this manuscript. Mrs. Cruson was initially guided by Mr. Lavon K. James in the necessary report format.

The following page is blank

TABLE OF CONTENTS

TABLE OF CONTENTS (cont'd)

TABLE OF CONTENTS (cont'd)

TABLE OF CONTENTS (cont'd)

TABLE OF CONTENTS (cont'd)

TABLE OF CONTENTS (cont'd)

TABLE OF CONTENTS (cont'd)

TABLE OF CONTENTS (cont'd)

LIST OF ILLUSTRATIONS

LIST OF ILLUSTRATIONS (cont'd)

LIST OF TABULAR DATA

1.0 INTRODUCTION

1.1 Objectives

The objectives of the study described in this report were:

a. to develop mathematical computer models for the M16A1 and XM19 Rifles.

b. to investigate alternative ways to model various events in the firing cycle.

c. to perform various sensitivity studies using the models.

d. to evaluate proposed design changes.

NOTE: The term "model" used in this report will indicate mathematical computer model.

This study was divided into two parts:

Volume I deals with the construction and the use of a model (M16 model) of the M16A1 Rifle. It is exploratory, philosophical, and it describes alternative ways to handle various forces and treats a variety of topics related to modeling in addition to providing a detailed description of the M16A1 model and results.

Volume II describes the development of a mathematical computer model of the XM19 Rifle (MXM model). In contrast, the MXM model is less exploratory and the report goes directly to the point of describing exactly what is in the model, what the results of exercising it are, and what conclusions can be drawn. The work was designed to be an application of present techniques that would directly result in a practical model.

1.2 Material Presented in This Volume

The material presented in Volume I of this report deals with the construction and the use of a mathematical model (M16 model) of the M16A1 Rifle. With the M16 model, the motions of the hammer, bolt, bolt-carrier, main gun, buffer body, buffer weights and an optional number of segments of the drive spring can be predicted. The M16 model has eleven degrees of freedom plus an extra number dependent upon how many element masses are chosen to represent the drive spring. For most purposes, other than an in-depth study of the spring itself, five element masses are adequate. One of the degrees of freedom accounts for the pitch motion of the weapon. The M16 model incorporates a simple model of the human operator (shooter) consisting of linear and torsional springs and dampers,

and it also includes a simple exterior ballistics analysis so that major trends in weapon dispersion can be evaluated. Detailed interior ballistics and gas-transmission analyses are not included; experimental pressure-time curves are used.

The construction of the M16 model of the M16A1 Rifle serves a number of purposes. It is first a vehicle for the extension of the state of the art in weapon modeling. For this role, the M16A1 Rifle is ideally suited. Rifles are readily available, and much information is already known with which theory can be compared. Second, a model of this weapon provides a logical basis for comparison of performance of other weapons such as the XM19 Rifle. Statements about sensitivity to changes in parameters in one weapon are more meaningful if one knows how another weapon responds to similar changes in these parameters. Third, the model serves as a practical tool for any proposed modifications to this weapon. Fourth, the model can be used for troubleshooting should any difficulties arise. In the past, manufacturing problems have arisen that are ideally suited for exploration through a model.[1] Fifth, as is demonstrated in this report, such a model can add to the present store of information about the M16A1 Rifle. Effects can be explored that are virtually impossible to study experimentally. Finally, the model provides a means of exploring and demonstrating the capabilities and limitations of mathematical weapon models.

Unique features of the M16 model include not only detailed and efficient analyses of the buffer, drive spring, and magazine, but also an exploration of weapon dispersion through a simple model of the shooter. An extensive sensitivity analysis was also performed that provides information on trends previously unavailable. Also, in connection with the development of the model, many new approaches were explored and some of these are discussed in the appendices to this report. Topics discussed include impact between masses, the coupling of complex mathematical models without simultaneous solution of all equations, and a

[1]Grandy, A.J.; Duffy, J.A.; Horchler, M.H.; and Ehle, P.E.; "Investigation of Bolt/Bolt-Carrier Clearances in the M16A1 Rifle", Technical Note TN-1159, Frankford Arsenal, Philadelphia, Pa. (May 1971)

unique fluid flow analysis.

One of the most significant aspects of the report is the sensitivity analysis. This analysis provides quantitative information about the M16A1 previously unavailable from experiment and demonstrates one of the important uses of a model. According to the M16 model, burst accuracy of this weapon can be improved by a stiffening of the shoulder and the upper torso of the shooter, a decrease in breech pressure, and increase in moment of inertia of the rifle, a decrease in drive-spring constant, and the positioning of the center of gravity of the buffer weights midway between the possible extremes. An increase in cyclic rate can be achieved, according to the model, by a stiffening of the shooter's shoulder, an increase in gas pressure in the bolt-carrier cavity and at the breech, a decrease in mass of the bolt and bolt-carrier, and the positioning of the center of gravity of the buffer weights in the most forward position possible. Many of these trends, but not their degree, are obvious.

The remainder of Volume I deals with the development and exercise of the model, and the discussion of study areas important for future model development. First, modeling philosophy is discussed that is essential for the placement of the subject of this report in proper perspective. Then after a brief description of weapon operation, the general equations of motion used to describe this rifle are discussed. From the solution of these equations, typical predictive capabilities of the model are demonstrated and many predictions are compared with experiment. For insight into the response of weapon performance to changes in various parameters, the sensitivity analysis is discussed. (Note that some of the model predictions were made while the model was in an advanced but not final state of development. However, the results are substantially representative of the present model. Continual changes and refinements are a natural part of the modeling process). A number of comparisons are made between the predictions of the M16 model and those of the MXM model of the XM19 Rifle described in Volume II. On the basis of the M16 model predictions, conclusions are drawn and recommendations are made. In the appendices, detailed derivations of each force expression are given. Various topics for future emphasis are also discussed.

A conversion table is included so that the reader can quickly relate cycle time to shots per minute and make conversions between English and metric systems. Finally, computer programs are provided to present a clearer impression of the M16A1 and drive spring models. Both computer programs are written in FORTRAN IV and were run on IBM 360/65 computers. Run times for a 3 shot burst generally was less than 1 minute, but this varied with the number of finite elements used to model the drive springs.

2.0 MATHEMATICAL COMPUTER MODELS

2.1 Modeling Philosophy

Since the M16A1 Rifle has been in service for a number of years and has undergone extensive tests and design changes, one may wonder why a mathematical model of the M16A1 was not undertaken long ago. In the past, weapon development has been basically a trial-and-error procedure. The techniques of mathematical modeling for the comprehensive description of small-caliber automatic weapons simply were not developed until recently. Some early modeling work was done at Frankford Arsenal in 1967[2]. However, one of the earliest attempts at a comprehensive model was made at Rock Island in 1969[3]. Models of artillery weapons had been developed before that time, but the problems of modeling these two types of weapons are quite different, especially in the areas of automatic fire and man-weapon interaction. Modeling efforts at WECOM and elsewhere have recently increased, and people now have a better idea of what can be modeled effectively, what is essential to model in detail, what modeling can provide, and what the problems and limitations are. In this section of the report, an attempt is made to present a clearer idea of current modeling philosophy upon which the M16A1 model is based.

2.1.1 Four Major Areas

A number of general purposes exist for which a model of any automatic weapon can be used. Eventually, with little or no resort to experimentation, highly developed math models will be constructed with which quick, inexpensive, accurate, and nearly complete information can be provided in four major areas: (1) weapon concept evaluation (2) design (3) evaluation of existing weapons (4) troubleshooting.

---

[2]Kucsan, S.; Shinaly, F.; Jaslow, H.; and Zaid, M.; "Small Arms Systems Simulation," Frankford Arsenal Report R-1848, Philadelphia, Pa. (Jun 1967)

[3]Ehle, P.E., "Mathematical Model of the Stoner 5.56mm Medium Machine Gun, XM207," WECOM Technical Report 70-114, AD 862081L, Research and Engineering Directorate, Rock Island, Ill (Oct 1969)

Today, this goal is partially realized. For concept work, one can use a model to predict gross operational characteristics, provide some reliability information, and partially explore compatibility with existing mounting systems. (A good example of this capability is contained in Ref [4].) For design, one can now use the models only as part of a trial-and-error procedure. At the very least, this procedure can be feasibly automated and many configurations can be analyzed by the computer until specified design criteria such as cyclic rate are met. To have the computer directly solve for the detailed specifications of a general configuration by which these criteria will be satisfied is also conceivable. Developments in optimization methodology will contribute to these design capabilities. However, the underlying design concept will still be the product of a human designer. Completely automated design is not in the foreseeable future. In the evaluation of existing weapons, the models can locate tendencies toward malfunctions, examine certain aspects of reliability and accuracy, and assess compatibility of the weapon with various mounting systems. For troubleshooting, one can use a model to locate the sources of many problems, to determine the ramifications, and to indicate alternative solutions. The full potential of mathematical modeling of weapons is far from being reached in the four major areas.

2.1.2 Simple Models

For many purposes, very simple models are the most effective. For example, in early concept studies, the inclusion of fine details is often unjustified. Also, one phenomenon may be very precisely modeled, but this advantage is somewhat negated by gross approximations in other parts of the model. In addition, when one divides a complicated physical process into a large number of smaller ones, often the result is that, instead of making one large guess, many smaller guesses are made; and the sum is no better than the accuracy of its parts. Also, computer time may soar unnecessarily. Thus, for a particular problem at hand, highly detailed approaches are sometimes neither necessary nor productive.

---

[4] Interim ADPACS Report - DESVAL - USAWECOM Task Group Report, SWERR-R, Rock Island, Ill (Jul 1972)

However, if one is to more fully explore the potential of math models, to look beyond the problems of the present, and to increase accuracy, one must at some time dig deeply into the details of the various physical phenomena. Thus, by the inclusion of seemingly unnecessary detail, especially in exploratory models, one is in effect planning for the future, increasing the ability of engineers to model future weapons, and advancing the state of the art. If one is to understand complex physical processes, these problems must be divided into parts that can be individually analyzed. Inclusion of these parts in a model also enables one to assess their relative importance. On balance, highly detailed models often serve a purpose beyond the immediate problem at hand and should be encouraged if time and resources permit.

2.1.3 Extreme Attitudes

One can often find two extreme attitudes concerning the value of math models of weapons. The first attitude is that these models are worthless because certain phenomena such as the complete human response of the shooter are too complex to model, or because some model predictions are not in agreement with experiment, or because certain expressions used in the models were not rigouously derived. The second attitude is that a model can do virtually everything and can even set the manufacturing tolerance limits on every part of the mechanism. The truth, of course, lies somewhere between these extremes.

2.1.3.1 First Attitude

The first attitude is unjustified because of the reasons stated below:

(a) Although phenomena exist too complex to analyze precisely now, an approximate model often retains much of the essence of the phenomenon and can be used for trend predictions that provide important insight into weapon characteristics. Perfection is desirable, but is not necessary.

(b) Inaccuracy of certain model predictions does not necessarily imply inaccuracy of others. For example, an incorrect peak force may not have much effect on cycle time predictions if the impulse level is basically correct. Also, disagreement with an experimental measurement does not automatically mean that the prediction is in error. In making

a presentation at a nonlinear mathematics conference held recently at Rock Island, Professor R. Rivlin of Lehigh University remarked that in his opinion, good experiments are more difficult to achieve than good theory. Even if the measurements are accurately made, considerable care must be exercised in their interpretation. For example, in the M16 model, extraction force is taken as the applied force acting on the cartridge case to resist motion: it does not include inertia forces because the case and bolt are considered to be a single mass during extraction. However, when measured by strain gages on the extractor, extraction force does include the force needed to overcome the inertia of the case. Many sources of experimental errors exist, just as many such sources in theory exist. Certainly, the final authority rests with accurate experimentation, but not all experimentation is accurate.

(c) Theoretical rigor should be sought where possible, but is not essential for useful weapon models. In many cases, it is unjustified. For example, one may naively assert that a model is seriously deficient because, in determination of the extraction force, no plastic effects were considered during the expansion of the cartridge case against the chamber wall. However, inclusion of these effects would not necessarily make the model more accurate because of the large uncertainties in coefficient of friction and gas-pressure distribution. Also, a power series used to obtain a reasonable approximation to a highly complex phenomenon may not converge in the mathematical sense. A model is not invalid because someone thinks that, for example, Coulomb damping rather than viscous damping should have been used in one of the force expressions; in reality, probably neither is correct. The ultimate criterion for an expression is whether it works satisfactorily for the purposes intended, not whether it was rigorously derived from some theory. The construction of weapon models is not a clean-cut process. No models would exist if one insisted on complete rigor for all complex processes in a weapon. In present models, a need exists to determine values of certain poorly understood variables such as friction. This is often done by adjustment of them within the bounds of reasonable values to force better

agreement between model and experiment. The true values are unknown anyway, so choosing them to improve model predictions makes sense. Rigor in weapon models is merely one means to an end, not an end in itself.

2.1.3.2 Second Attitude

The second extreme attitude is also unjustified for reasons stated below:

(a) Mathematical modeling has many limitations. High confidence-levels in the accuracy of certain predictions are presently not within the realm of feasibility. For example, although manufacturing tolerances may be set on certain orifices, model capability in the tolerance area is virtually nonexistent. How often a weapon will malfunction; how a weapon will be affected by cold weather, sand, fouling, and moisture; how much rough usage a weapon can be subjected to before it malfunctions; and many other important areas of study cannot be defined on the basis of present models.

(b) Experimentation and experience are still essential in many areas of weapon design, effectiveness, and reliability. Models are merely useful tools. One of the areas of model development in need of further exploration is that of model validation. "Verification" or "validation" of a complex weapon model by experiment is a nebulous concept. The problem is complicated by (1) experimental uncertainty (2) random processes by which measurements are caused to change from round-to-round (3) an extremely large number of possible predictions from a model, some of which will be in better agreement with experiment than others, and most importantly, (4) a lack of criteria that can be applied to determine when experimental and theoretical curves are in satisfactory agreement, which curves, and how many such curves must be in satisfactory agreement before a model can be considered "verified".

2.2 Authors' Approach

The approach taken by the authors in modeling weapons is to use Newton's laws to describe the motion of each significant mass in the mechanism. Each force acting on each mass is individually analyzed, and mathematical expressions are obtained. Some of these forces do not

act during various parts of the firing cycle. The logic capability of the computer is used to insert or remove these forces at the correct times. By this approach, the entire cycle is considered at once, and no "phases" are established.

The philosophy outlined above and followed in this report is not claimed to be either entirely unique or even best. It has produced successful results and was carefully and thoughtfully developed over a period of several years. Mr. Robert H. Coberly, Weapons Technology Division, RIA, made many significant contributions to this development.

2.3 Related Work

In addition to the mathematical computer model M16 of the M16A1 Rifle described in this volume, other models also exist. One of these was developed at Frankford Arsenal under the direction of F. Shinaly primarily for the study of malfunction dynamics. An early version of the Frankford model was used for the work described in Reference[1]. At BRL, H. Gay and E. Wineholt constructed an analog-computer model[5].

The advantages of an analog-computer are principally in short computation time and in ease of making parametric variations. However, one is usually much more limited in the size and complexity of a problem that can be solved on this computer than one is when using commonly available digital computers. Also, large modifications in the model can usually be more easily accomplished on a digital computer. Modeling work with a hybrid computer, in which analog and digital capabilities are combined, has also been done at BRL. The use of such a computer for weapon models appears to be very promising. One present disadvantage is that generally the memory capacity of the digital portion is considerably less than that of a computer such as the IBM 360/65.

Perhaps the greatest differences between the model described in this report and other existing models lie in the larger amount of detail incorporated into this model, the capacity of this model to approximately analyze weapon dispersion, the specific modeling approaches used, and the purposes for which the models were designed.

---

[1]Grandy, A.J.; Duffy, J.A.; Horchler, M.H.; and Ehle, P.E.; "Investigation of Bolt/Bolt-Carrier Clearances in the M16A1 Rifle," Technical Note TN-1159, Frankford Arsenal, Philadelphia, Pa. (May 1971)

[5]Gay, H.P. and Wineholt, E.M., "Analog Simulation of the Mechanism of the M16A1 Rifle," BRL Report No. 1596, Aberdeen Proving Ground, Md. (Jun 1972)

3.0 M16A1 RIFLE MODEL

3.1 Brief Description of Weapon Operation

The M16A1 Rifle (Fig. 1) is a hand-held gas-operated 5.56mm weapon and has both full-automatic and semi-automatic modes of operation. Initially the bolt is locked to the barrel extension, and the hammer is in cocked position. When the trigger is pulled, the hammer is released by the sear and strikes the firing pin. The firing pin then strikes the primer, from which action the propellant is ignited. (The main components of the M16A1 are shown in Fig. 2). The pressure from the propellant gases acts on the main gun through the base of the cartridge case and the locked bolt. When the projectile reaches the gas port, which is located approximately 16 inches from the chamber, some gas is redirected rearwardly along a gas tube to a cavity in the bolt-carrier. The pressure in this cavity forces the bolt forward and the bolt-carrier

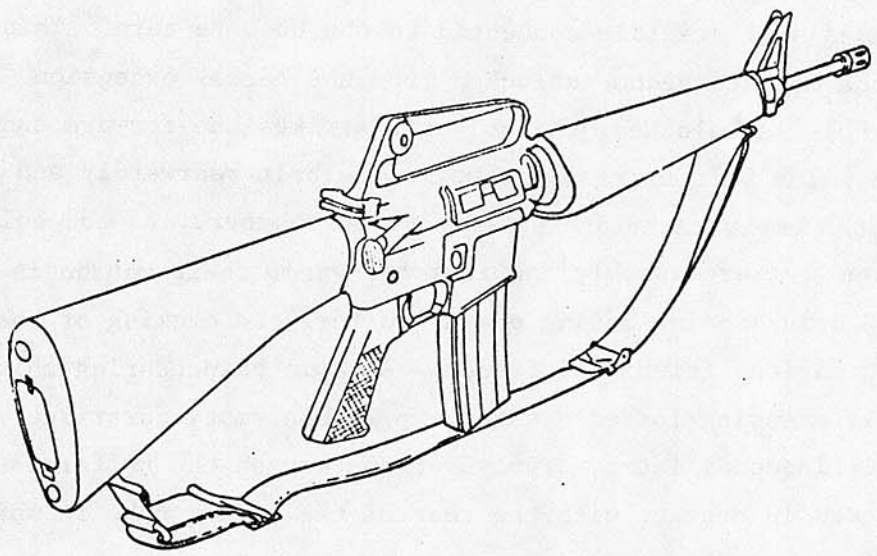

Figure 1 M16A1 Rifle

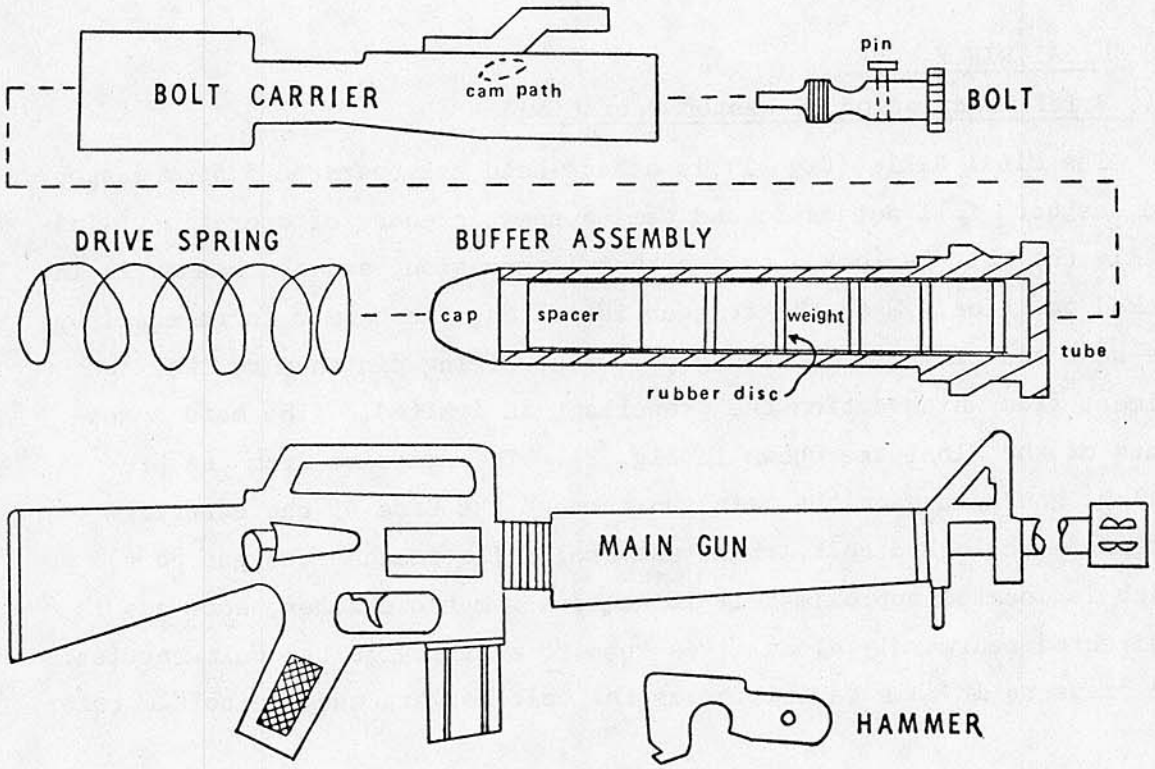

Figure 2 Components of M16A1 Rifle

rearward. As the bolt-carrier moves rearwardly, a cam path cut in the the carrier causes a pin rigidly connected to the bolt to turn. This action causes the bolt to become unlocked from the barrel extension. Just after the bolt is unlocked, the bolt pin strikes the forward end of the cam path. The bolt-carrier now pulls the bolt rearwardly and the bolt pulls the empty cartridge case from the chamber. As the bolt, bolt-carrier, and buffer assembly continue rearward, their motion is resisted by the drive spring acting on the buffer, the cocking of the hammer, and the various frictional forces. At some point during this rearward travel, a spring-loaded ejector expels the empty cartridge case. A few milliseconds later, a polyurethane cap on the buffer assembly usually comes in contact with the rear of the buffer tube in which the entire buffer assembly and drive spring are housed; then the counter recoil begins. Part of the energy of the bolt, bolt-carrier, and buffer is imparted to the main gun and mount, part is lost to permanent

deformations and heat, and part is retained by the drive spring, which must push the bolt, bolt-carrier, and buffer assembly forward again.

In counter recoil, the bolt impacts against the face of the top cartridge in the magazine, strips it, and loads it into the chamber. The bolt-carrier continues forward and, by means of the cam path, causes the bolt to become locked to the barrel extension once again. Weights in the buffer body continue to move forward a small distance and to strike the end of the body. This impact counteracts a tendency for the bolt-carrier to rebound and thus prevents premature unlocking. In the full-automatic mode, just prior to completion of locking, the bolt-carrier trips the sear by which action the hammer is released from its cocked position. The hammer moves forward and strikes the firing pin; the operating cycle is repeated. In the semi-automatic mode, the sear is not tripped, and the hammer does not move forward until the trigger is depressed again.

3.2 General Equations of Motion for the M16A1 Rifle

In writing the equations of motion, the authors followed a Newtonian rather than a Lagrangian approach. For the present problem, where there were not a large number of irrelevant constraint forces, the equations could be found more simply through Newton's laws. Both approaches ultimately yield the same results.

Separate coordinate systems are established for each component mass. One coordinate system is constructed for rifle rotation, and the rotation angle is defined as zero when the barrel is horizontal. The origin of each coordinate system is fixed with respect to the ground. Positive axial directions are in the direction of initial bullet velocity. Positive rotation is that which causes the muzzle to move away from the ground.

The equations of motion and their initial conditions are listed below. These are written with only general expressions for the forces. A summary of forces is given (after this list of equations of motion) in which a brief physical description of each is provided (Table 1). The detailed mathematical descriptions of both axial and rotational forces are included in Appendix A.

a. Bolt

$$M_{B(E)}\ddot{X}_B = FB(1) + FB(2) + FB(3) + FB(4) + FB(5) + FB(6) + FB(7) + FB(8) + FB(9) + FB(11) + FB(12)$$

At $t = 0$: $\dot{X}_B = 0$, $X_B = X_{B_o}$

X_B = position of center of gravity of bolt

$FB(i)$ = ith force acting on bolt as discussed in Appendix A.

$M_{B(E)}$ =
- = effective mass of bolt = .156 lb after a new round has been stripped from the magazine, but before the round is fired
- = .143 lb after the round has been fired, but before the case is ejected
- = .130 lb after the cartridge case has been ejected, but before a new round is obtained from the magazine

$X_{B_o} = 0$

b. Bolt-Carrier

$$M_{BC}\ddot{X}_{BC} = FBC(1) + FBC(2) + FBC(3) + FBC(4) + FBC(5) + FBC(6) + FBC(7) + FBC(8) + FBC(9) + FBC(10) + FBC(11) + FBC(12)$$

At $t = 0$: $\dot{X}_{BC} = 0$, $X_{BC} = X_{BC_o}$

X_{BC} = position of center of gravity of bolt-carrier

$FBC(i)$ = ith force acting on bolt-carrier as discussed in Appendix A.

M_{BC} = mass of bolt-carrier = .586 lb

$X_{BC_o} = .7 \times 10^{-3}$ inch

c. Main gun structure

$$M_{MG(E)}\ddot{X}_{MG} = FMG(1) + FMG(2) + FMG(3) + FMG(4) + FMG(5) + FMG(6) + FMG(7) + FMG(8) + FMG(9) + FMG(10) + FMG(11) + FMG(12) + FMG(13) + FMG(14) + FMG(15)$$

At $t = 0$: $\dot{X}_{MG} = 0$, $X_{MG} = X_{MG_o}$

X_{MG} = position of center of gravity of main gun

$FMG(i)$ = ith force acting on main gun as discussed in Appendix A.

$M_{MG(E)}$ = Effective mass of main gun = 6.2 + .0252(N-19) lb

N = Number of rounds of ammunition in magazine at any given time

$X_{MG_o} = 0$

d. Buffer tube

$$M_{BUFF}\ \ddot{X}_{BUFF} = FBUFF(1) + FBUFF(2) + FBUFF(3) + FBUFF(4) + FBUFF(5) + FBUFF(6)$$

At t = 0: $\dot{X}_{BUFF} = 0, \quad X_{BUFF} = X_{BUFF_o}$

X_{BUFF} = position of center of gravity of empty buffer tube

FBUFF(i) = ith force acting on buffer tube

M_{BUFF} = mass of empty buffer tube =.0987 lb

$X_{BUFF_o} = 1.4 \times 10^{-3}$ inch

e. Buffer weights

Option 1: Lumped mass system

$$M_{TOTAL}\ \ddot{X}_{WTS} = F_{WTS}$$

At t = 0: $\dot{X}_{WTS} = 0, \quad X_{WTS} = X_{WTS_o}$

X_{WTS} = position of center of gravity of buffer weight system

F_{WTS} = force acting on buffer weights as described in Appendix A.

M_{TOTAL} = Total mass of all buffer weights = .224 lb

X_{WTS_o} = .0014 inch when weights are completely forward in tube
= -.129 inch when weights are completely rearward in tube

Option 2: Individual masses

$$M_i\ \ddot{X}_i = FM_{i,1} + FM_{i,2} + FM_{i,3} + FM_{i,4} \quad (i = 1,2,3,4,5)$$

At t = 0: $\dot{X}_i = 0, \quad X_i = X_{i_o}$

X_i = position of center of gravity of ith mass

$FM_{i,j}$ = jth force acting on ith mass as described in Appendix A.

M_i = mass of ith buffer weight ($M_1 = M_2 = M_3 = M_4 = .0406$ lb, $M_5 = .0616$ lb)

X_{i_o} = .0014 inch when weights are completely forward in tube
=-.129 inch when weights are completely rearward in tube

f. Hammer

$$I_H \ddot{\theta} = T_{SPRING} - r_2 \cos(\alpha_2 + \theta)\, FMG(7) - r \cos(\alpha + \theta)\, FBC(8) - M_H [r_o \cos\theta]\, \ddot{X}_H$$

At $t = 0$: $\dot{\theta} = 0$, $\theta = \theta_o$

θ = rotational position of hammer

T_{SPRING} = torque exerted by hammer spring = 6 in-lb

FMG(7) and FBC(8) are forces acting between hammer and main gun and between hammer and bolt-carrier as discussed in Appendix A.

I_H = moment of inertia of hammer about an axis through the pivot point = .000015 slug-ft^2

$\theta_o = -70°$

M_H = mass of hammer = .0683 lb

r_o = distance from c.g. of hammer to pivot point of hammer = .75 inch

g. Rifle rotation

$$I_G \ddot{\theta}_G = T_{SHOULDER} + T_{BODY} + T_{\substack{INTERNAL \\ GUN\ MOTION}}$$

At $t = 0$ $\dot{\theta}_G = 0$, θ_G = any angle of elevation, typically 0°

$T_{SHOULDER}$, T_{BODY}, and $T_{\substack{INTERNAL \\ GUN\ MOTION}}$ are torques acting on the rifle as described in Appendix A.

I_G = Moment of inertia of the rifle about its center of gravity = .135 slug-ft^2

h. Exterior ballistics (neglecting drag)

$$Z = -\frac{1}{2} g \frac{(R-y_i)^2}{\dot{y}_i^2} + \dot{Z}_i \frac{R-y_i}{\dot{y}_i} + Z_i$$

z = vertical coordinate of projectile impact point at range R

R = horizontal coordinate of projectile impact point

z_i = vertical coordinate of projectile at exit from barrel

$\dot{z}_i$ = vertical velocity of projectile at exit from barrel

$\dot{y}_i$ = horizontal velocity of projectile at exit from barrel

See Appendix H for derivation.

3.3 A Note on Initial Conditions

Initially, unbalanced forces must not be present on any of the weapon components. Forces that must be balanced are the preload force from the drive spring that acts on the buffer tube and gravity forces that act on the masses when the weapon is elevated. These forces are balanced by the allowance of extremely small penetrations of the bolt pin into the forward end of the cam path, and the buffer tube into the bolt-carrier. Thus, if $F_{PRELOAD}$ = drive spring preload force, then

$$X_{BC_o} = [F_{PRELOAD} - g(\sin \theta_E)(M_{BC} + M_{BUFF})] / K_{BC} = .7 \times 10^{-3} \text{inch}$$

and

$$X_{BUFF_o} = X_{BC_o} + [F_{PRELOAD} - g(\sin \theta_E)M_{BUFF}] / K_{BUFF} = 1.4 \times 10^{-3} \text{ inch}$$

TABLE 1 SUMMARY OF FORCES

BRIEF DESCRIPTION OF FORCE	MASS RECEIVING THE FORCE									
	BOLT	BOLT CARRIER	MAIN GUN	BUFF BODY	HAMMER	BUFF. MASS 1	BUFF. MASS 2	BUFF. MASS 3	BUFF. MASS 4	BUFF. MASS 5
1. Breech force	FB(1)									
2. Friction between bolt and ammo	FB(2)		FMG(2)							
3. Impact between bolt and barrel and engagement of extractor	FB(3)		FMG(3)							
4. Friction between bolt and bolt carrier	FB(4)	FBC(1)								
5. Force at end of cam path when rifle is not locked	FB(5)	FBC(2)								
6. Unlocking force	FB(6)	FBC(3)								
7. Locking force	FB(7)	FBC(5)								
8. Force at end of cam path when rifle is locked	FB(8)	FBC(4)								
9. Stripping of ammo from magazine	FB(9)		FMG(15)							
10. Pressure in bolt carrier cavity	FB(10)	FBC(9)								
11. Extraction force	FB(11)		FMG(10)							
12. Gravity force on bolt	FB(12)									
13. Interaction between bolt carrier and buffer body		FBC(6)	**FBUFF(1)**							
14. Friction between bolt carrier and main gun		FBC(7)	FMG(4)							
15. Constraint force between hammer and bolt carrier		FBC(8)			FHAM(1)					
16. Friction between bolt carrier and ammo		FBC(10)	FMG(12)							
17. Friction between hammer and bolt carrier		FBC(11)	FMG(13)							
18. Gravity force on bolt carrier		FBC(12)								
19. Mount force			FMG(1)							
20. Drive spring force			FMG(5)	FBUFF(3)*						
21. Bore friction			FMG(6)							
22. Impact between hammer and main gun			FMG(7)		FHAM(2)					
23. Constraint force between hammer and main gun			FMG(8)		FHAM(3)					
24. Impact between buffer tube and backplate			FMG(9)	FBUFF(2)						
25. Gravity force on main gun			FMG(11)							
26. Friction between buffer tube and main gun			FMG(14)	FBUFF(6)						
27. Gravity force on buffer tube				FBUFF(4)						

* NOTE: FBUFF(3) is equal and opposite to FMG(5) under static conditions

TABLE 1 SUMMARY OF FORCES (cont'd)

	BRIEF DESCRIPTION OF FORCE	MASS RECEIVING THE FORCE									
		BOLT	BOLT CARRIER	MAIN GUN	BUFF BODY	HAMMER	BUFF. MASS 1	BUFF. MASS 2	BUFF. MASS 3	BUFF. MASS 4	BUFF. MASS 5
28.	Interaction between buffer and all buffer weights						$FM_{1,3}$ & $FM_{1,1}$	$FM_{2,3}$	$FM_{3,3}$	$FM_{4,3}$	$FM_{5,3}$ & $FM_{5,2}$
29.	Spring interaction between **tube** and 1st buffer weight				$FBUFF(5)_1$		$FM_{1,1}$				
30.	Spring interaction between 1st and 2nd buffer weights						$FM_{1,2}$	$FM_{2,1}$			
31.	Friction between **tube** and 1st buffer weight				$FBUFF(5)_2$		$FM_{1,3}$				
32.	Gravity force on 1st buffer weight						$FM_{1,4}$				
33.	Spring interaction between 2nd and 3rd buffer weights							$FM_{2,2}$	$FM_{3,1}$		
34.	Friction between **tube** and 2nd buffer weight				$FBUFF(5)_3$			$FM_{2,3}$			
35.	Gravity force on 2nd buffer weight							$FM_{2,4}$			
36.	Spring interaction between 3rd and 4th buffer weights								$FM_{3,2}$	$FM_{4,1}$	
37.	Friction between **tube** and 3rd buffer weight				$FBUFF(5)_4$				$FM_{3,3}$		
38.	Gravity force on 3rd buffer weight								$FM_{3,4}$		
39.	Spring interaction between 4th and 5th buffer weights									$FM_{4,2}$	$FM_{5,1}$
40.	Friction between tube and 4th buffer weight				$FBUFF(5)_5$					$FM_{4,3}$	
41.	Gravity force on 4th buffer weight									$FM_{4,4}$	
42.	Spring interaction between **tube** and 5th buffer weight				$FBUFF(5)_6$						$FM_{5,2}$
43.	Friction between **tube** and 5th buffer weight				$FBUFF(5)_7$						$FM_{5,3}$
44.	Gravity force on 5th buffer weight										$FM_{5,4}$

NOTE: That $FBUFF(5) = \sum_{i=1}^{7} FBUFF(5)_i$

3.4 Examples of Model Predictions

A number of predictions are now presented as examples of data that can be generated from the model. These predictions include peak forces, impulses, energies, force shapes, and component motions.

3.4.1 Summary of Predicted Peak Forces, Impulses, and Energies

Predicted peak forces that act on the bolt-carrier, bolt, main gun, and buffer tube are contained in Tables 2 thru 5. Computed impulses and energies associated with these forces are represented by bar graphs in Figures 3 to 6. To evaluate the significance of a particular force, one must consider all three indicators. A force can have a high value in one category, but a low value in another. Regardless of impulse or energy value, a high peak force can be significant for material strength and fatigue considerations.

From these tables and figures, one can draw quantitative conclusions about the influence of each force in the model. A number of qualitative conclusions are mentioned below:

a. Forces applied at the ends of the cam paths and the gas pressure in the bolt-carrier cavity are of greatest significance to the motion of the bolt-carrier. In the nominal case, friction forces are the least significant, although in some circumstances they can, in practice, be large enough to stop weapon operation. The most likely areas for fatigue are at the ends of the cam paths.

b. The motion of the bolt is strongly influenced by the force between the bolt pin and the end of the cam path, and the gas pressure in the bolt-carrier cavity.

c. The mount, breech force, bore friction, drive spring, and the impact between buffer tube and backplate are most significant to the motion of the main gun. Thus, these are factors that affect accuracy.

d. The motion of the buffer tube is strongly affected by interaction with the bolt-carrier, impact with the backplate, the drive spring, and interaction with the buffer weights.

Although the forces mentioned are those that are most influential from the point of view of magnitude, the weapon could not be operated without the many small forces that cause events to occur in the right sequence at the right time.

TABLE 2 CALCULATED PEAK FORCES IMPARTED IN THE FIRST CYCLE TO THE BOLT-CARRIER

FORCE SYMBOL AND BRIEF DESCRIPTION		PEAK FORCE (lb)
FBC(1)	Friction between bolt and bolt-carrier	.26
FBC(2)	Force at end of cam path when rifle is not locked	440.
FBC(3)	Unlocking force	35.
FBC(4)	Force at end of cam path when rifle is locked	308.
FBC(5)	Locking force	18.4
FBC(6)	Interaction between bolt-carrier and buffer tube	310.
FBC(7)	Friction between bolt-carrier and main gun	.37
FBC(8)	Constraint force between hammer and bolt-carrier	52.
FBC(9)	Pressure in bolt-carrier cavity	520.
FBC(10)	Friction between bolt-carrier and ammo	2.67
FBC(11)	Friction between hammer and bolt-carrier	1.21
FBC(12)	Gravity force on bolt-carrier	0.0

TABLE 3 CALCULATED PEAK FORCES IMPARTED IN THE FIRST CYCLE TO THE BOLT

FORCE SYMBOL AND BRIEF DESCRIPTION		PEAK FORCE (lb)
FB(1)	Breech force	2185.
FB(2)	Friction between bolt and ammo	2.67
FB(3)	Impact between bolt and barrel and engagement of extractor	158.
FB(4)	Friction between bolt and bolt-carrier	.26
FB(5)	Force at end of cam path when rifle is not locked	440.
FB(6)	Unlocking force	35.
FB(7)	Locking force	18.4
FB(8)	Force at end of cam path when rifle is locked	308.
FB(9)	Stripping of ammo from magazine	6.91
FB(10)	Pressure in bolt-carrier cavity	520.
FB(11)	Extraction force	.94
FB(12)	Gravity force on bolt	0.0

TABLE 4 CALCULATED PEAK FORCES IMPARTED IN THE FIRST CYCLE TO THE MAIN GUN

FORCE SYMBOL AND BRIEF DESCRIPTION		PEAK FORCE (lb)
FMG(1)	Mount force	44.3
FMG(2)	Friction between bolt and ammo	2.67
FMG(3)	Impact between bolt and barrel and engagement of extractor	158.
FMG(4)	Friction between bolt-carrier and main gun	.37
FMG(5)	Drive spring force	22.
FMG(6)	Bore friction	325.
FMG(7)	Impact between hammer and main gun	258.
FMG(8)	Constraint force between hammer and main gun	85.5
FMG(9)	Impact between buffer tube and backplate	318.
FMG(10)	Extraction force	.94
FMG(11)	Gravity force on main gun	0.0
FMG(12)	Friction between bolt-carrier and ammo	2.67
FMG(13)	Friction between hammer and bolt-carrier	1.21
FMG(14)	Friction between buffer tube and main gun	.33
FMG(15)	Stripping of ammo from magazine	6.91

TABLE 5 CALCULATED PEAK FORCES IMPARTED IN THE FIRST CYCLE TO THE BUFFER TUBE

FORCE SYMBOL AND BRIEF DESCRIPTION		PEAK FORCE (lb)
FBUFF(1)	Interaction between bolt carrier and buffer tube	310.
FBUFF(2)	Impact between buffer tube and backplate	318.
FBUFF(3)	Drive spring force	19.0
FBUFF(4)	Gravity force on buffer tube	0.0
FBUFF(5)	Interaction between buffer tube and all buffer weights	144.
FBUFF(6)	Friction between buffer tube and main gun	.33

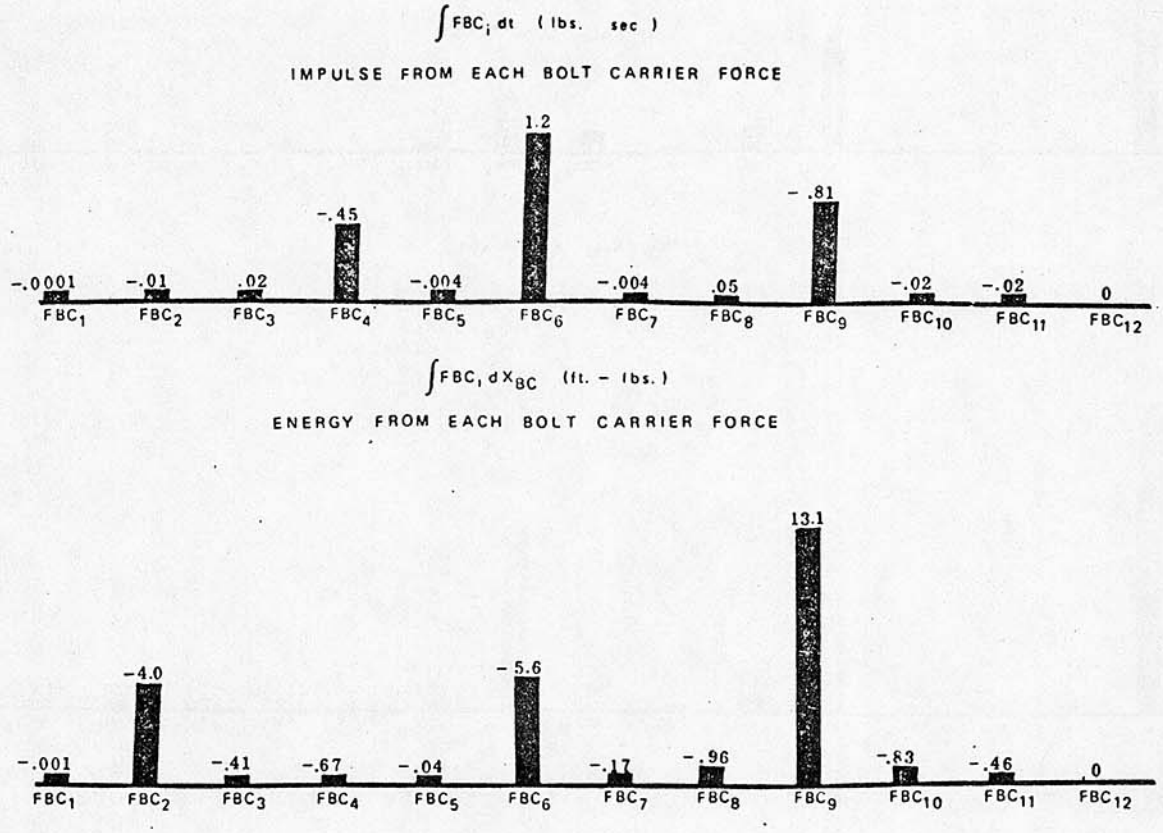

Figure 3 Computed Impulse and Energy Imparted by Each Bolt-Carrier Force

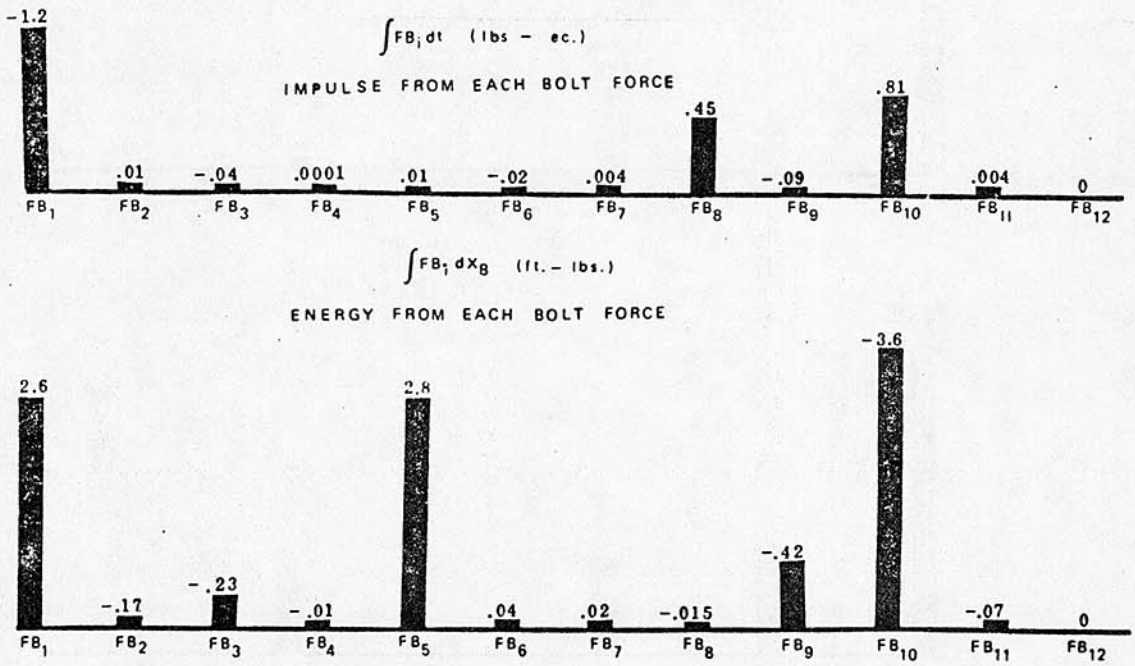

Figure 4 Computed Impulse and Energy Imparted By Each Bolt Force

NOTE: All integrals are for the first cycle, and rifle is rigidly mounted.

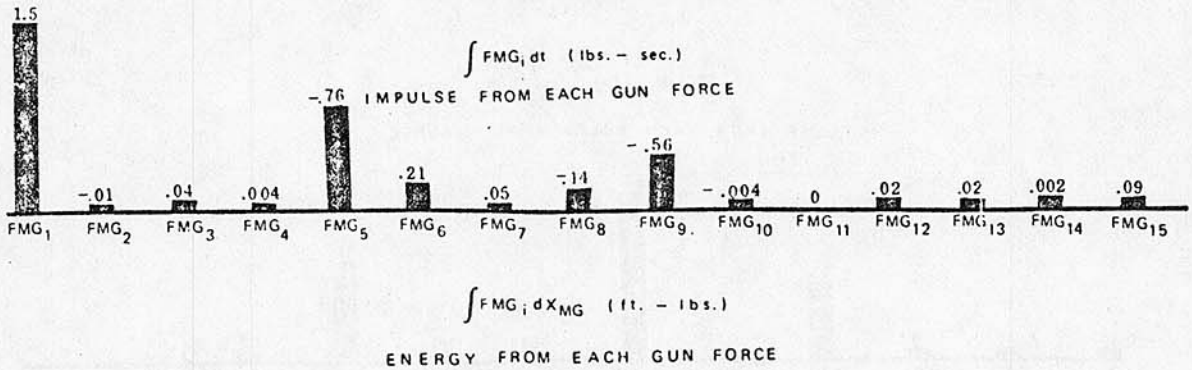

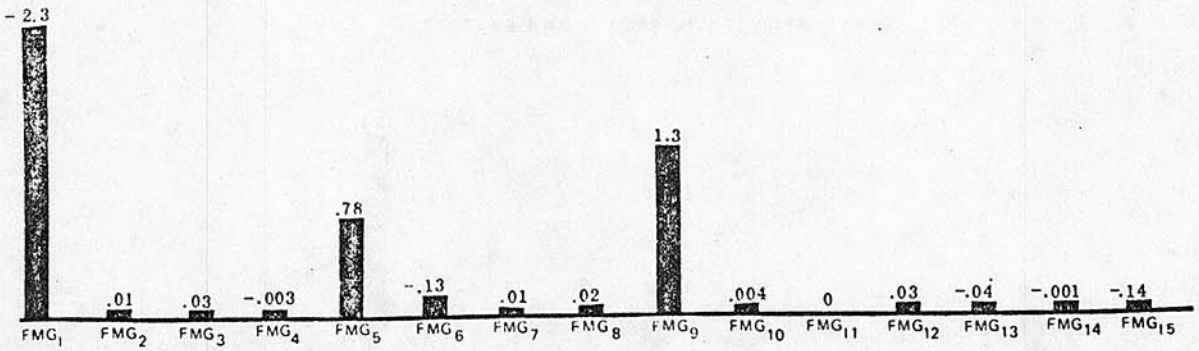

Figure 5 Computed Impulse and Energy Imparted By Each Main-Gun Force

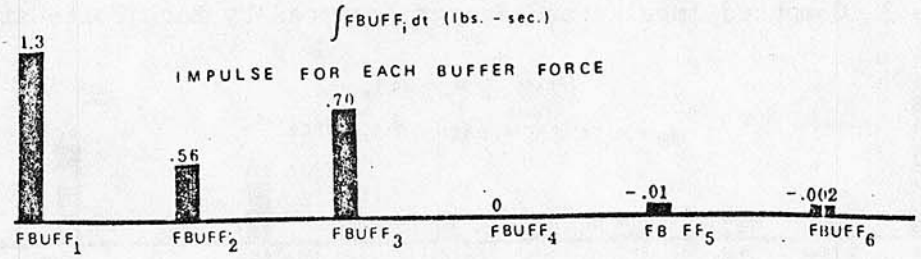

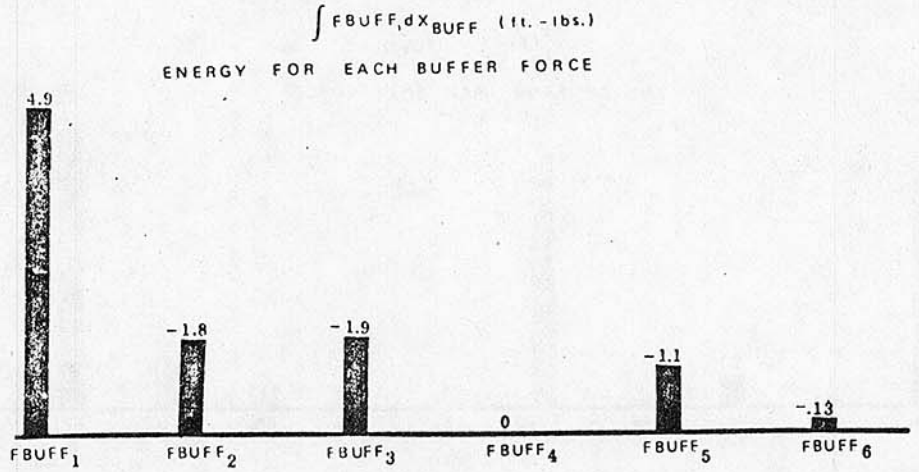

Figure 6 Computed Impulse and Energy Imparted By Each Buffer-Tube Force

NOTE: All integrals are for the first cycle, and rifle is rigidly mounted

3.4.2 Predicted Force Shapes (Cocking, Unlocking, Mount, Drive-Spring)

Cocking and unlocking forces on the bolt-carrier are shown in Figure 7. With this model, a very sharp rise and a gradual decay over approximately two milliseconds are predicted for both forces.

The force felt at the shooter's shoulder during one cycle is shown in Figure 8. Peaks occur as results of the breech pressure and the impact of the buffer tube on the backplate.

Drive-spring forces are shown in Figure 32. Note the delay in the response of the rearward end of the drive-spring after the forward end is displaced.

3.4.3 Predicted Component Motions

Displacement and velocity are predicted as functions of time for the bolt, bolt-carrier, main gun, and hammer (Figures 9-12). Key events are also noted on these graphs. Accelerations have such large fluctuations that they cannot be plotted effectively on graphs of this size. All graphs shown begin with hammer release at time equal to zero.

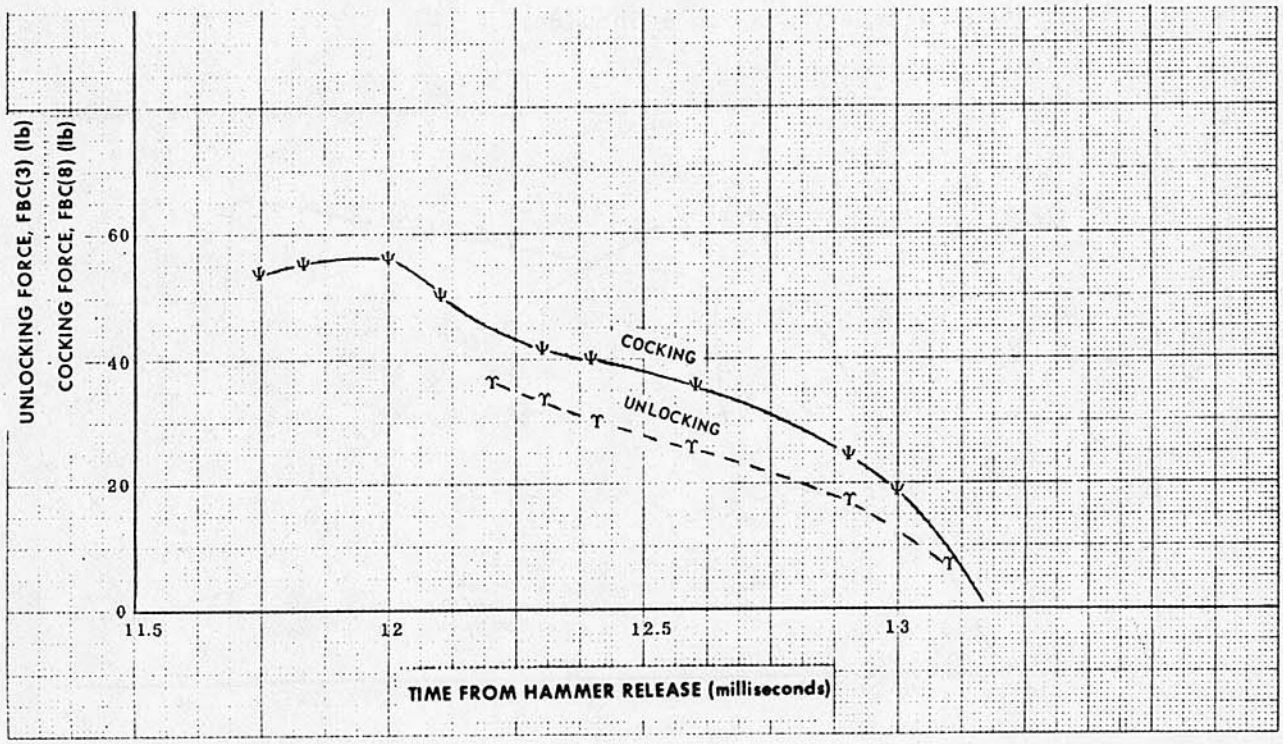

Figure 7 Computed Cocking and Unlocking Forces on Bolt-Carrier vs Time

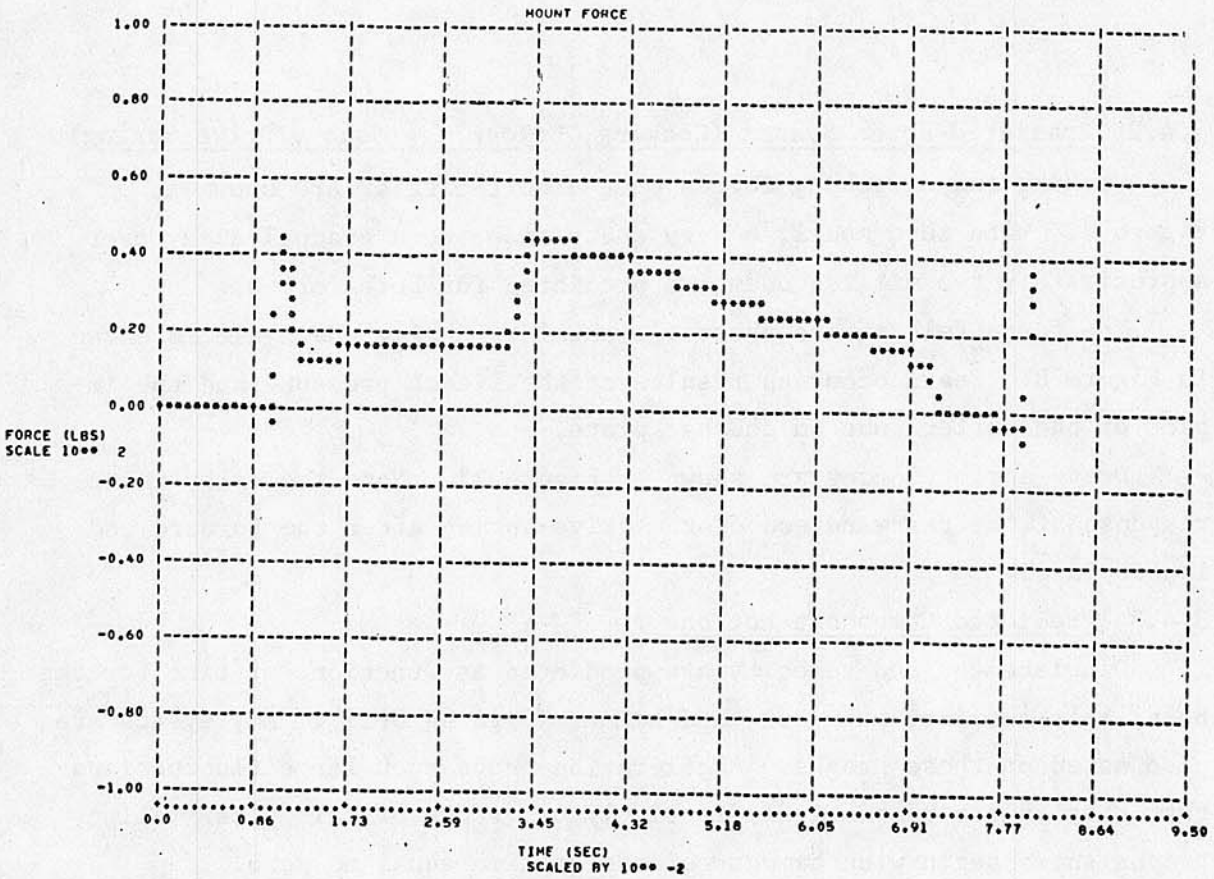

Figure 8 Computed Force at Shooter's Shoulder

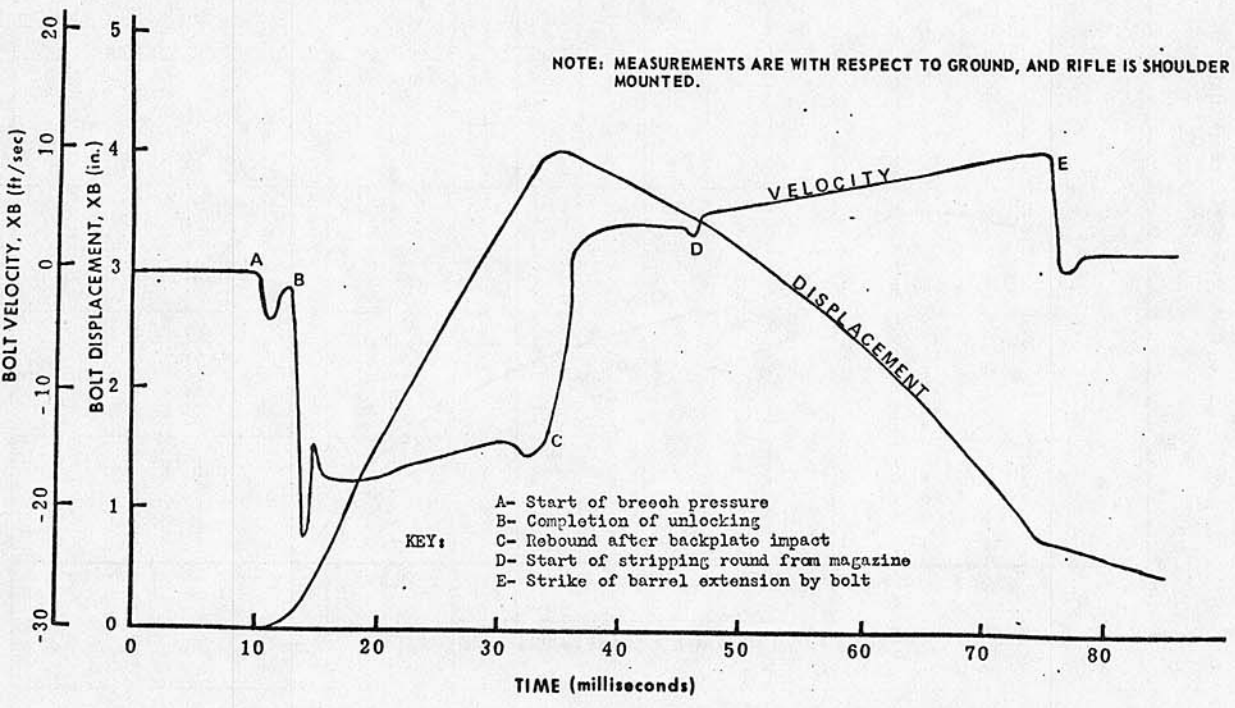

Figure 9 Computed Displacement and Velocity of Bolt vs Time

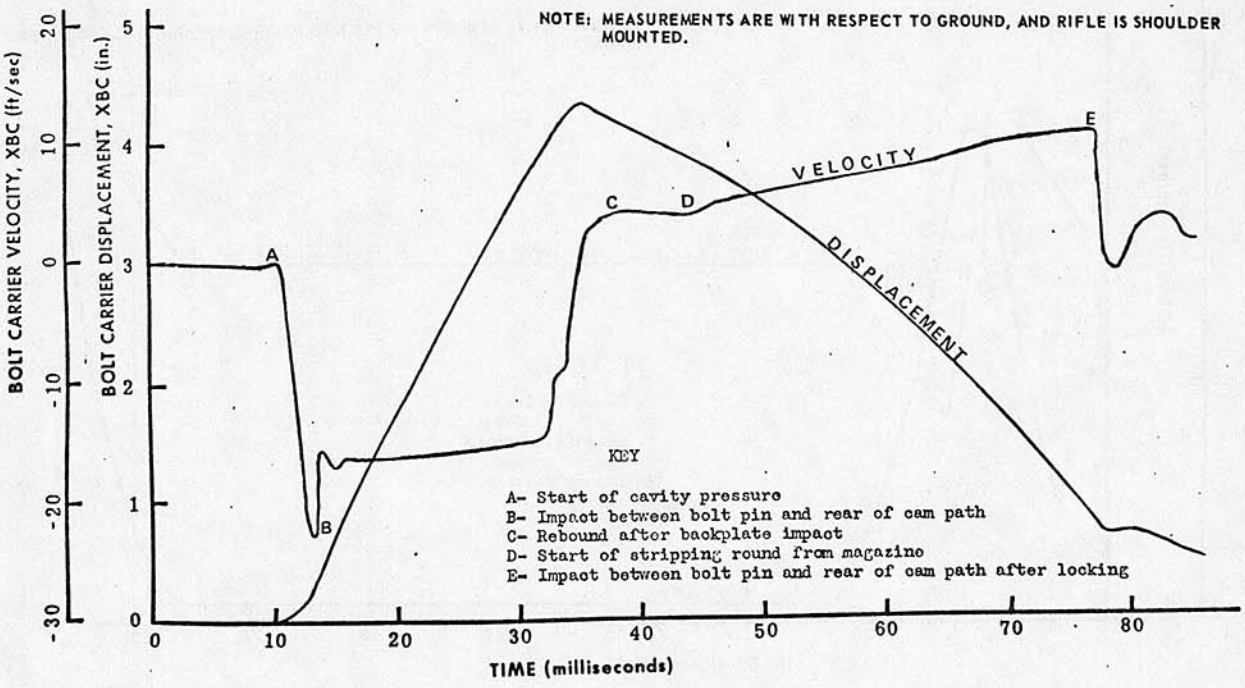

Figure 10 Computed Displacement and Velocity of Bolt-Carrier vs Time

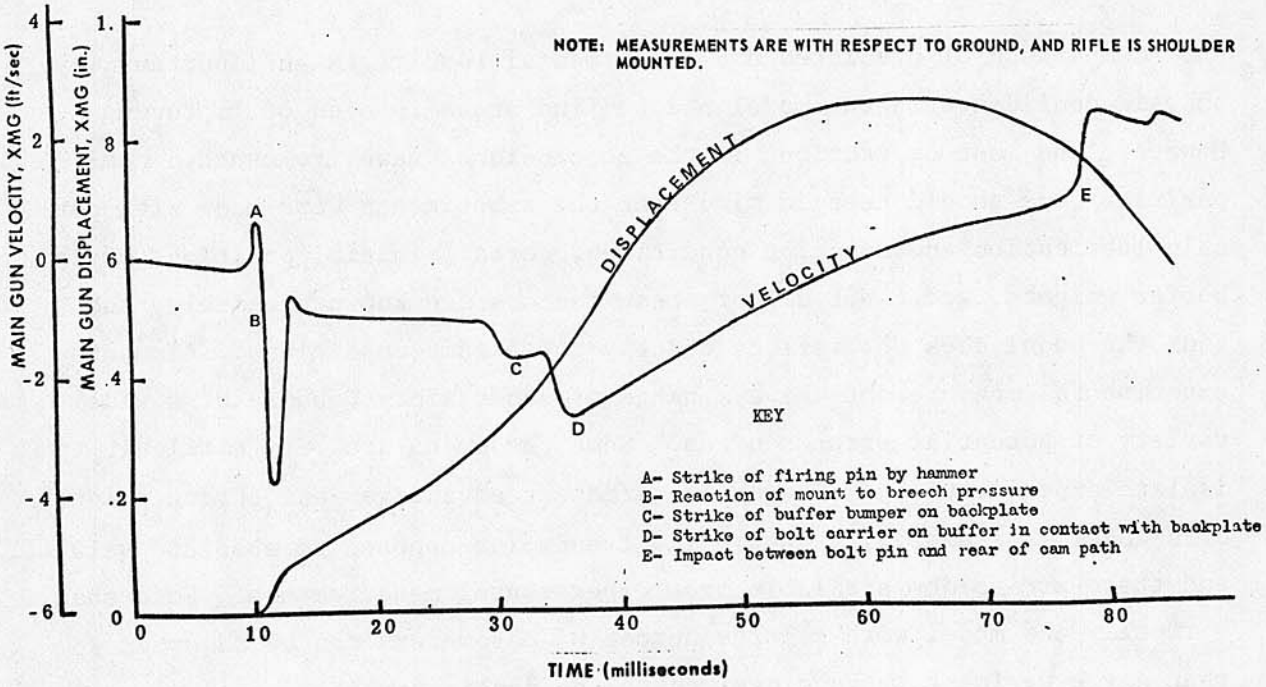

Figure 11 Computed Displacement and Velocity of Main Gun vs Time

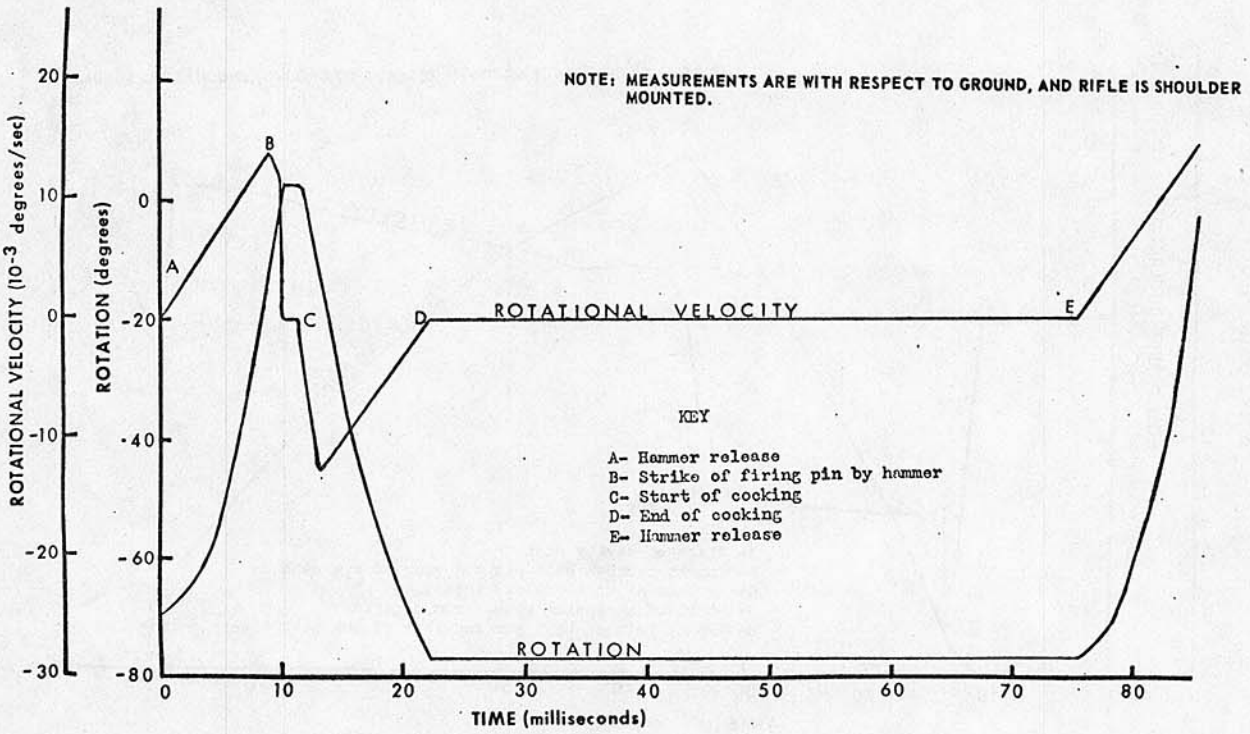

Figure 12 Computed Rotational Displacement and Velocity of Hammer vs Time

3.5 Agreement with Experiments

Comparison of predicted and experimental results is an important way to gain confidence in the model and to find areas in need of improvement. However, one must be cautious in the conclusions drawn from such a comparison. One should keep in mind that the experiments were made with certain lubrication and mounting conditions, certain initial positions of the buffer weights, etc. Not all of these factors are known precisely, and thus the model does not reflect exactly these same conditions. Also, the experimental measurements have a range of uncertainty because of a wide variety of potential error sources. Some phenomena are very difficult to isolate experimentally. One of the greatest advantages and strong points of a model is its ability to predict trends (as opposed to absolute values), and these are seldom available from experimental measurements. Note that virtually any model with a large number of parameters can be adjusted so that any experimental trace desired can be duplicated.

The key question is whether, once the parameter values are set on

the basis of one curve, these values remain valid when other curves are predicted. Thus, the validity and usefulness of a model is not determined by whether cyclic time, extraction force, or other measured values coincide exactly with predicted values. The whole area of model validation is presently a nebulous one. No established criteria exist that, if met, render the model "verified." This aspect of weapon modeling deserves much additional study.

A number of model predictions will now be compared with published experimental data. These predictions include bolt-carrier velocities, cycle time, time for hammer fall, cocking-and-friction energy, drive-spring energy, friction energies, and time-displacement data.

3.5.1. Bolt-carrier velocities for rigid mount

TABLE 6 COMPARISON OF PREDICTED AND EXPERIMENTAL BOLT-CARRIER VELOCITIES

POSITION OF BOLT-CARRIER	COMPUTED VALUE ft/sec	EXPERIMENTAL VALUE ft/sec	EXPERIMENTAL RANGE ft/sec
.64 in from locked position (recoil stroke)	17.8	18.4	(16.6 to 20.2)
.64 in. forward of position at time of buffer/backplate impact (recoil stroke)	15.7	15.2	(13.7 to 16.7)
.64 in. forward of position at time of buffer/backplate impact (counterrecoil stroke)	6.26	7.9	(7.1 to 8.7)
.64 in. rearward of position at which impact with bolt pin occurs (counterrecoil stroke)	10.6	10.8	(9.7 to 11.9)

The source of the experimental values in Table 6 is Ref [1]. The experimental accuracy stated in this report is ±10%.

---

[1]Grandy, A.J.; Duffy, J.A.; Horchler, M.H.; and Ehle, P.E.; "Investigation of Bolt/Bolt-Carrier Clearances in the M16A1 Rifle," Technical Note TN-1159, Frankford Arsenal, Philadelphia, Pa. (May 1971)

3.5.2. Cycle time

Note that recoil time is defined here as the time from when the bolt-carrier first begins rearward motion until the buffer body rebounds from the closed end of the buffer tube. Counterrecoil time is the time from when the bolt-carrier begins to move forward until the end of the cam path strikes the bolt pin after locking. The dwell time is defined as the time from when the end of the cam path strikes the bolt pin until the bolt-carrier begins to move rearward again. Cycle time is the sum of recoil, counterrecoil, and dwell times. These times are compared in Table 7.

TABLE 7 COMPARISON OF PREDICTED AND EXPERIMENTAL RECOIL, COUNTERRECOIL, DWELL, AND CYCLE TIMES

	Recoil Time	Counterrecoil Time	Dwell Time	Cycle Time
Experimental	23	38	10	71
Computed	21	39	10	70

NOTE: All times are in milliseconds

3.5.3. Hammer-fall time

In the automatic mode of fire, the time for hammer-fall is computed to be 10.3 milliseconds. Experimental measurements of the time for hammer-fall after sear release varied between 10 and 11 milliseconds during 20 trials. See page 13 of Ref[1]. (In the semi-automatic mode, the computed time is 9.9 milliseconds.)

3.5.4. Cocking-and-friction energy

The subject of this comparison is the integral, over bolt-carrier displacement, of the cocking force acting on the bolt-carrier and of the frictional force acting between the bolt-carrier and the hammer as the bolt-carrier is recoiling. Some of the difference between computed and experimental values can be attributed to the fact that the experimental measurements were not under realistic dynamic conditions; quasi-steady measurements were made with an Instron testing machine.

---

[1]Grandy, A.J.; Duffy, J.A.; Horchler, M.H.; and Ehle, P.E.; "Investigation of Bolt/Bolt-Carrier Clearances in the M16A1 Rifle," Technical Note TN-1159, Frankford Arsenal, Philadelphia, Pa. (May 1971)

The results[6]:

Experimental	14.0 in-lb
Computed	17.7 in-lb

Computer results indicate that more than enough energy is imparted to the hammer to fully cock it.

3.5.5. Drive-spring energy

The computed integral of spring force over buffer-body displacement is compared to quasi-steady experimental results obtained with an Instron testing machine[6].

Computed	45.5 in-lb
Experimental	36.2 in-lb

3.5.6. Frictional energies

a. Integral, over bolt-carrier displacement, of the drag force acting on the bolt-carrier in counterrecoil.[1]

Computed	3.2 in-lb
Experimental	3.0 in-lb

b. Integral, over bolt-carrier displacement, of the drag force acting on the bolt-carrier as it moves rearward over the uppermost round in the magazine[5].

19 rounds in magazine:	Computed	8.1 in-lb
	Experimental	8.1 in-lb
10 rounds in magazine:	Computed	6.3 in-lb
	Experimental	7.1 in-lb
2 rounds in magazine:	Computed	4.7 in-lb
	Experimental	5.5 in-lb

c. Integral, over bolt displacement, of the stripping force required to remove a round from the magazine[5].

---

[1]Grandy, A.J.; Duffy, J.A.; Horchler, M.H.; and Ehle, P.E.; "Investigation of Bolt/Bolt-Carrier Clearances in the M16A1 Rifle", Technical Note TN-1159, Frankford Arsenal, Philadelphia, Pa. (May 1971)

[5]Gay, H.P. and Wineholt, E.M., "Analog Simulation of the Mechanism of the M16A1 Rifle,"BRL Report No. 1596, Aberdeen Proving Grd, Md. (Jun 1972) Pg 23

[6]Brosseau, T.L., "Kinematic Study of the M16A1 Rifle," Ballistic Research Laboratories Report No. 2153, Aberdeen Proving Grd, Md. (Jan 1972)

19 rounds in magazine:	Computed	7.4 in-lb
	Experimental	7.4 in-lb
10 rounds in magazine:	Computed	5.7 in-lb
	Experimental	6.3 in-lb
2 rounds in magazine:	Computed	4.2 in-lb
	Experimental	3.2 in-lb

3.5.7. Time-displacement data

In Figure 13, one can compare theoretical and experimental time-displacement curves and the times of occurrence for various events. The exact conditions under which the experimental curve was established are not known. The curve was simply matched with a typical predicted curve that had about the same cycle time. Note that the cycle time varies widely, depending on the number of shots previously fired, the number of rounds in the magazine, the initial buffer weight positions, etc. Such a comparison cannot show that either the experimental or the theoretical results are correct, but only that they are in general agreement. Nothing more could be said even if the curves were to match perfectly.

3.5.8. Effect of mounting conditions

Experimental results indicate that cycle time is somewhat longer for soft mounting conditions than for stiff mounting conditions. The reason is that, when the recoiling parts strike the backplate of a soft-mounted weapon, they impart more of their momentum to the main gun. Thus, the initial counterrecoil velocity of the operating parts is slower, and more time is required for these parts to return to battery. For a stiff-mount spring constant of 10,000 pounds per foot, and a soft-mount spring constant of 300 pounds per foot, the difference in cycle time ranged from 3 to 4 milliseconds. Reference [1] indicates an experimental variation in cycle time of 1.7 to 4.7 milliseconds.

---

[1] Grandy, A.J.; Duffy, J.A.; Horchler, M.H.; and Ehle, P.E.; "Investigation of Bolt/Bolt-Carrier Clearances in the M16A1 Rifle", Technical Note TN-1159, Frankford Arsenal, Philadelphia, Pa. (May 1971)

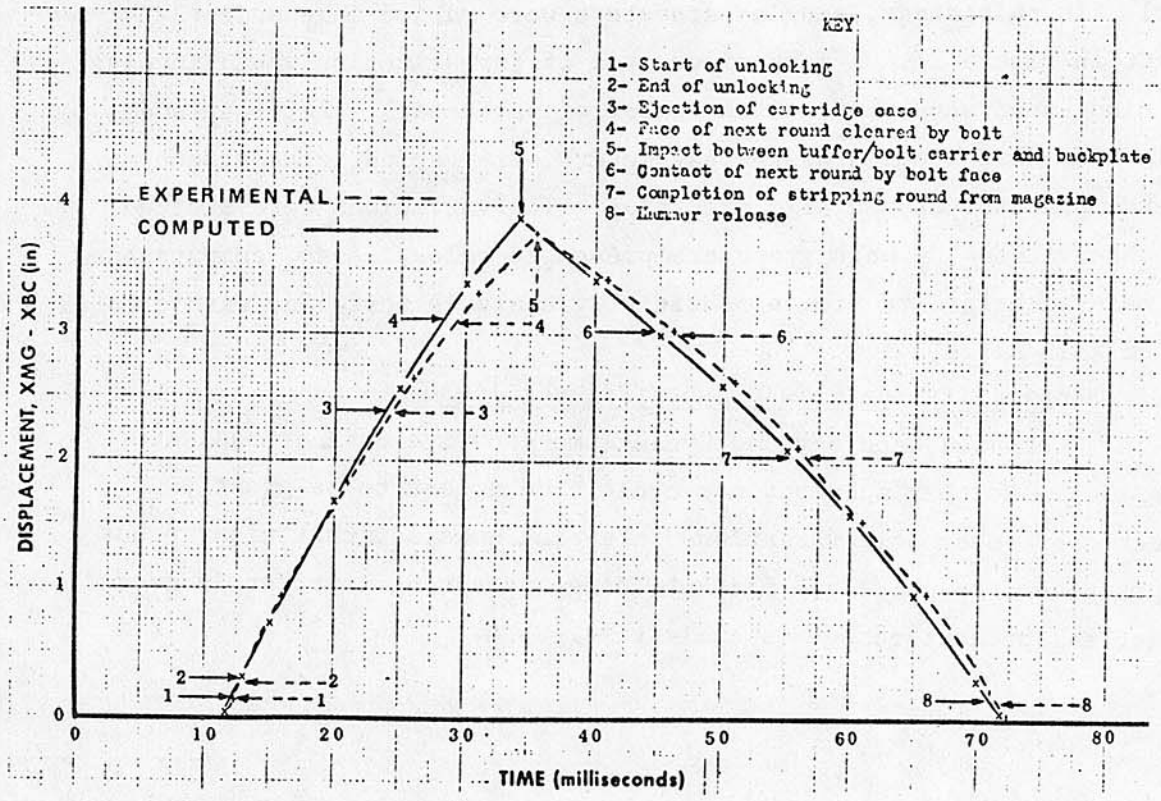

Figure 13 Computed and Experimental Bolt-Carrier Displacement vs Time

3.6 Sensitivity Analysis

One important use of a math model of a weapon is the conduct of a sensitivity analysis through parametric variations. Such a study is often very costly and difficult to perform experimentally because of the need to physically alter weapon components and the need to repeat many tests a large number of times to remove random variations from causes other than part modification. A sensitivity analysis is a very helpful tool with which to uncover potential malfunctions. In practice, small variations in parameters such as drive spring stiffness actually occur, and a model can be used to determine just how great these variations can be before performance is adversely affected. Also, one acquires a good idea of what particular design change might improve performance.

A sensitivity analysis was performed with the use of the M16A1 model. In this study, single parameters were varied independently, except in Figure 21. A much wider area of investigation would involve the simultaneous variation of a number of parameters. Accuracy and cycle time were studied as the parameters were varied. The effect on several peak forces was also predicted. The variations were plotted, and observations on each graph are presented below. Also, comparisons are made with results from a sensitivity analysis performed with a model of the XM19 Rifle.

3.6.1 Sensitivity Analysis Graphs (Figures 14-30)

a. Computed Accuracy and Cycle Time vs Drive Spring Constant (Fig. 14). Neither accuracy nor cycle time appear to be greatly affected by reasonable variations in spring constant that might occur in practice. Roughly, a 6 percent change in spring constant is needed to get a 1 percent change in cycle time.

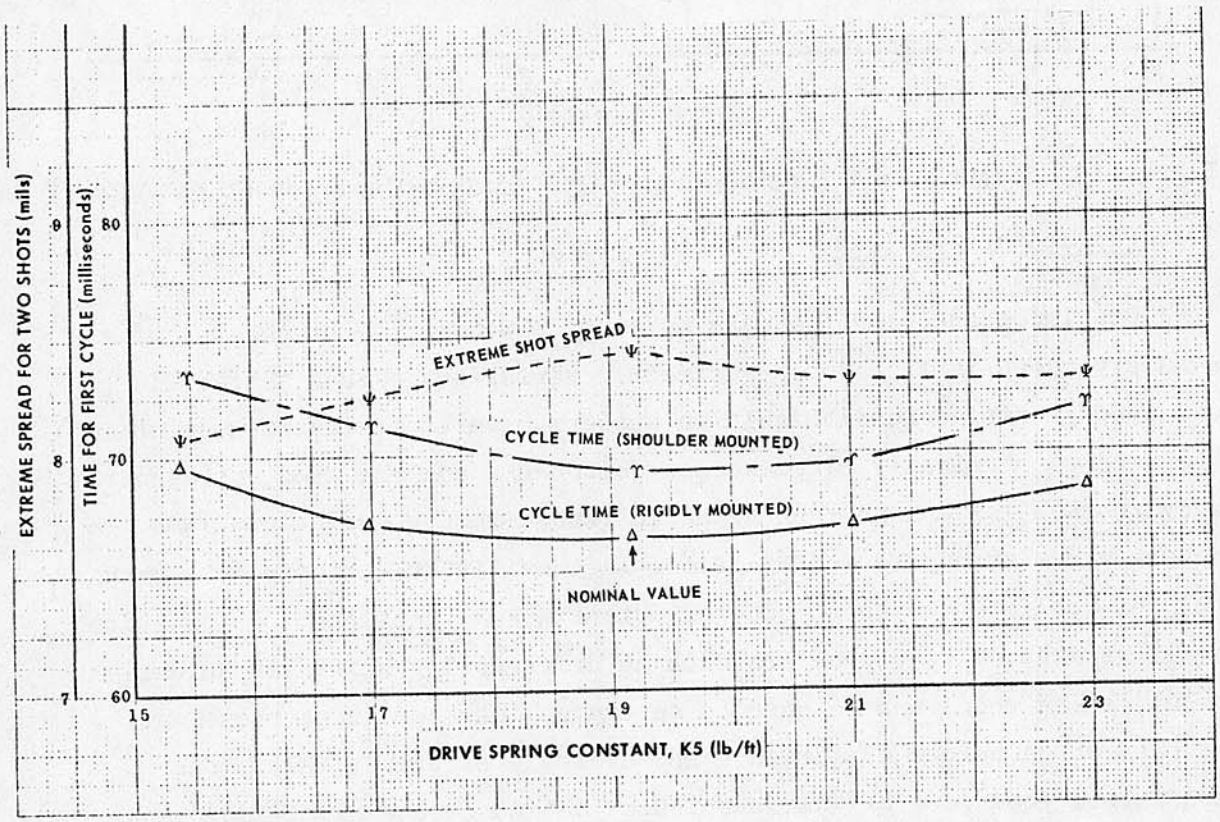

Figure 14 Computed Accuracy and Cycle Time vs Drive Spring Constant

b. Computed Accuracy and Cycle Time vs Linear Mount Spring Constant (Fig. 15). The spring referred to here represents the shooter's shoulder and should be distinguished from the torsional spring that represents the rest of the body. In the lower range of spring stiffnesses, characteristic of most men's shoulders, cycle time is moderately sensitive to spring stiffness and tends to decrease as stiffness increases. At higher values, sensitivity is low. Accuracy is also moderately sensitive to the spring constant in the lower range of values and tends to increase with spring stiffness. Accuracy tends to decrease with stiffness in the higher range, but this range is not realistic for a shoulder mount.

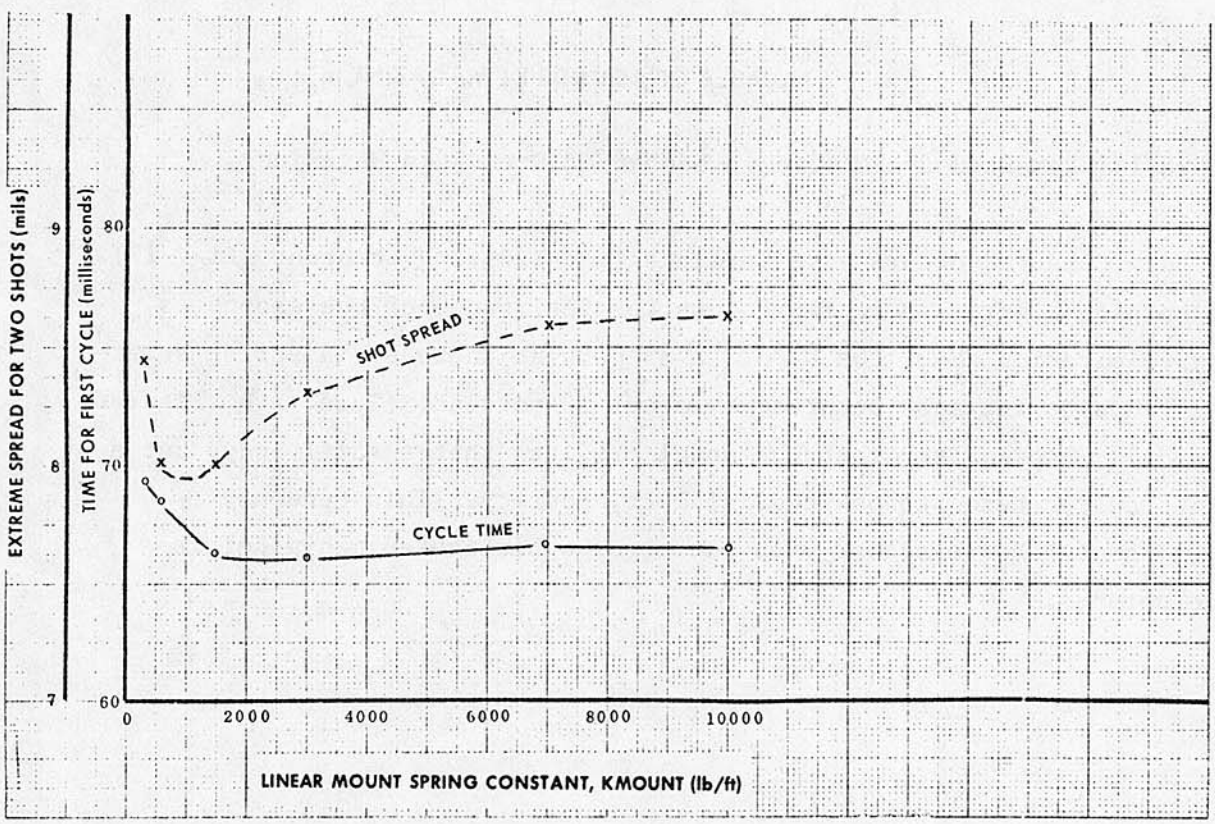

Figure 15 Computed Accuracy and Cycle Time vs Linear Mount Spring Constant

c. Computed Cycle Time vs Number of Rounds in Magazine (Fig. 16). Cycle time shows a slight increase with number of rounds. Variation up to about 1/4 millisecond can be expected from a 20-round magazine.

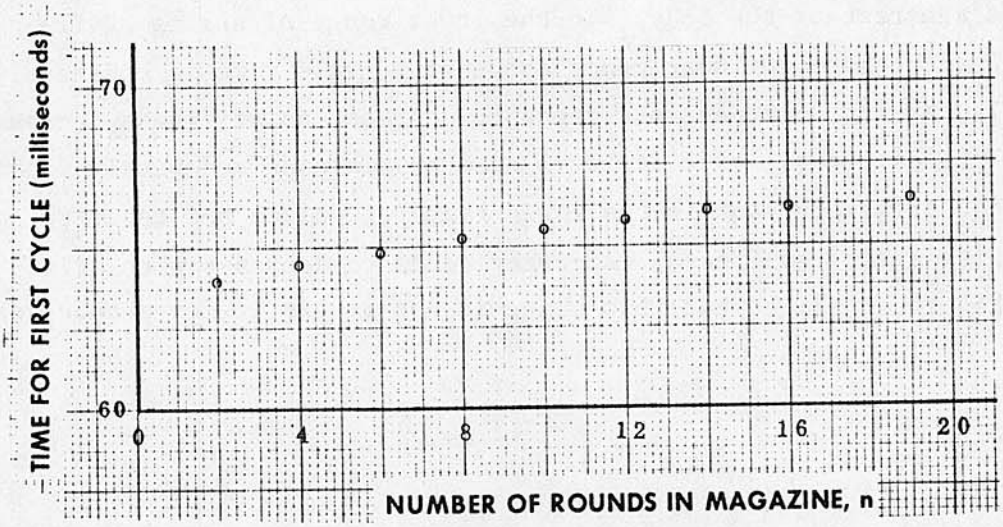

Figure 16 Computed Cycle Time vs Number of Rounds in Magazine

d. Computed Accuracy vs Torsional Mount Spring Constant (Fig. 17). The torsional spring here represents the resistance of the shooter's body to pivoting about the hips. A 33 percent increase in spring stiffness tends to increase accuracy by about 13 percent. Thus, from Figures 15 and 17, one can see that the model predicts that a stiff body, but a soft shoulder tends to be beneficial to accuracy. This tendency should be further explored when the more sophisticated man-model is incorporated.

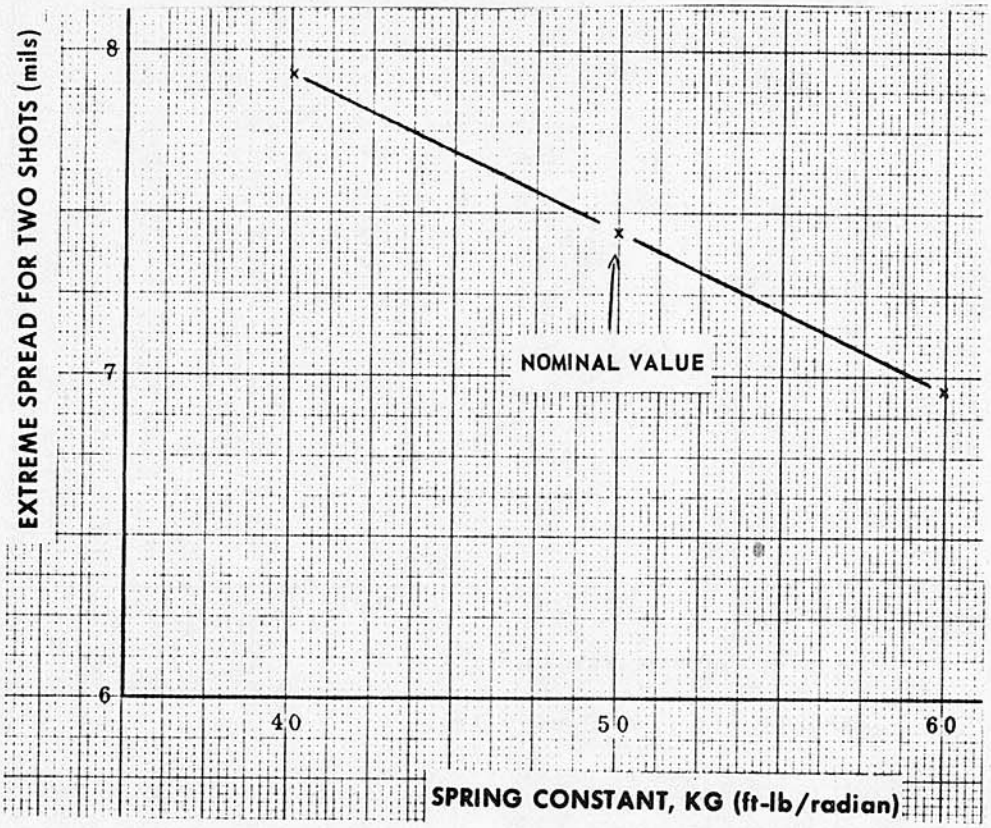

Figure 17 Computed Accuracy vs Torsional Mount Spring Constant

e. Computed Cyclic Time vs Cavity Area (Fig. 18). This variation in area is equivalent to a uniform increase in pressure over the nominal cavity area in the bolt-carrier. Cycle time is sensitive to this variation. An 18 percent increase in cavity area (or pressure) causes about a 16 percent decrease in time for the first cycle. Thus, one can expect that this weapon is sensitive to round-to-round variations in ammunition.

f. Computed Stripping and Friction Forces vs Number of Rounds in Magazine (Fig. 19). One can expect that stripping force may vary about three pounds, and that friction between bolt-carrier and ammunition may vary about one pound as rounds are removed from the magazine.

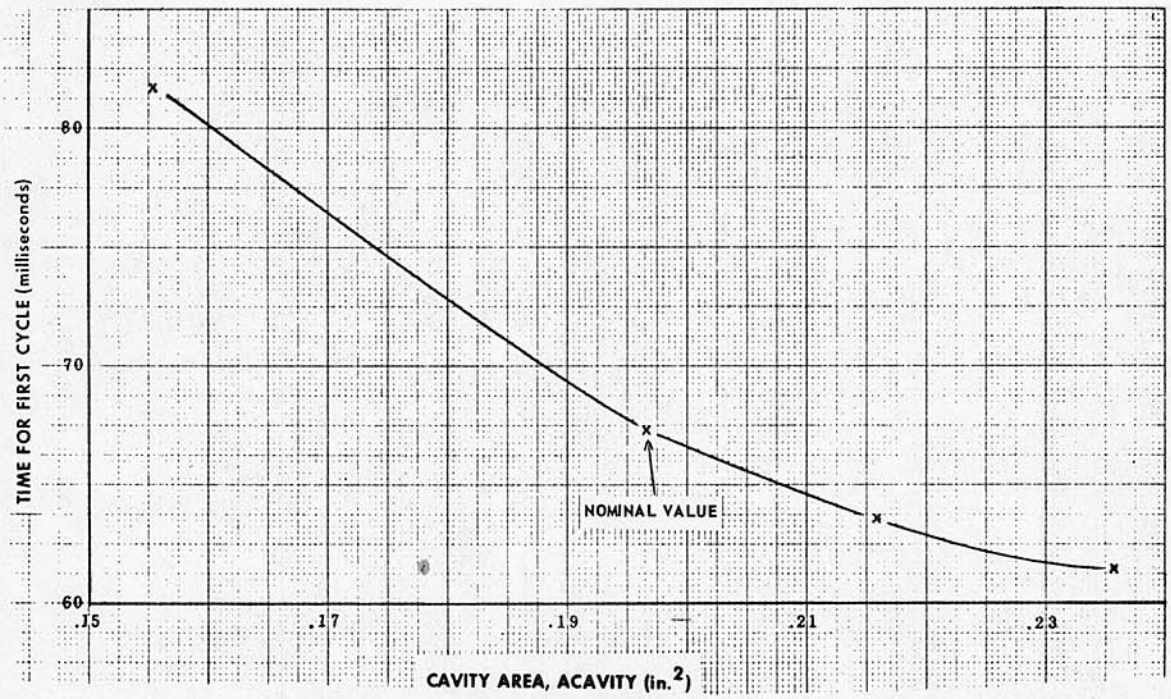

Figure 18 Computed Cyclic Time vs Cavity Area

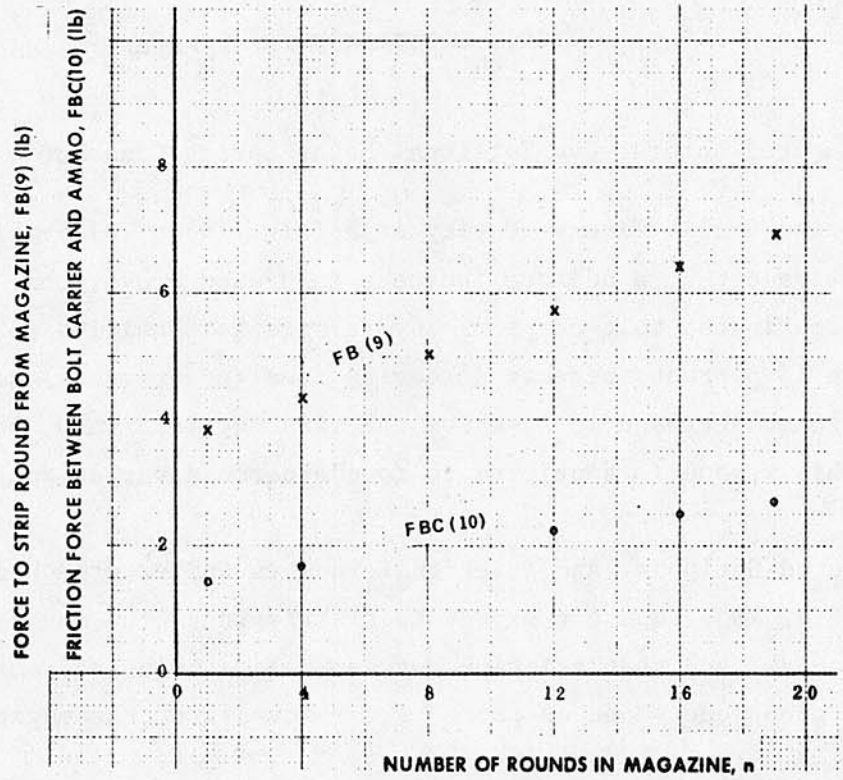

Figure 19 Computed Stripping & Friction Forces vs Number of Rounds in Magazine

g. Computed Accuracy and Cycle Time vs Breech Pressure Impulse (Fig. 20). This weapon exhibits a very high sensitivity of accuracy to breech pressure impulse. A 10 percent increase in breech pressure impulse can result in an accuracy loss of roughly 17 percent and a decrease in cycle time of about 4 percent. Thus, round-to-round variations in ammunition can be expected to significantly affect performance.

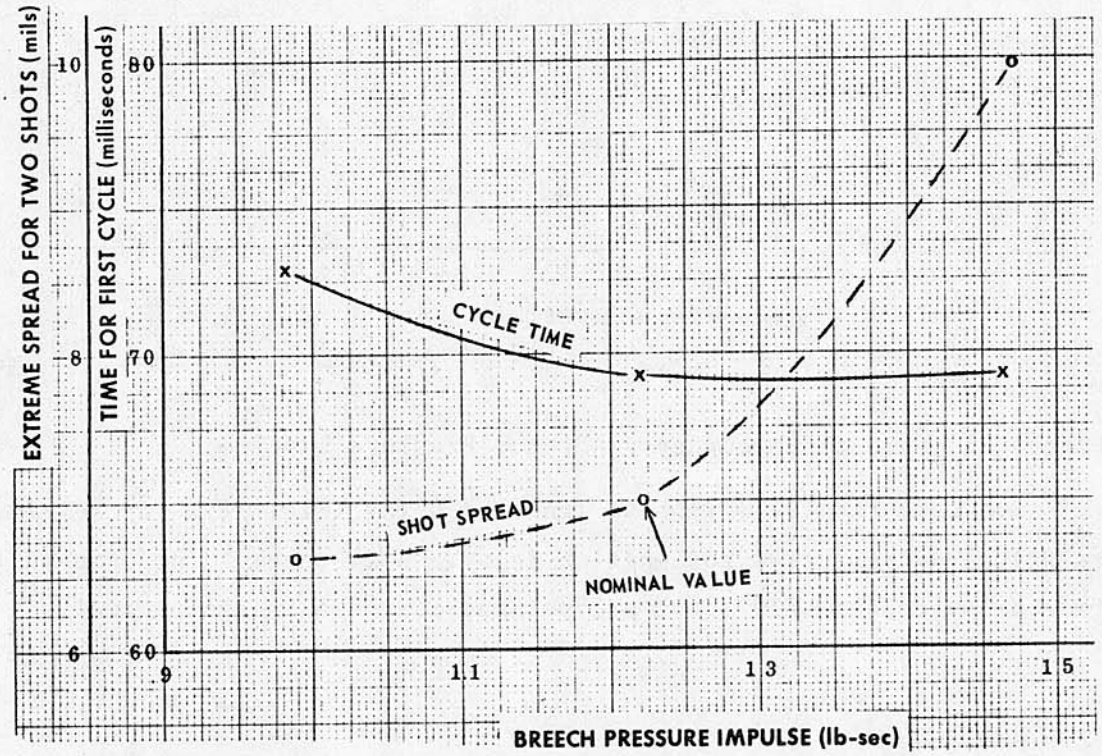

Figure 20 Computed Accuracy and Cycle Time vs Breech Pressure Impulse

h. Computed Accuracy vs Breech Pressure Impulse (Fig. 21). The difference between Figure 21 and Figure 20 is that here the pressure in the bolt-carrier cavity is allowed to change with breech pressure. A 1 percent increase in breech pressure impulse accompanied by a 1 percent increase in cavity pressure impulse results in about a 1 percent decrease in accuracy.

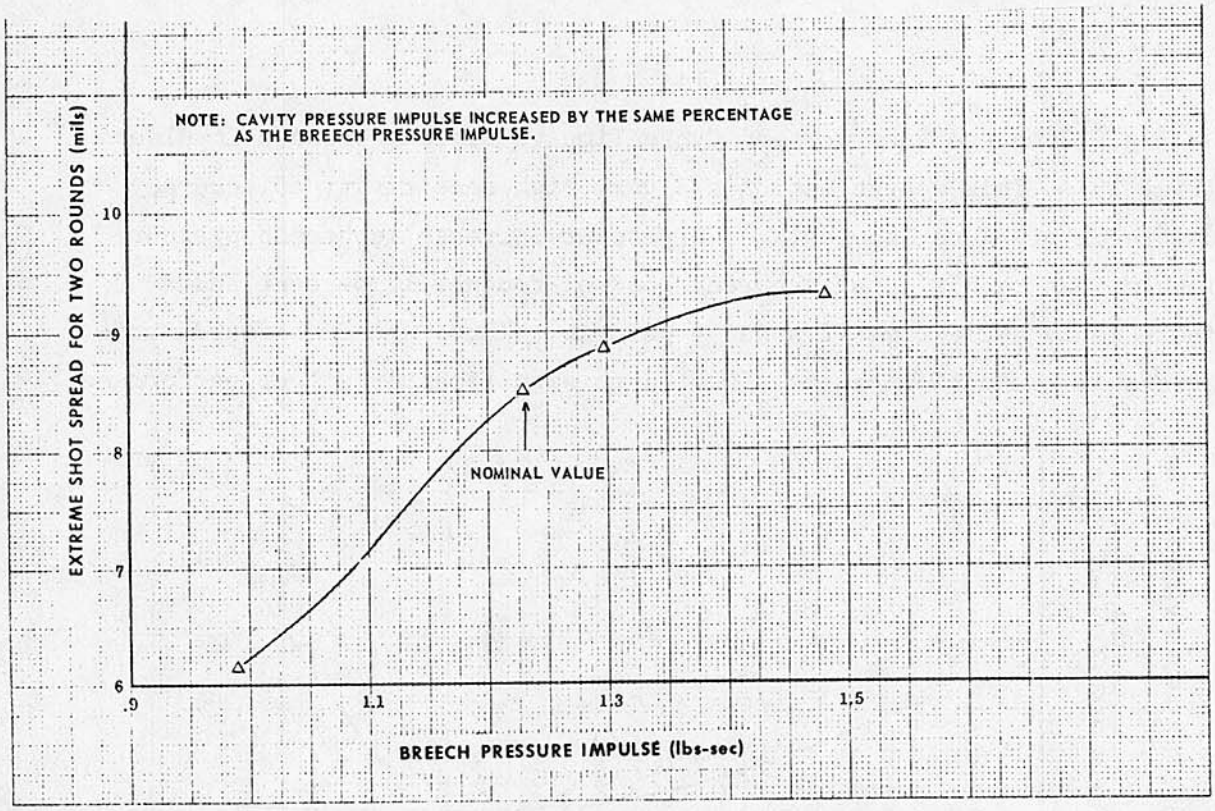

Figure 21 Computed Accuracy vs Breech Pressure Impulse

i. Computed Cycle Time vs Ignition Delay (Fig. 22). Cycle time is relatively insensitive to ignition delay. A 14 percent increase in ignition delay causes only about a 1 percent increase in cycle time.

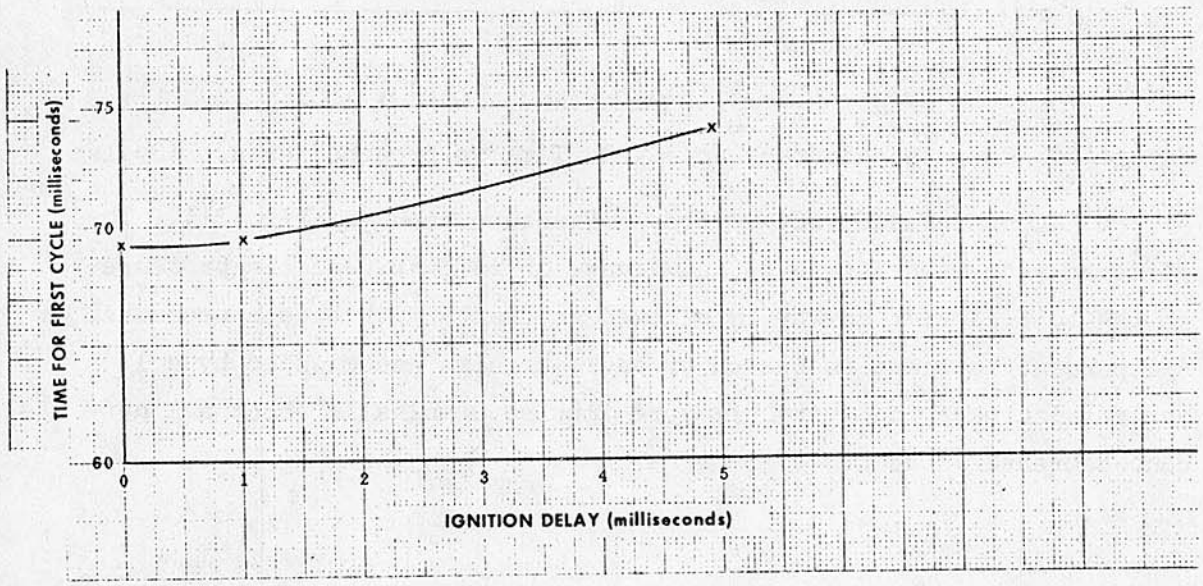

Figure 22 Computed Cycle Time vs Ignition Delay

j. Computed Cycle Time vs Ignition Delay (Fig. 23). The difference between this graph and Figure 20 is that here the ignition delay is in a more realistic range. Very little effect on cycle time is observed. This behavior is in contrast with that of the XM19 Rifle where the effect is much more significant. (See Part II of this report).

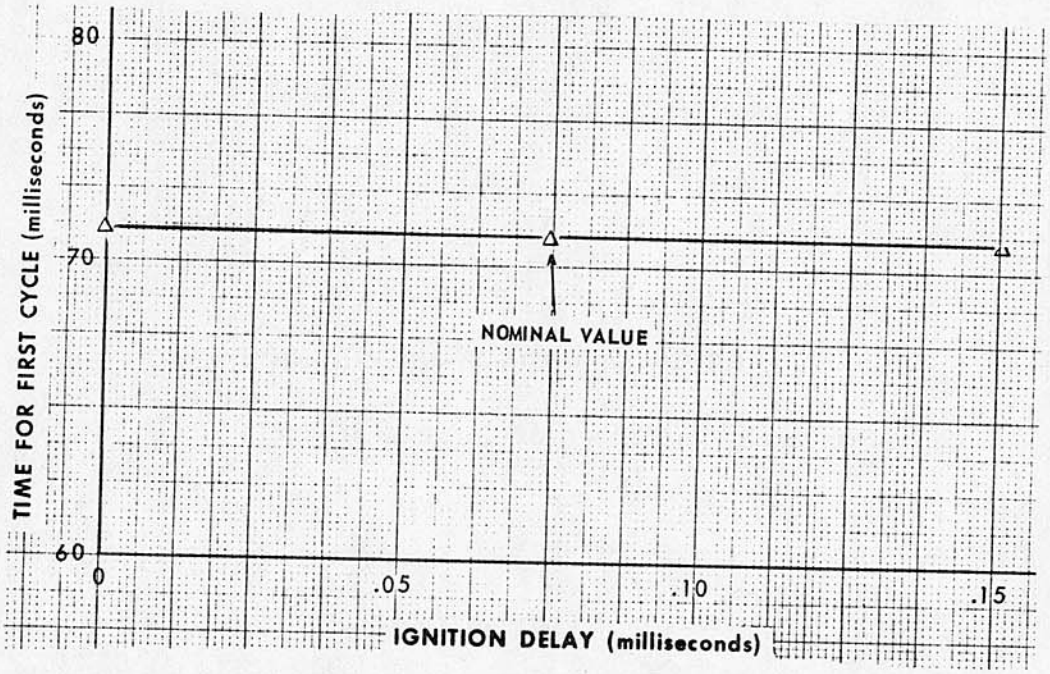

Figure 23 Computed Cycle Time vs Ignition Delay

k. Computed Accuracy vs Moment of Inertia of Rifle (Fig. 24). Accuracy of the M16A1 does not appear to be highly sensitive to the moment of inertia of the rifle about an axis through the center of gravity and perpendicular to the bore and gravity axes. A 10 percent increase in moment of inertia increases accuracy by about 3 percent.

1. Computed Unlocking Force and Cycle Time vs Length of Cam Path (Fig. 25). The peak unlocking force and the cycle time have a definite tendency to decrease as the length of the cam path in the bolt is increased. The force is more sensitive than is cycle time.

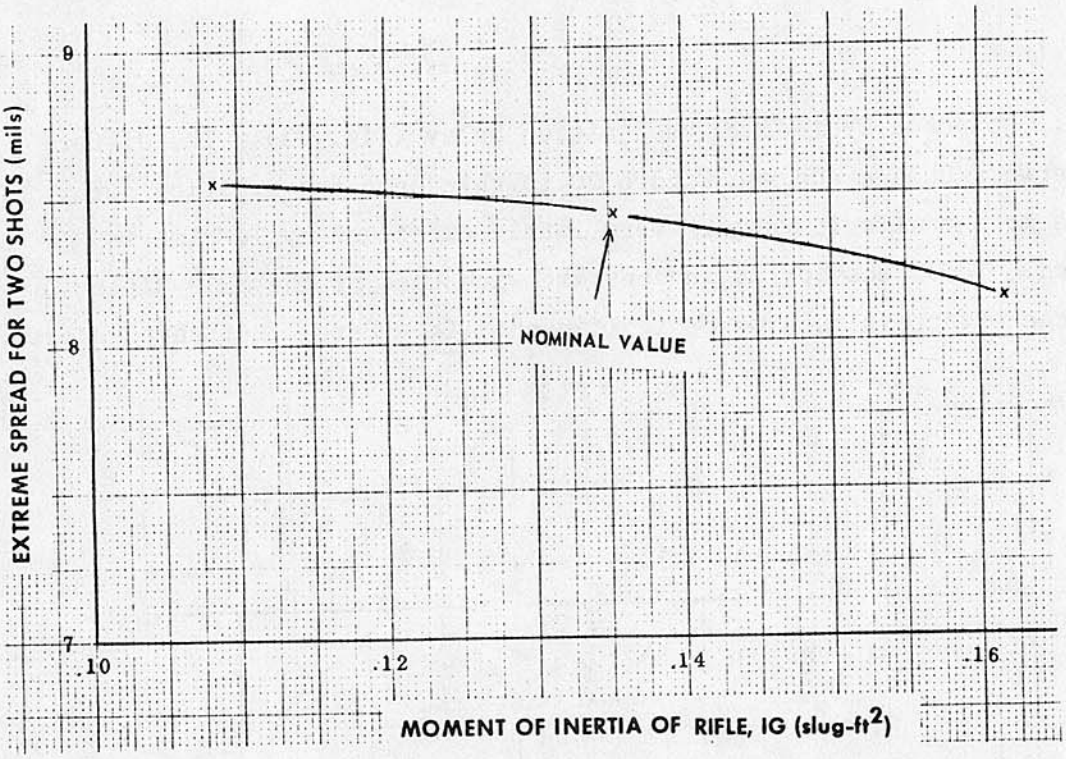

Figure 24 Computed Accuracy vs Moment of Inertia of Rifle

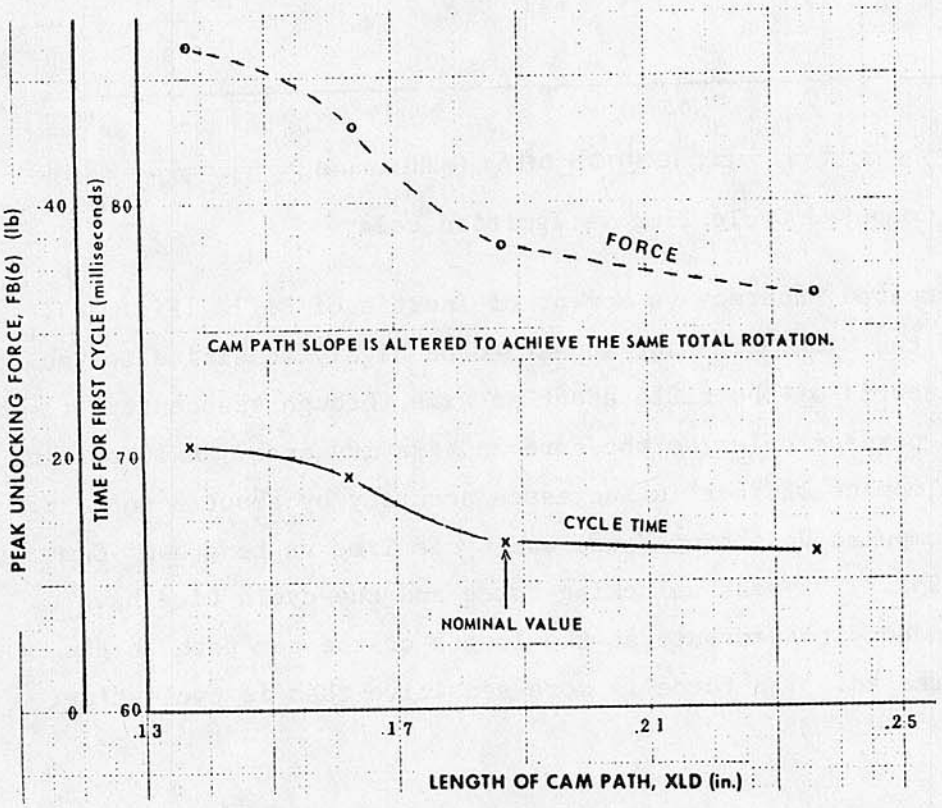

Figure 25 Computed Unlocking Force and Cycle Time vs Length of Cam Path

m. Computed Accuracy and Cycle Time vs Mass of Bolt (Fig. 26). A 10 percent increase in the mass of the bolt leads to only a 2 percent increase in cycle time and less than a 1 percent change in accuracy. Accuracy both increases and decreases with bolt mass. Thus, the mass of the bolt does not appear to be highly critical.

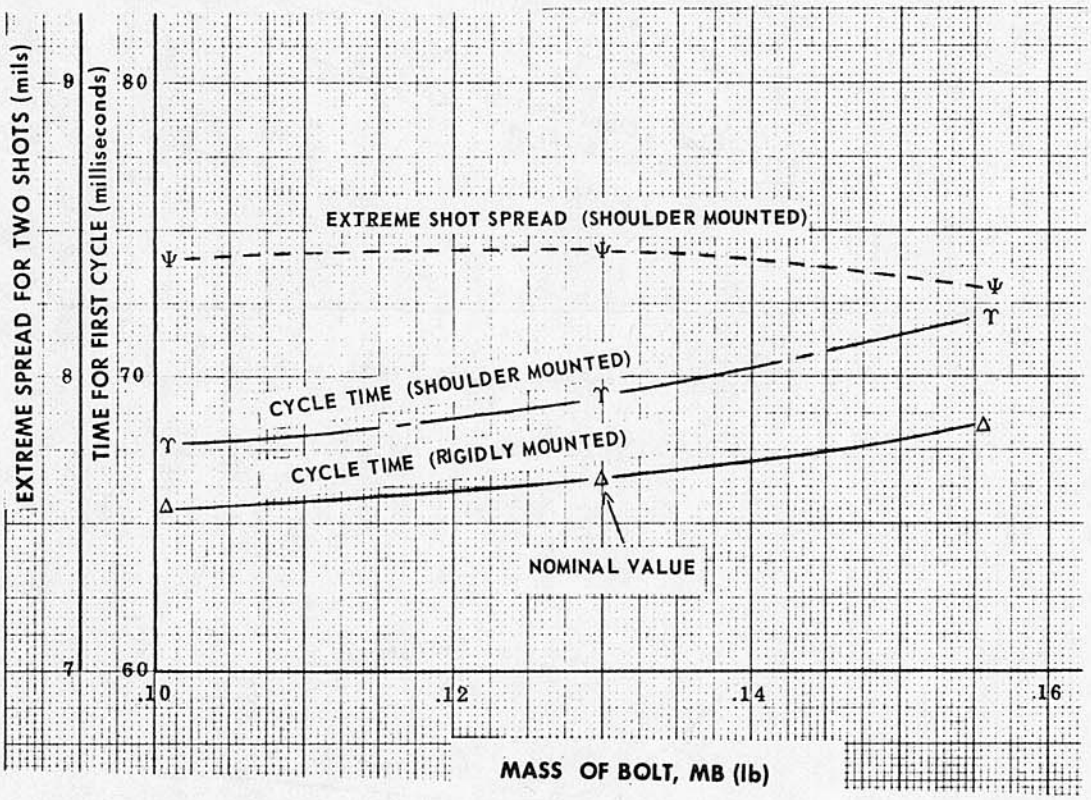

Figure 26 Computed Accuracy and Cycle Time vs Mass of Bolt

n. Computed Accuracy and Cycle Time vs Mass of Bolt-Carrier (Fig. 27). A 10 percent increase in the mass of the bolt-carrier leads to roughly a 4 percent increase in cycle time. No definite trend is apparent for accuracy. Performance appears to be only slightly more sensitive to variations in bolt-carrier mass than to variations in bolt mass.

o. Computed Accuracy and Cycle Time vs Drive Spring Preload (Fig. 28). Cycle time and accuracy appear to be more sensitive to reductions in preload rather than to increases in preload. A 10 percent reduction in preload leads to a 3 percent increase in cycle time and a 7 percent increase in accuracy.

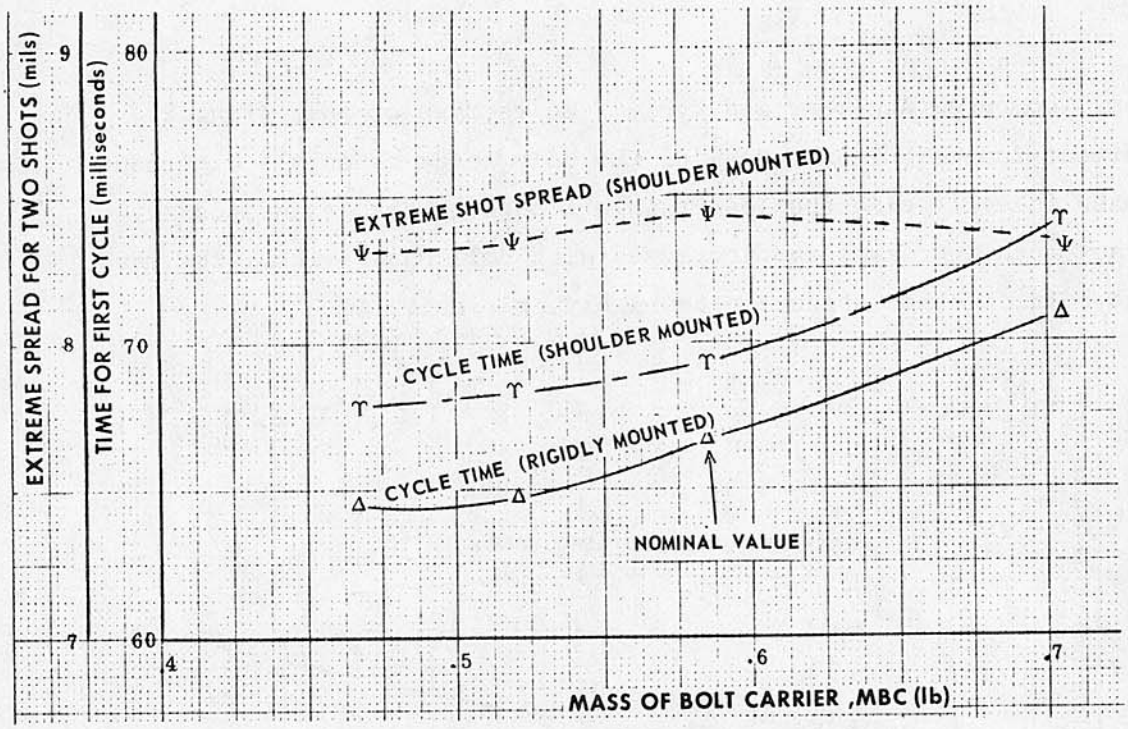

Figure 27 Computed Accuracy and Cycle Time vs Mass of Bolt-Carrier

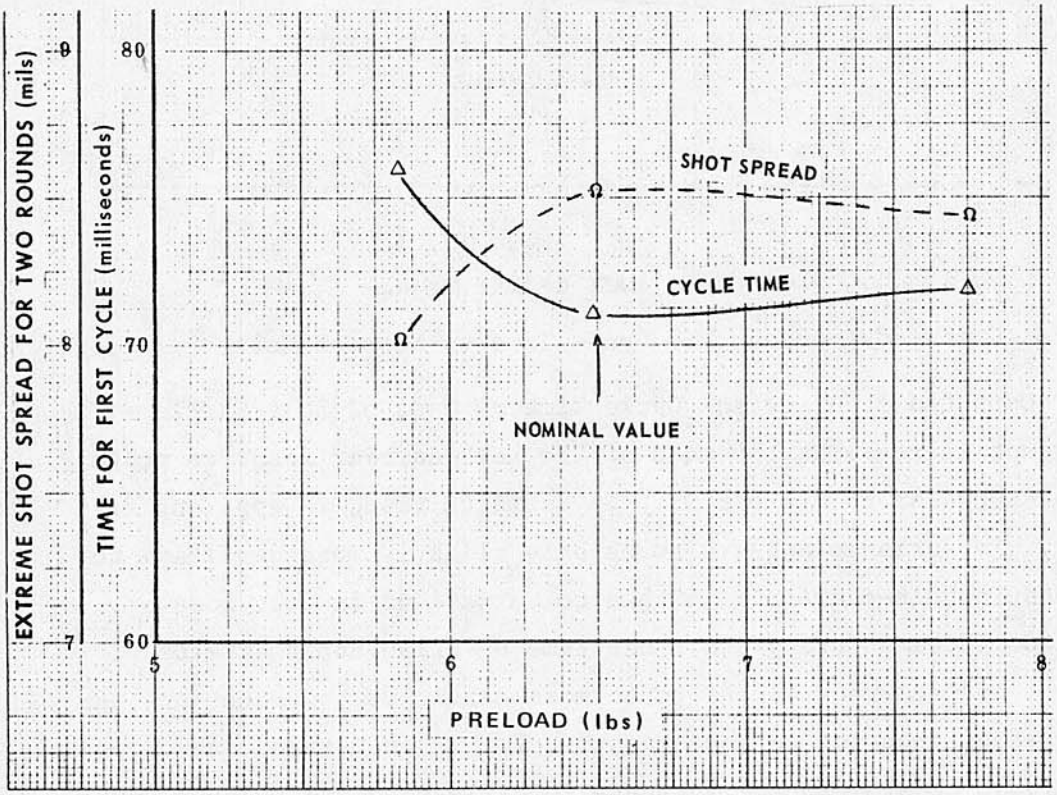

Figure 28 Computed Accuracy and Cycle Time vs Drive Spring Preload

p. Computed Accuracy and Cycle Time vs Initial Buffer Weight Positions (Fig. 29). According to the model, cycle time for the first shot is highly dependent on the initial positions of the buffer weights and can vary as much as 10 milliseconds. However, the effect tends to quickly diminish in succeeding shots. Shot spread for two rounds can vary by as much as 1 milliradian.

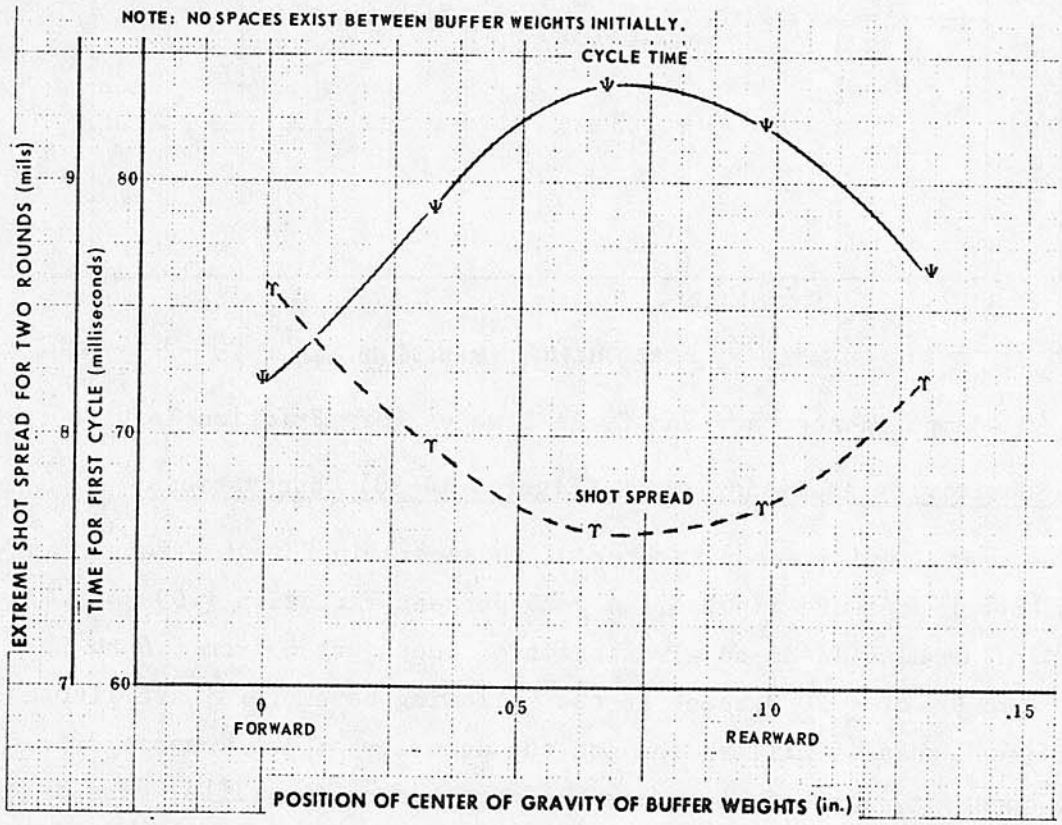

Figure 29 Computed Accuracy & Cycle Time vs Initial Buffer Weight Positions

q. Computed Accuracy and Cycle Time vs Bore Friction Impulse (Fig. 30). Cycle time is not affected by bore friction for the first shot. However, a 5 percent increase in bore friction impulse increases accuracy by about 1 percent. The reason is that bore friction tends to counteract the breech impulse.

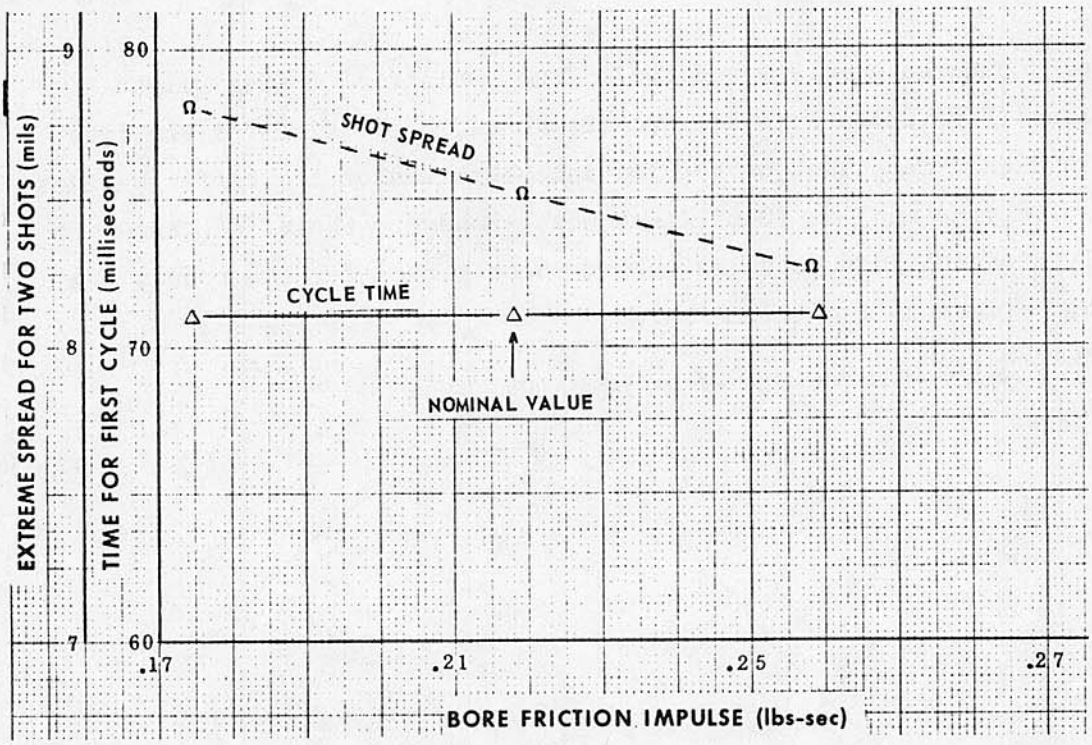

Figure 30 Computed Accuracy and Cycle Time vs Bore Friction Impulse

3.6.2 Sensitivity Analysis Graphs (Figures 14-30) Observations

The most significant parameter of those examined that affect accuracy is breech-pressure impulse. A $\pm$ 20 percent variation (.99 to 1.47 lb-sec) of impulse leads to a variation of shot spread from 6.6 to 10 mils. Changes of $\pm$ 20 percent in the following parameters have little effect (less that .5 milliradian) on the accuracy of the weapon: drive spring constant, mass of bolt moment of inertia of the rifle, mass of the bolt-carrier, and bore-friction impulse. Mechanical properties of the shooter are seen to have a significant effect on accuracy. Drive spring preload has a moderate effect.

The most significant parameter of those examined that affect cycle time is the cavity area in the bolt-carrier. A 20 percent variation about the nominal area causes cycle time to vary from 61 to 82 milliseconds. The initial positions of the buffer weights appear to be highly significant for the first round. The number of rounds in the magazine appears to have little effect. With two rounds in the magazine,

the cycle time is 64 milliseconds, whereas the cycle time is 66 milliseconds with nineteen rounds. A decrease in the length of the cam path by 20 percent causes the cycle time to change from 66.5 to 70.5 milliseconds. The reason is that the gas forces have a shorter time over which to impart momentum to the bolt-carrier.

In Part II of this two-report series, a complete discussion appears in which performance of the M16A1 Rifle is compared with that of the XM19 Rifle. The results are based on mathematical models of both weapons. From this study, accuracy appears to be slightly more sensitive to changes in moment of inertia of the rifle in the M16A1. Also, the M16A1 cycle time is more sensitive to changes in the drive spring constant, in mount stiffness, and in ignition delay. However, sensitivity to changes in drive spring preload appears to be somewhat greater in the XM19.

3.7 Additional Comments on the Buffer and Drive Spring

The buffer assembly in the M16A1 was designed to provide a secondary impulse to the bolt-carrier. This impulse is needed to prevent the bolt-carrier from bouncing rearward just after locking. If the bounce is too great, a misfire can result. With the use of the model, a check was made to determine if the buffer does indeed perform this function. By setting the spring constants and damping coefficients between the buffer weights to zero, one effectively removes the influence of the buffer weights on the weapon. When this is done, the model predicts a bolt-carrier rebound of about 1/16th of an inch. The weapon begins to unlock, but the drive spring on the buffer body prevents complete unlocking. When the influence of the buffer weights is included in the model, virtually no rebound occurs. The reason is attributed to the secondary impact of the buffer weights on the forward end of the buffer body. The model predicts that this impact occurs 1.2 milliseconds after the bolt-carrier strikes the bolt pin at the end of locking.

The inertial effects of the drive spring have a very significant effect on the operation of the M16A1 Rifle. Initially, the drive spring was considered to behave linearly, and inertial effects were accounted for by the addition of one-third of its mass to the mass of the buffer body. With this kind of model, the bolt-carrier and buffer body were observed to separate just after unlocking and the buffer continued rearwardly at a faster rate than the bolt-carrier. The reason is that the picking up of the bolt by the bolt-carrier decreases the rearward acceleration of the bolt-carrier while the buffer is free to continue rearwardly since only compressive forces can act between the buffer and the bolt-carrier. The buffer was found to rebound from the closed end of the buffer body, strike the bolt-carrier, and bounce back toward the closed end again. Large variations in cyclic rate occurred. The operating parts entered the counterrecoil phase with less velocity than if all parts were together at the time of impact with the closed tube end. No experimental evidence could be found to indicate that the buffer rebounds from the closed end of the buffer body more than once per cycle. Thus, a more sophisticated model of the drive spring seemed to be required. As described in Appendices A and C, a finite-element method was used. With even a small number of elements, the inertia effects from this model were sufficient to cause the bolt, bolt-carrier, and buffer to strike the backplate together, and thus to eliminate the problem. In some instances, cycle time was reduced by as much as nine milliseconds. Two principal effects result from this more realistic model. The first is that the effective drive spring seen by the buffer body is initially greatly stiffened. The second is that the main gun is unaffected by the buffer body motion until a stress wave travels the entire length of the spring. The M16A1 drive spring can, for most purposes, be modeled with as few as five elements. To consider coil clashing in a detailed evaluation of the spring itself, one can use a number of elements equal to the number of coils as discussed in Appendix C. The difference in spring behavior with various numbers of elements is shown in Figures 31 to 33.

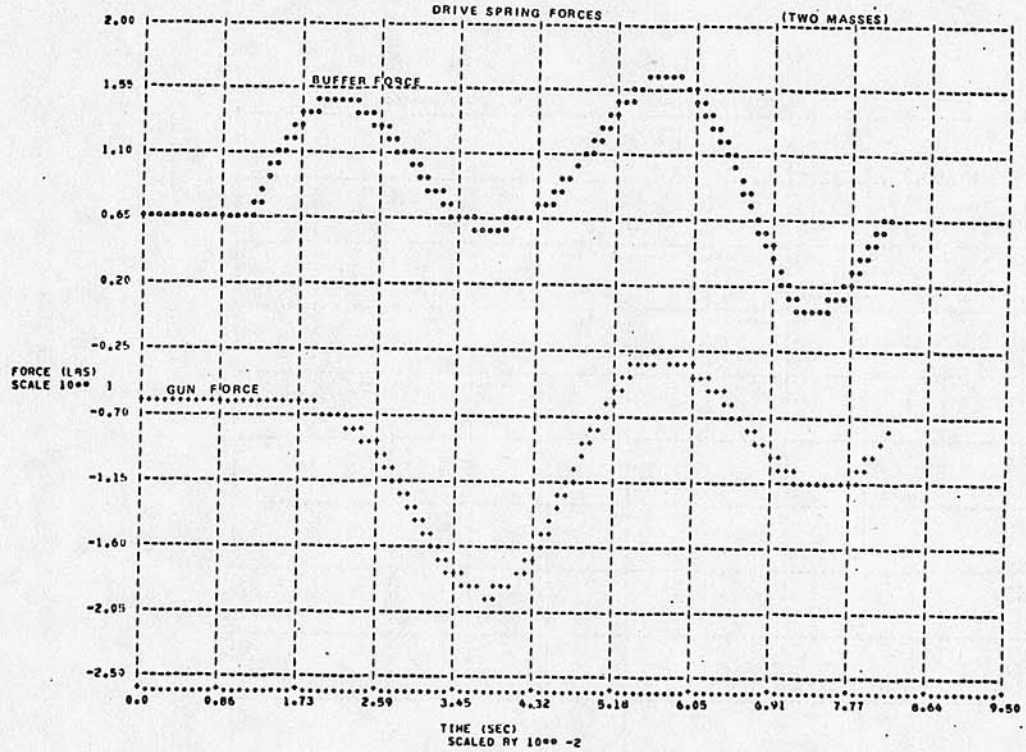

Figure 31 Drive Spring Forces (2 - Element Model)

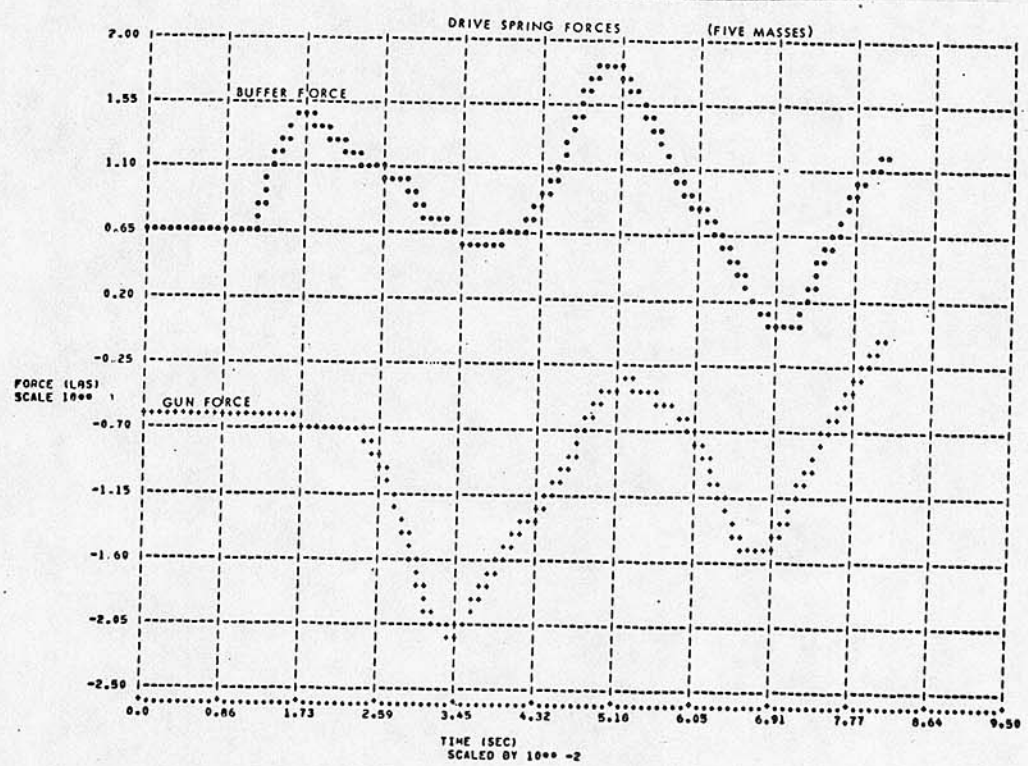

Figure 32 Drive Spring Forces (5 - Element Model)

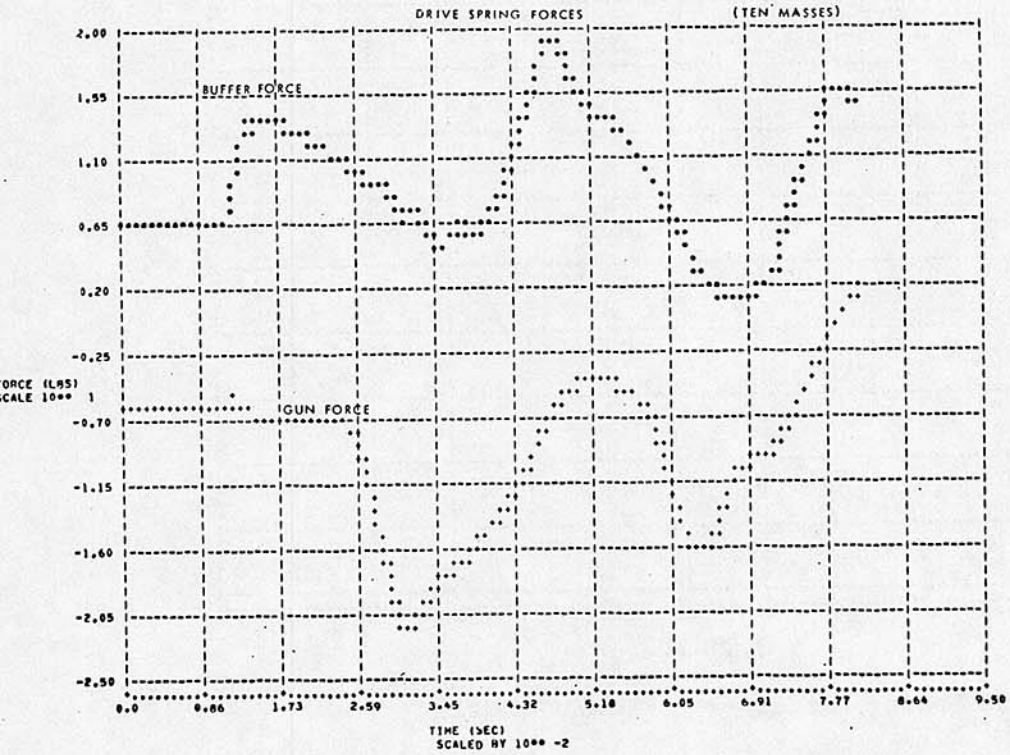

Figure 33 Drive Spring Forces (10 - Element Model)

4.0 CONCLUSIONS AND RECOMMENDATIONS

4.1 Conclusions

a. A digital-computer model of the M16A1 Rifle has been constructed and is suitable for the study of effects on mechanical performance and weapon dispersion as changes are made in various weapon parameters. From this model, information about the M16A1 can be obtained that would be extremely difficult and costly to determine by experiment.

b. As a result of the work associated with the development of this model, modest extensions of the state of the art in weapon modeling have been realized. For example, both continuum and finite-element approaches to impact have been explored (Appendix F), and three approaches for the analysis of cam forces are presented in Appendix A. A new area of study, the coupling of complex computer models, is presented in Appendix F. Another new approach to the modeling of weapons is that of the extension of deterministic models to the probabilistic regime (Appendix G). The concept of finite elements in solid mechanics has been extended to fluid mechanics, and the result is a unique approach to gas flow (Ref[7]). For the first time, very detailed small-caliber weapon models have been developed by which weapon dispersion can be approximately analyzed. Also, detailed models of spring surging, coil clashing, and buffer-weight behavior have become integral parts of the weapon model. Hammer and magazine dynamics have been extensively analyzed. However, much work remains in these and other areas of weapon modeling such as dynamic friction.

c. Accuracy of the M16A1 Rifle can be improved, in accordance with the model, by a stiffening of the shoulder and upper torso of the shooter, a decrease in breech-pressure impulse, and increase in moment of inertia of the rifle, an increase in bore-friction impulse (provided this increase is obtained without a corresponding increase in the time that the projectile is in the barrel), decreases in both drive spring constant and preload, and by the initiation of the firing cycle with the buffer weights in their most central location. Of course, these changes also have other ramifications that must be explored, and not all of these

[7]Ehle, P.E. and Rahe, A.E., "Development of a Finite Element Approach for Approximate Analysis of Unsteady Compressible Fluid Flow," WECOM Technical Report, SWERR-TR-72-36, AD 746234, Rock Island, Ill (Jun 1972)

may be beneficial. Also, the combined effect of the simultaneous changing of two or more parameters was not explored, although this could be done.

d. An increase in cyclic rate can be achieved in accordance with the model, by a stiffening of the shooter's shoulder, an increase in gas pressure in the cavity and at the breech, decreases in bolt and bolt-carrier masses, and the initiation of the firing cycle with the buffer weights at either extreme end of their allowed positions. Again, these changes would have other ramifications, none of which were explored in this study.

e. Techniques developed for the M16A1 Rifle model are applicable to the analyses of other shoulder-fired automatic weapons. Examples of these techniques are those used to model the drive spring, magazine, cam forces, weapon dispersion, and hammer dynamics. The preliminary results from the investigations of impact, stochastic methods, coupling of complex models, and fluid flow are also applicable.

f. Detailed analyses of the buffer assembly, shooter, and drive spring are important factors for accuracy and realism in an M16A1 Rifle model. These factors have important influences on weapon operation and dispersion.

g. The model provides a suitable base for the comparison of performance of other weapons.

h. In the section of this report on modeling philosophy, "verification" of a complex weapon model by experiment is mentioned as a concept not well defined. One often uses the term without a clear idea of its meaning. Since no established verification criteria exist, the present model will not be presented as either verified or unverified. Many of the model predictions are in excellent agreement with experiment; this can be seen in the section on comparison with experiment. Without doubt, other predictions such as a peak force value may be found that are not as good. Some uses for the model require better accuracy in certain areas than in others. All that can be said about validation is that the model is sufficiently accurate that it can be used with a high degree of confidence for many important studies, but that the model is by no means infallible.

4.2 Recommendations

a. Use of the M16A1 Rifle model should be continued as a vehicle for the development of modeling techniques.

b. A number of important areas exist in which development work should be emphasized. First, a detailed mathematical model of the shooter should be added to the M16A1 model. This man-model is already available at RIA and comprises springs, levers, masses, and dampers to simulate the passive response of a man's body to recoil. The sensitivity analysis in this report demonstrates that such response significantly affects both weapon operation and accuracy. Second, better models of friction should be developed with an instrument designed to simulate and measure friction forces typical of many different weapons. Cams capable of providing time-displacement histories found in a given weapon can be manufactured and inserted in this machine. Normal force, temperature, humidity, velocity, displacement, acceleration, and lubricant are some of the parameters that can be varied. Delivery of this instrument to the Weapons Laboratory, RIA, is expected during FY73. Third, an analysis of gas transmission should be included. A relatively simple analysis is needed that can be run with an already complex model without excessive computation time. Development of such an analysis is nearing completion (Ref[7]). Fourth, stochastic techniques should be developed and incorporated into the M16A1 Rifle model so that probabilistic data can be accepted as input and confidence levels can be established for predicted results (Appendix D). Fifth, improved models of impact should be developed that more accurately reflect the true stress levels involved (Appendix F). Sixth, methods should be explored for the direct coupling of complex computer models (Appendix G). Seventh, optimization and design methodologies should be developed so that models will have a more significant place in the design process. Eighth, the development of reliability data obtained from a model before a record of performance is established should be emphasized. Ninth, cartridge case

---

[7]Ehle, P.E. and Rahe, A.E., "Development of a Finite Element Approach for Approximate Analysis of Unsteady Compressible Fluid Flow," WECOM Technical Report, SWERR-TR-72-36, AD 746234, Rock Island, Ill (Jun 1972)

extraction and bore friction are study areas important for the construction of accurate models and should become the subjects of in-depth studies.

c. Special emphasis should be focused upon the semiphilosophical problem of model verification and the development of suitable validation criteria.

d. The M16A1 Rifle model should be used as a basis for the comparison of performance of other automatic shoulder-fired weapons and for the improvement of the M16A1 itself.

APPENDIX A

DERIVATION OF FORCE EXPRESSIONS

A.1 BASIC NOMENCLATURE

1. X_{MG} = position of center of gravity (cg) of main gun structure with no operating parts
2. X_B = position of cg of bolt
3. X_{BC} = position of cg of bolt-carrier
4. X_{BUFF} = position of cg of buffer body
5. X_{WTS} = position of cg of buffer weight system
6. θ_B = angle through which bolt rotates during locking and unlocking
7. θ_H = angle through which hammer rotates
8. θ_E = angle of elevation of Rifle
9. $M_{B(E)}$ = effective mass of the bolt at time t
10. g = acceleration of gravity
11. t = time

A.1.1 Coordinate System

Each mass has an associated coordinate system fixed with respect to the ground. These are such that when t = 0, the coordinate values are all zero if the masses are in the locked position and completely forward.

A.2 Force acting on the bolt

A.2.1 FB(1) Breech force - For several milliseconds after propellant ignition, the bolt is locked to the main gun and is considered a part of it; at this time only, FB(1) is considered to act on the main gun. After unlocking occurs, the FB(1) acts only on the bolt. FB(1) is a digitized function of time and becomes nonzero when the hammer strikes the firing pin. At this time, the mass of the bolt is reduced by an amount equal to the mass of the projectile plus the mass of the propellant.

Then,

$$FB(1) = -P_{BREECH}(t)\, A_{BORE} \qquad \text{(A-1)}$$

Nominal values are: $A_{BORE} = .0377\ in^2$,

$P_{BREECH}(t)$ = See Table 8 below.

TABLE 8 NOMINAL BREECH PRESSURE vs TIME

t (sec)	$P_{BREECH}(t)$ (lbs/in^2)
0	0
.0001	1000
.0002	3000
.0003	5000
.0004	11000
.0005	36000
.0006	50000
.0007	58000
.0008	50000
.0009	35000
.0010	25000
.0011	19000
.0012	15000
.0013	12000
.0014	10000

A.2.2 FB(2) Friction between bolt and ammo - This force is caused by the friction between the top round of ammunition in the magazine and the bolt during the recoil stroke. It becomes nonzero just after the bolt-carrier has passed over the ammunition and the bolt contacts the top round in the magazine. Three conditions exist that must be met for the force to continue to be nonzero:

a. The bolt has not reached the position where it "picks up" a new round,

b. The weapon is still in recoil,

c. The bolt-carrier is not in contact with the ammunition.

Then,

$$FB(2) = 2\mu_1 \text{sgn}(\dot{X}_B - \dot{X}_{MG}) \left((M_E g \cos \theta_E) + K_M (Y - Y_o) \right) \qquad \text{(A-2)}$$

if

the weapon is in recoil,

if

$X_{BC} - X_{MG} \leq -2.34$ in.,

And if

$X_B - X_{MG} \geq -2.81$ in.

FB(2) is zero otherwise.

The derivation of the expression used for this force is the same as the derivation of FBC(10). Nominal values of the parameters are also chosen to be the same.

An equal and opposite force FMG(2) acts on the main gun.

A.2.3 FB(3) Impact between bolt and barrel and engagement of extractor The contribution to FB(3) from the engagement of the extractor is assumed to be a constant 7.5 pounds. The contribution to this force from the impact between bolt and barrel is determined by a stiff spring and damper hypothetically placed between these two parts. When, during impact, the spring is about to decompress, the bolt and main gun are considered to be a single mass since locking has just occurred. This is a completely inelastic collision between bolt and barrel.

Then,

$$FB(3) = -E_{XTF} + K_{\substack{BARREL \\ IMPACT}} (X_{MG} - X_B) + C_{\substack{BARREL \\ IMPACT}} (\dot{X}_{MG} - \dot{X}_B) \qquad (A-3)$$

E_{XTF} is nonzero if weapon is in counterrecoil and $-.13" \leq X_B - X_{MG} \leq 0$.

$K_{\substack{BARREL \\ IMPACT}}$ and $C_{\substack{BARREL \\ IMPACT}}$ are nonzero if weapon is in counterrecoil,

if

$$X_{MG} - X_B \leq 0,$$

and if

$$\dot{X}_B \geq \dot{X}_{MG}.$$

Nominal values are:

E_{XTF} = 7.5 lbs

$K_{\substack{BARREL \\ IMPACT}}$ = 100,000 lb/ft

$C_{\substack{BARREL \\ IMPACT}}$ = 18 lb-sec/ft

For the two-mass system consisting of the bolt and the main gun, 18 lb-sec/ft represents 45 percent of critical damping where

$$C_{CRITICAL} = 2\sqrt{\frac{K_{\substack{BARREL \\ IMPACT}} M_{B(E)} M_{MG}}{M_{B(E)} + M_{MG}}}$$

This definition is made in analogy to the single mass-spring system where a mathematical change in the form of the solution for the governing equations occurs at this value of damping.

NOTE: FB(3) is zero after the bolt is locked, and an equal and opposite force FMG(3) acts on the main gun.

A.2.4 FB(4) Friction between bolt and bolt-carrier - The friction force between bolt and bolt-carrier acts continuously.

Then,

$$FB(4) = -C_B \left(\dot{X}_B - \dot{X}_{BC} \right) + \mu_B \, M_{B(E)} \, g \, \text{sgn} \left(\dot{X}_{BC} - \dot{X}_B \right) \cos \theta_E \qquad \text{(A-4)}$$

$$C_B = .01 \text{ lb-sec/ft}$$

$$\mu_B = .2$$

The first term in this expression represents viscous damping and the second term is Coulomb friction due to the weight of the bolt.

NOTE: An equal and opposite force FBC(1) acts on the bolt-carrier.

A.2.5 FB(5) Force at the end of the cam path when weapon is not locked - This force is the means by which the bolt-carrier transmits motion to the bolt. A 1/16 inch play exists between the bolt and the bolt-carrier. A stiff spring is assumed to act on both sides of this 1/16 inch distance.

Thus,

$$FB(5) = -K_{BBC} \left(X_B - X_{BC} - X_{BBC} \right) - C_{BBC} \left(\dot{X}_B - \dot{X}_{BC} \right) \qquad \text{(A-5)}$$

if

$$\left(X_B - X_{BC} - X_{BBC} \right) \leq 0$$

and if

$$FB(5) > 0.$$

NOTE: X_{BBC} is the total distance the bolt moves relative to the bolt-carrier (5/16 inch).

Therefore,

$$FB(5) = -K_{BBC} \left[X_B - X_{BC} - \left(X_{BBC} - 1/16" \right) \right] - C_{BBC} \left(\dot{X}_B - \dot{X}_{BC} \right) \qquad \text{(A-6)}$$

if the bolt is not about to be locked or unlocked,

if

$$X_B - X_{BC} - (X_{BBC} - 1/16") \geq 0,$$

and if

$$FB(5) < 0.$$

This situation is represented in Figure 34.

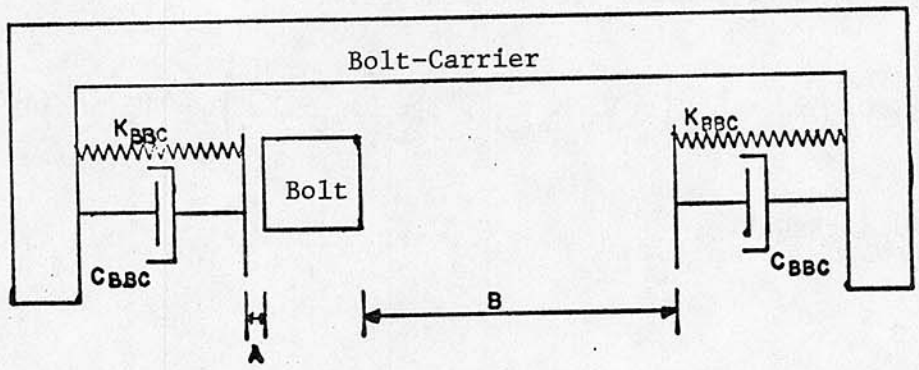

$A+B = 1/16"$

K_{BBC} = Assumed Spring Constant Between Bolt and Bolt-Carrier

C_{BBC} = Assumed Damping Constant Between Bolt and Bolt-Carrier

Figure 34 Schematic of Bolt/Bolt-Carrier Interaction (Unlocked Weapon)

Nominal values are: K_{BBC} = 100,000 lbs/ft,

C_{BBC} = 18 lb-sec/ft (49 percent of critical)

NOTE: An equal and opposite force FBC(2) acts on the bolt-carrier.

A.2.6 FB(6) Locking force, FB(7) Unlocking force

These are constraint forces that act between the bolt and bolt-carrier during locking and unlocking. They are the axial components of the forces needed to rotate the bolt in accordance with the cam path in the bolt-carrier. Two derivations of the force expressions are presented. In the first, the Newtonian approach is used; and in the second, the Lagrangian approach is followed. Finally, an alternate formulation of the problem is discussed.

A.2.6.1 Newtonian approach

Figures 35 illustrates the Newtonian approach to resolving the forces acting between bolt and bolt-carrier during locking and unlocking.

Newtonian approach:

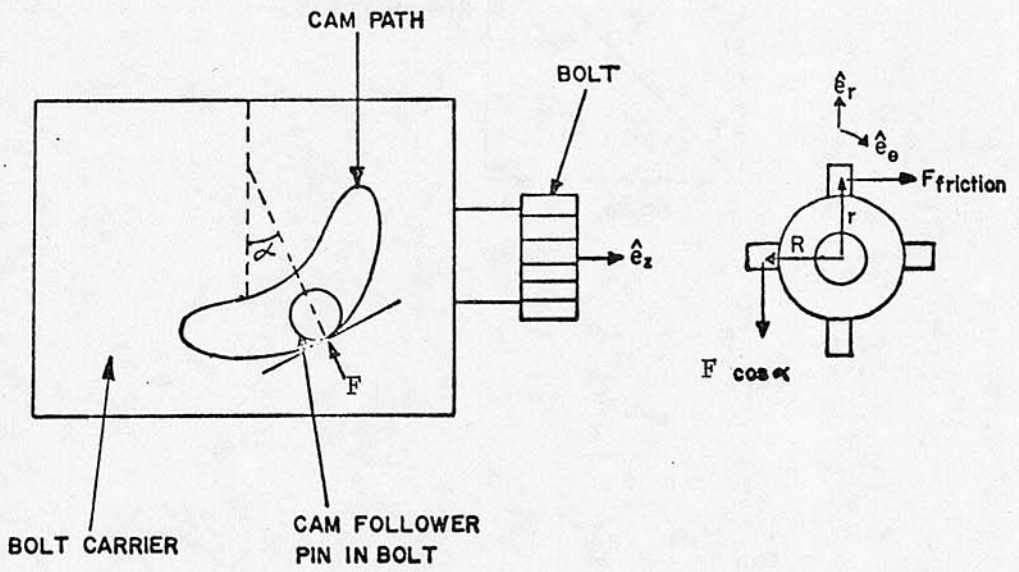

Figure 35 Schematic of Bolt/Bolt-Carrier Interaction during Locking and Unlocking

From Fig. 35, $F \cos \alpha$ = the force that tends to rotate the bolt.

I_B = moment of inertia of bolt about longitudinal axis

$\overrightarrow{N} = \overrightarrow{\dot{L}}$ sum of torques equals rate of change of angular momentum

$$I_B \ddot{\theta}\, \hat{e}_z = r\, \hat{e}_r \times (-F_{friction})\, \hat{e}_\theta + R\, \hat{e}_r \times F \cos \alpha\, \hat{e}_\theta$$

$$I_B \ddot{\theta} = -r F_{friction} + R F \cos \alpha$$

$$F = \frac{I_B \ddot{\theta} + r F_{friction}}{R \cos \alpha}$$

$$FB(6,7) = F \sin \alpha \qquad \text{(A-7)}$$

$$FB(6,7) = \frac{I_B \ddot{\theta} + r F_{friction}}{R \cot \alpha} \qquad \text{(A-8)}$$

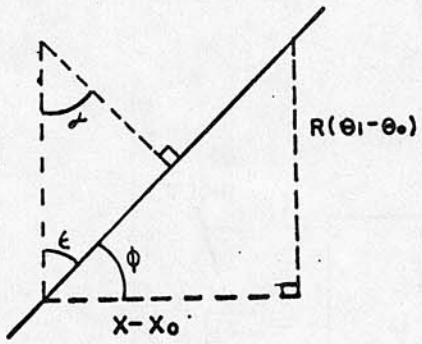

$$\begin{cases} \varepsilon = \frac{\pi}{2} - \phi \\ \alpha + \varepsilon = \frac{\pi}{2} \end{cases}$$

$$\therefore \quad \alpha = \phi$$

$$\phi = \tan^{-1}\left(R \frac{d\theta}{dx} \right)$$

$$FB(6,7) = \frac{I_B \ddot{\theta} + r F_{friction}}{R \cot\left[\tan^{-1}(R\frac{d\theta}{dx})\right]} = \frac{I_B \ddot{\theta} + r F_{friction}}{R} \tan = \left[\tan^{-1}(R\frac{d\theta}{dx})\right] \quad \text{(A-9)}$$

$$FB(6,7) = \frac{d\theta}{dx}\left(I_B \ddot{\theta} + r F_{friction}\right) \quad \text{(A-10)}$$

From the chain rule of differentiation,

$$\ddot{\theta} = \frac{d^2\theta}{dx^2} \dot{X}^2 + \frac{d\theta}{dx} \ddot{x}$$

where

$$X = \left(X_{BC} - X_{BC_o} \right) - \left(X_B - X_{B_o} \right)$$

A.2.6.2 Lagrangian approach

The rotation is assumed to be a linear function of relative position between the bolt and bolt-carrier. For the M16A1 Rifle, this is an accurate assumption.

Let $q_i (i = 1,2, \cdots n)$ represent generalized coordinates.

Let $\sum_{i=1}^{n} a_i \, dq_i = 0$ be the constraint equation.

Let L be the Lagrangian, which is the kinetic energy minus the potential energy of the system.

Let F_i $(i = 1,2, \cdots n)$ represent dissipative forces in the system.

Then $\frac{d}{dt}\left(\frac{\partial L}{\partial \dot{q}_i}\right) - \frac{\partial L}{\partial q_i} = \lambda \, a_i + F_i \qquad i = 1,2, \cdots n$

The constraint forces are $\lambda \, a_i$, where λ is a Lagrangian multiplier. (See, for example, pg 269 of Ref[8])

For the problem at hand, generalized coordinates are the rotation of the bolt, θ, the displacement of the bolt, X_B, and the displacement of the bolt-carrier, X_{BC}.

The constraint equation is then $\theta_B = -.131 + \left[\frac{d\theta_B}{d(X_B - X_{BC})}\right](X_B - X_{BC})$

This equation can be put into the form $\sum_{i=1}^{n} a_i \, dq_i = 0$ as follows:

$$- d\theta_B + \left[\frac{d\theta_B}{d(X_B - X_{BC})}\right] dX_B - \left[\frac{d\theta_B}{d(X_B - X_{BC})}\right] dX_{BC} = 0$$

The Lagrangian is $L = \frac{1}{2} I_B \dot{\theta}_B^2 + \frac{1}{2} M_B \dot{X}_B^2 + \frac{1}{2} M_{BC} \dot{X}_{BC}^2$

Let F_B and F_{BC} be other forces acting on the bolt and bolt-carrier.

The only forces acting on the bolt in the rotational direction are the constraint force and friction.

Substitution into $\frac{d}{dt}\left(\frac{\partial L}{\partial \dot{q}_i}\right) - \frac{\partial L}{\partial q_i} = \lambda \, a_i + F_i$ yields the following

---

[8] Greenwood, D.T., Principles of Dynamics, Prentice-Hall, 1965

three equations of motion:

$$\begin{cases} I_B \ddot{\theta}_B = -\lambda + T_{FRICTION} & \text{(A-11)} \\ M_B \ddot{X}_B = \lambda \dfrac{d\theta_B}{d(X_B - X_{BC})} + F_B & \text{(A-12)} \\ M_{BC} \ddot{X}_{BC} = -\lambda \dfrac{d\theta_B}{d(X_B - X_{BC})} + F_{BC} & \text{(A-13)} \end{cases}$$

$T_{FRICTION}$ is the torsional friction moment due to the compression of the bolt on the base of the cartridge case. This force is assumed to be uniformly distributed over the base.

Let F_N denote the normal force between bolt and case that acts on the bolt. Then

$$T_{FRICTION} = + \int_{r_1}^{r_2} r \mu_c \frac{F_N}{\pi(r_2^2 - r_1^2)} 2\pi r \, dr$$

$$= + \frac{2}{3} \mu_c F_N \frac{r_2^3 - r_1^3}{r_2^2 - r_1^2}$$

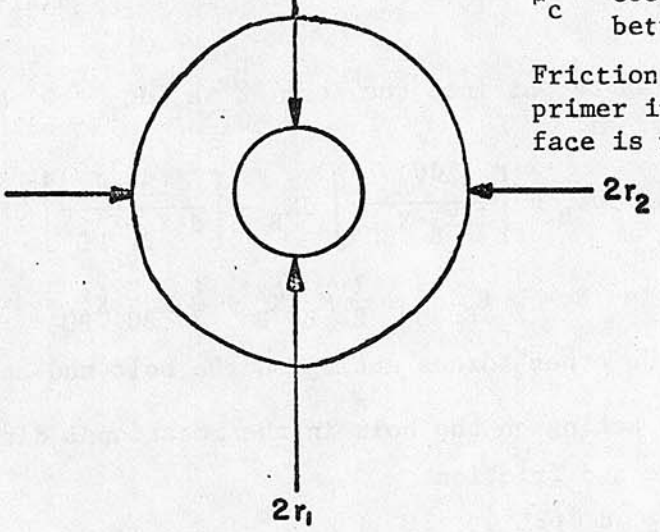

μ_c = coefficient of friction between bolt and case

Friction from portion of primer in contact with bolt face is neglected.

r_1 = radius of primer

r_2 = radius of base of cartridge case

Figure 36 Diagram of Cartridge Case Base

From the first equation of motion, $\lambda = -I_B \left[\frac{d\theta_B}{d(X_B - X_{BC})}\right] (\ddot{X}_B - \ddot{X}_{BC})$ (A-14)

$+ T_{FRICTION}$

$FB(6) = \lambda a_2$ where $a_2 = \frac{d\theta_B}{d(X_B - X_{BC})}$ (A-15)

$$FB(6) = \frac{d\theta_B}{d(X_B - X_{BC})} T_{FRICTION} + I_B \left[\frac{d\theta_B}{d(X_B - X_{BC})}\right]^2 (\ddot{X}_{BC} - \ddot{X}_B) \quad \text{(A-16)}$$

$$FB(6) = + \frac{d\theta_B}{d(X_B - X_{BC})} \left[\frac{2}{3} \mu_c \frac{(r_2^3 - r_1^3)}{(r_2^2 - r_1^2)}\right] F_N + I_B \left[\frac{d\theta_B}{d(X_B - X_{BC})}\right]^2 (\ddot{X}_{BC} - \ddot{X}_B) \quad \text{(A-17)}$$

$= FB(7)$

if $-.0625$ inch $\geq X_{BC} - X_B \geq -X_{LD} = -.25$ inch where X_{LD} is the distance the bolt and bolt-carrier must move relative to each other to achieve locking or unlocking

Nominal values are: $\frac{d\theta_B}{d(X_B - X_{BC})} = 2.09$ radians/inch

$I_B = 10.5 \times 10^{-7}$ slug-ft^2

$r_1 = .0938$ inch

$r_2 = .1875$ inch

$\mu_c = .2$ for FB(6) and 0 for FB(7)

Friction on unlocking is very high because of gas pressure, but is considered insignificant on locking. See Figure 37.

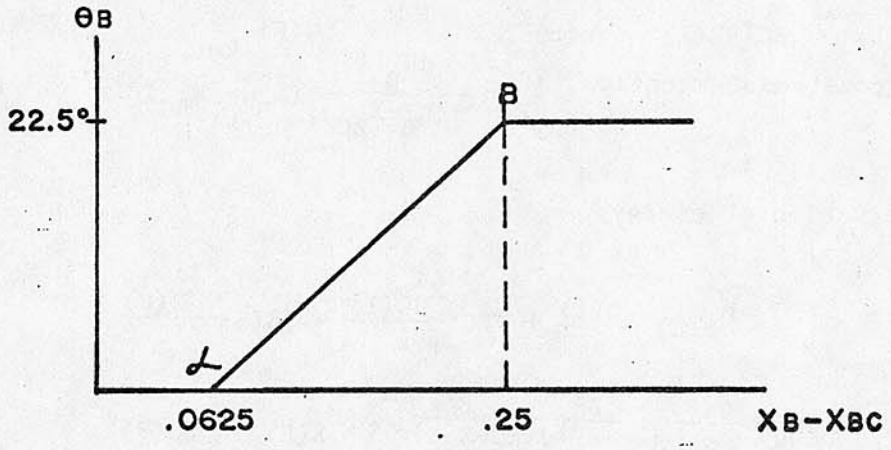

Figure 37 Rotation of Bolt vs Separation Distance Bolt and Bolt-Carrier

Note that θ_B as a function of $X_B - X_{BC}$ is discontinuous in the first derivative just prior to rotation and after rotation is completed. The points of discontinuity are at α and B in Fig. 37. Prior to rotation, $\dot{\theta}_B = 0$; on the other side of the discontinuity, $\dot{\theta}_B = [\frac{d\theta_B}{d(X_B - X_{BC})}] (\dot{X}_B - \dot{X}_{BC})$. This instantaneous change in angular momentum can be considered to be caused by impulsive constraint forces acting between the bolt and bolt-carrier. The instantaneous changes of bolt and bolt-carrier momenta will be computed from conservation of linear momentum and conservation of energy equations. This situation is unlike impact with a spring where a decrease in time interval leads to a smaller jump in force.

Now, make the following definitions:

$M_{B(E)}$ is the effective mass of the bolt when the discontinuity is encountered.

M_{BC} is the mass of the bolt-carrier.

$\dot{X}_{B(I)}$ is the velocity of the bolt prior to the discontinuity.

$\dot{X}_{B(F)}$ is the computed velocity of the bolt after the discontinuity.

$\dot{X}_{BC(I)}$ is the velocity of the bolt-carrier prior to the discontinuity.

$\dot{X}_{BC(F)}$ is the velocity of the bolt-carrier after the discontinuity.

Here, only the case where the bolt begins to unlock will be considered. The other three cases, unlocking completed, beginning of locking, and locking completed, are treated similarly.

From the conservation of linear momentum:

$$M_{B(E)}\dot{X}_{BC(I)} + M_{BC}\dot{X}_{BC(I)} = M_{B(E)}\dot{X}_{B(F)} + M_{BC}\dot{X}_{BC(F)} \tag{A-18}$$

From the constraint equation, $\dot{\theta}_B = \frac{d\theta_B}{d(X_B - X_{BC})} (\dot{X}_B - \dot{X}_{BC})$ (A-19)

and conservation of energy:

$$M_{B(E)} \frac{\dot{X}^2_{B(I)}}{2} + M_{BC} \frac{\dot{X}^2_{BC(I)}}{2} = M_{B(E)} \frac{\dot{X}^2_{B(F)}}{2} + M_{BC} \frac{\dot{X}^2_{BC(F)}}{2} + \frac{I_B}{2} [\frac{d\theta_B}{d(X_B - X_{BC})}]^2 (\dot{X}_{B(F)} - \dot{X}_{BC(F)})^2 \tag{A-20}$$

The variables $\dot{X}_{BC(I)}$ and $\dot{X}_{B(I)}$ are known; and from the conservation of momentum and energy equations, $\dot{X}_{BC(F)}$ and $\dot{X}_{B(F)}$ can be computed. In doing so, one must solve a quadratic algebraic equation and the appropriate sign of the discriminate must be chosen.

In obtaining the accelerations during locking and unlocking, one must solve simultaneously the equations of motion for the bolt and bolt-carrier.

NOTE: Equal and opposite forces, FBS(3) and FBC(5), act on the bolt-carrier.

The inclusion of the analysis of the discontinuity is an important addition. If it is not included, an implicit assumption exists in the remaining analysis that, when unlocking begins, the bolt is already rotating. In reality, a relatively large impulse must be provided to cause the bolt to overcome its initially zero rotational velocity. The value of the force required to accomplish this momentum change depends on the time it is assumed to act. If the change is instantaneous, an infinite force is needed. Another approach is to replace the discontinuity with a smooth curve of small radius. In this analysis, no attempt was made to calculate the force, but the impulse was calculated. In comparing the results of measurements of unlocking force with the computer results, one must remember that what is labeled as unlocking force does not include the force needed to put the bolt into rotation initially.

A.2.6.3 Alternate formulation of the problem

Now, an alternative formulation of the locking and unlocking problem will be discussed. The strong point of the formulation is that it does not require the treatment of discontinuities. It also can be modified to include chatter. In the math model of the XM19 Rifle, Part II of this report, the following approach was used.

F = [Spring Constant] x [Penetration of bolt pin into bolt-carrier cam path in direction perpendicular to cam path surface]

F = K [distance bolt pin moves relative to bolt-carrier C.G. in direction normal to cam path surface minus distance point of contact between bolt pin and cam path moves in direction normal to cam path surface]

$$F = K\,[(X_B - X_{BC} - a)\sin\alpha - R\theta\cos\alpha] \qquad \text{(A-21)}$$

$a = X_B - X_{BC}$ at start of rotation

K = spring constant for hypothetical stiff spring whose location is at the point of contact between cam path and bolt pin

$$I\ddot{\theta} = RF\cos\alpha, \quad \dot{\theta}(0) = \theta(0) = 0 \qquad \text{(A-22)}$$

Solve for θ and substitute in the following equation:

$$FB(6,7) = F\sin\alpha = K[(X_B - X_{BC} - a)\sin\alpha - R\theta\cos\alpha]\sin\alpha \qquad \text{(A-23)}$$

A.2.7 FB(8) Force between bolt and bolt-carrier while weapon is locked

The interface between the bolt and bolt-carrier while the weapon is locked is assumed to be characterized by a stiff spring.

$$FB(8) = -K_{BC}(X_B - X_{BC}) - C_{BC}(\dot{X}_B - \dot{X}_{BC}) \text{ if } X_B - X_{BC} \leq 0 \text{ and } FB(8) \geq 0. \qquad \text{(A-24)}$$

Nominal values are:

K_{BC} = 100,000 lbs/ft

C_{BC} = 37 lb-sec/ft = 45% critical

A.2.8 FB(9) Stripping force used to remove a round of ammo from the magazine

The collision between the bolt and the uppermost round in the magazine is assumed to be inelastic. At impact, a simultaneous change in the mass and velocity of the bolt is assumed to occur. Make the following definitions:

$\dot{X}_{MG(I)}$ is the velocity of the rifle just prior to the collision between bolt and cartridge

$\dot{X}_{B(I)}$ is the velocity of the bolt just prior to the collision between bolt and cartridge

$\dot{X}_{B(F)}$ is the velocity of the bolt just after collision between bolt and cartridge

M_B is the mass of the bolt

M_R is the mass of the cartridge

From conservation of momentum, $M_B\dot{X}_{B(I)} + M_R\dot{X}_{MG(I)} = (M_B + M_R)\dot{X}_{B(F)}$ (A-25)

$$\therefore\ \dot{X}_{B(F)} = \frac{M_B\dot{X}_{B(I)} + M_R\dot{X}_{MG(I)}}{M_B + M_R} \qquad \text{(A-26)}$$

Note that, at the time of collision, the cartridge is considered to be part of the main gun and, therefore, the velocity of the cartridge is assumed to be that of the rifle. Also, at this instant, the effective

mass of the bolt is increased by M_R and the mass of the rifle is decreased by M_R. The foregoing development provides the values for the simultaneous changes in mass and velocity. Now the stripping force itself will be found. Consider the geometry and forces shown in Fig. 38.

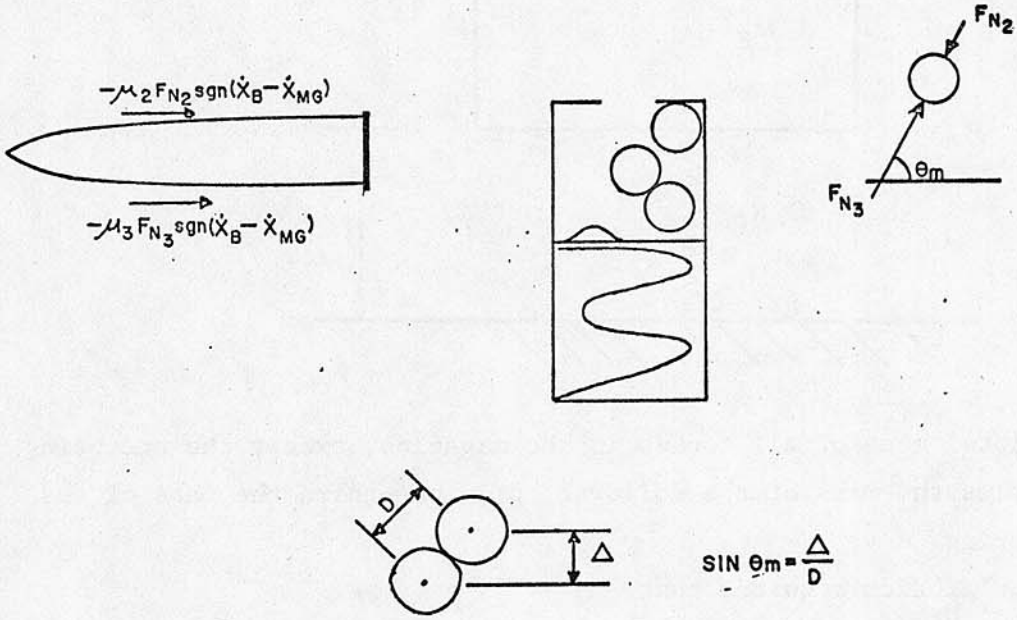

μ_2, μ_3 are coefficients of friction

For vertical equilibrium, $F_{N_2} = F_{N_3}$

Figure 38 Schematic of Magazine

Note that Δ is the displacement of the spring per round of ammo and D is the diameter of the cartridge case. To establish the value of Δ, one divides the difference between the height of the magazine spring when the magazine is full and the height when empty by the round capacity of the magazine.

To continue the analysis, one must compute F_{N_2} and F_{N_3}. Assume that the magazine can be idealized as follows:

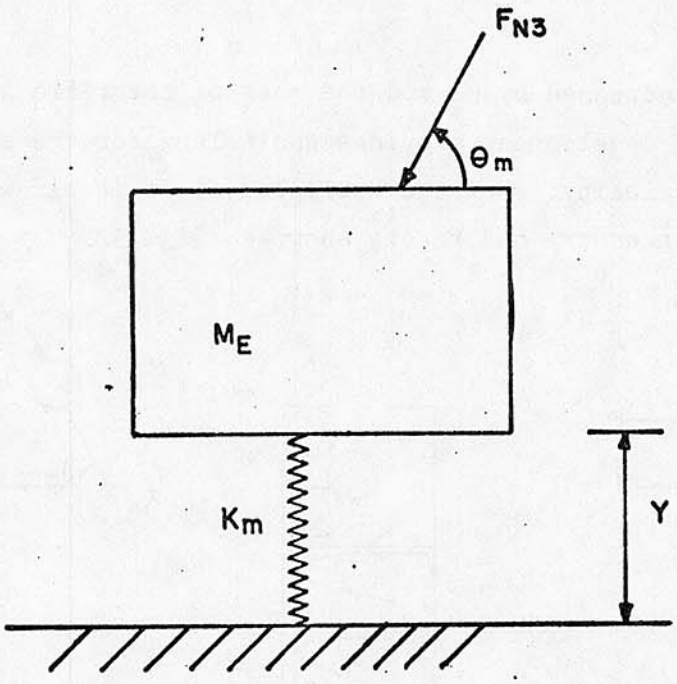

M_E is the total mass of all rounds in the magazine, except the one being stripped, plus the mass of the follower, plus one-third the mass of the magazine spring.

Vertical equilibrium requires that

$$-F_{N_3} \sin \theta_M - M_E g \cos \theta_E - K_M(Y - Y_o) = 0 \qquad \text{(A-27)}$$

The free length of the magazine spring is Y_o, and K_M is the spring constant. The angle of elevation of the rifle is θ_E.

$$F_{N_2} = F_{N_3} = -\frac{1}{\sin\theta_M} [M_E g \cos \theta_E + K_M (Y - Y_o)] \qquad \text{(A-28)}$$

The stripping force is then:

$$FB(9) = \left(\frac{\mu_2 + \mu_3}{\sin\theta_M}\right) [M_E g \cos \theta_E + K_M (Y - Y_o)] \operatorname{sgn} (\dot{X}_B - \dot{X}_{MG}) \qquad \text{(A-29)}$$

This force is nonzero when the weapon is in counterrecoil and $-2.81 \text{ inch} \leq X_B - X_{MG} \leq -1.84 \text{ inch}$.

The parameters that are invariant during the firing of the weapon are Δ, D, $(M_F + \frac{1}{3} M_K)$ (mass of the follower plus 1/3 the mass of the magazine spring), M_R, μ_2, μ_3, K_M and Y_o. After each round is stripped, M_E and Y are recomputed. $Y = Y_E - n\Delta$, where Y_E is height of magazine

spring when magazine is empty, and n is number of rounds in magazine.

Nominal values for the parameters of a twenty-round magazine are:

Δ = .18 in

D = .375 in

$M_F + \frac{1}{3} M_K$ = .03 lb

M_R = .025 lb

μ_2 = .30

μ_3 = .30

K_M = 10.8 lbs/ft

Y_o = 7.77 in

Y_E = 4.5 in

NOTE: An equal and opposite force, FMG(15), acts on the main gun.

A.2.9 FB(10) Force from bolt cavity pressure

This force is caused by the gases in the bolt-carrier cavity. These gases enter the cavity by means of a long tube connected to the gas port on the barrel. This pressure is the main source of energy for weapon actuation. This force can be calculated by the method of matched asymptotic expansions. (See Ref[9]) Finite element methods also show promise for such calculations. (See Ref[7]) For present work, the following nominal values were experimentally obtained for:

$$FB(10) = -P_{CAVITY}(t)\, A_{CAVITY}, \text{ where} \qquad \text{(A-30)}$$

A_{CAVITY} = .1967 in^2.

---

[9]Spurk, J.H., "The Gas Flow in Gas-Operated Weapons," Ballistic Research Laboratories Report No. 1475, Aberdeen Proving Ground, Md. (Feb 1970)

[7]Ehle, P.E. and Rahe, A.E., "Development of a Finite Element Approach for Approximate Analysis of Unsteady Compressible Fluid Flow," WECOM Technical Report, SWERR-TR-72-36, AD 746234, Rock Island, Ill (Jun 1972)

TABLE 9 NOMINAL PRESSURE vs TIME IN BOLT-CARRIER CAVITY

Time (milliseconds	$P_{CAVITY}(t)$ (lb/in^2
0.0	0.0
.264	1250
.528	2500
.792	2650
1.056	2400
1.32	2000
1.584	1500
1.844	1100
2.112	600
2.376	400
2.64	300
2.904	250
3.168	200
3.432	150
3.696	100
3.96	100
4.224	50
4.488	50

The delay between the time that the breech pressure becomes nonzero and the time that the cavity pressure becomes nonzero is $t_{port} + t_{cav}$. Nominal values are t_{port} = 1.1 milliseconds = time required by projectile to reach gas port, and t_{cav} = .2 milliseconds = time required by the pressure wave to travel from the gas port to the bolt cavity.

NOTE: An equal and opposite force FBC(9) acts on the bolt-carrier.

A.2.10 FB(11) Extraction of the cartridge case from the chamber

This force becomes nonzero just after the bolt is unlocked, and the bolt and main gun are again two separate masses. The first problem is that of determining when the bolt becomes separated from the main gun. Once the bolt-carrier reaches the end of the cam path in the unlocking process, the accelerations of the rifle and the bolt

are computed from the following equations:

$$M_{B(E)} \ddot{X}_B = \sum_{i=1}^{K} FB(I) + F_{CON} \tag{A-31}$$

$$M_{MG(E)} \ddot{X}_{MG} = \sum_{i=1}^{n} FMG(I) - F_{CON} \tag{A-32}$$

$$\ddot{X}_B = \ddot{X}_{MG} \tag{A-33}$$

F_{CON} represents the constraint force that causes the bolt and main gun to move together. When this constraint force overcomes the static stiction force between cartridge case and chamber wall, then the bolt and main gun begin to separate. At this point, FB(11) becomes non-zero.

From the three equations given above,

$$F_{CON}\left[\frac{1}{M_{B(E)}} + \frac{1}{M_{MG(E)}}\right] = -\frac{1}{M_{B(E)}} \sum_{i=1}^{K} FB(I) + \frac{1}{M_{MG(E)}} \sum_{i=1}^{n} FMG(I) \tag{A-34}$$

$\therefore$ Separation occurs when

$$\frac{1}{M_{B(E)}+M_{MG(E)}} \left[-M_{MG(E)} \sum_{i=1}^{K} FB(I) + M_{B(I)} \sum_{i=1}^{n} FMG(I) \right] > F_{STICTION} \tag{A-35}$$

Model predictions are very insensitive to reasonable values of $F_{STICTION}$, therefore, $F_{STICTION}$ is set equal to zero. Experimentally, extraction forces have been obtained by placement of a strain gauge on the extractor. Such measurements include the force needed to impart the velocity of the bolt-carrier to the empty cartridge case in addition to the friction force between chamber wall and cartridge case. In the model, the force needed to impart the velocity of the bolt-carrier to the cartridge case is automatically taken into account by the addition of the cartridge case mass to that of the bolt. Thus, to use the experimental data, that component must be removed. The remainder will be an approximation of the friction force between chamber and cartridge case.

Let $\int F_{EXT}\, dt$ be the measured impulse on the extractor, $M_c V_c$ be the momentum of the cartridge case after it acquires the velocity of

the bolt-carrier, and $F_{CHAMBER}$ be the friction force between cartridge case and chamber.

Then $\int F_{EXT}\, dt - \int F_{CHAMBER}\, dt = M_c\,(V_c - V_{c_o})$ (A-36)

Assume $V_{c_o} \simeq 0$ and $V_c \simeq \dot{X}_{MG} - \dot{X}_{BC} = 17$ ft/sec when case assumes bolt-carrier velocity. Further assume V_c is constant in time during extraction. This value for V_c obtained from a computer run is in agreement with Reference[10].

Assume $F_{CHAMBER}$ has the following shape:

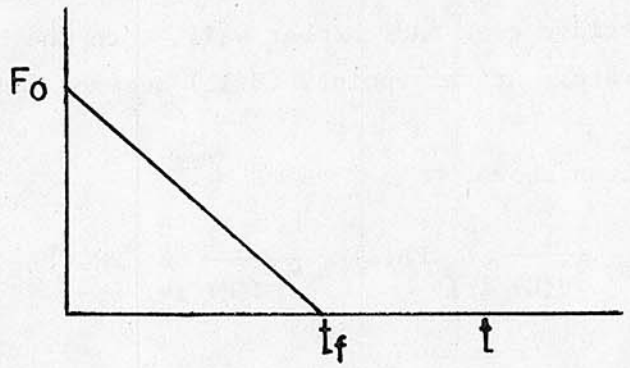

$$F_{CHAMBER} = F_o \frac{t_f - t}{t_f} \qquad t_f = \frac{L}{V_c} \tag{A-37}$$

where L = length of cartridge case.

$$F_{CHAMBER} = F_o \left[\, 1 - \frac{V_c}{L} t \,\right] \tag{A-38}$$

$$\int_o^{t_f} F_{CHAMBER}\, dt = \frac{1}{2} F_o \frac{L}{V_c} \tag{A-39}$$

From Eq. (A-36),

$$\int F_{EXT}\, dt - \frac{1}{2} F_o \frac{L}{V_c} = M_c V_c \tag{A-40}$$

$$F_o = \frac{2V_c}{L} \left[\int F_{EXT}\, dt - M_c V_c \right] \tag{A-41}$$

---

[10] Werner, W.M., "Comparison of a Theoretical and Experimental Study of the Gas System in the M16A1 Rifle," BRL Report No. 1548, Aberdeen Proving Ground, Md., (Aug 1971) Pg 23.

V_c = 17 ft/sec

$\int F_{EXT}\, dt$ = .011 lb/sec

(See WECOM DF, 5 Jun 68, from SWERI-RDT 9280 to AMSWE-RDSR (C.F. Packard), Subject: "M16A1 Test Equipment Instrumentation.")

M_c = .000411 slug

L = 1.75 in

F_o = .94 lb

$$F_{CHAMBER} = FB(11) = F_o \left[1 - \frac{V_c}{L} t \right] \qquad \text{(A-42)}$$

$$FB(11) = .94 \left[1 - 116.6\, t \right]$$

Time is zero when the criterion for separation of bolt and main gun is met.

FB(11) is zero after $t \geq \frac{L}{V_c}$

NOTE: An equal and opposite force FMG(10) acts on the main gun.

A.2.11 FB(12) Gravity force acting on bolt

This force acts continuously.

$$FB(12) = -M_{B(E)}\, g \sin \theta_E \qquad \text{(A-43)}$$

$$g = 32.2 \text{ ft/sec}^2$$

NOTE: $M_{B(E)}$ varies with time.

$M_{B(E)}$ = .156 lb after a new round has been stripped from the magazine, but before round is fired

.143 lb after the round has been fired, but before the case is ejected

.130 lb after the case has been ejected but before a new round is obtained from the magazine

Forces acting on the bolt-carrier

A.2.12 FBC(1) = -FB(4) (See previous derivation)

A.2.13 FBC(2) = -FB(5) (See previous derivation)

A.2.14 FBC(3) = -FB(6) (See previous derivation)

A.2.15 FBC(4) = -FB(8) (See previous derivation)

A.2.16 FBC(5) = -FB(7) (See previous derivation)

A.2.17 FBC(6) Interaction force between buffer tube and bolt-carrier

A hypothetical stiff spring is placed between the buffer tube and the bolt-carrier at their interface.

$$FBC(6) = K_{BUFF}\,(X_{BUFF} - X_{BC}) + C_{BUFF}\,(\dot{X}_{BUFF} - \dot{X}_{BC}) \quad \text{if } FBC(6) \geq 0. \tag{A-44}$$

K_{BUFF} = 100,000 lb/ft

C_{BUFF} = 14.06 lb-sec/ft = 37% critical

NOTE: An equal and opposite force FBUFF(1) acts on the buffer.

A.2.18 FBC(7) Friction force between bolt-carrier and main gun

This force acts continuously.

$$FBC(7) = -C_{BC}\,(\dot{X}_{BC} - \dot{X}_{MG}) - \mu_{BC}(M_{BC} + M_{B(E)})\; g\; [sgn(\dot{X}_{BC} - \dot{X}_{MG})]\; \cos\theta_E \tag{A-45}$$

The first term represents viscous damping, and the second term represents Coulomb friction caused by the weight of the bolt-carrier.

Nominal values are: C_{BC} = .01 lb-sec/ft

μ_{BC} = .2

NOTE: An equal and opposite force FMG(4) acts on the main gun.

A.2.19 FBC(8) Constraint force between hammer and bolt-carrier

This is the force that cocks the hammer. Consider the following diagram where θ is zero when the hammer is fully forward.

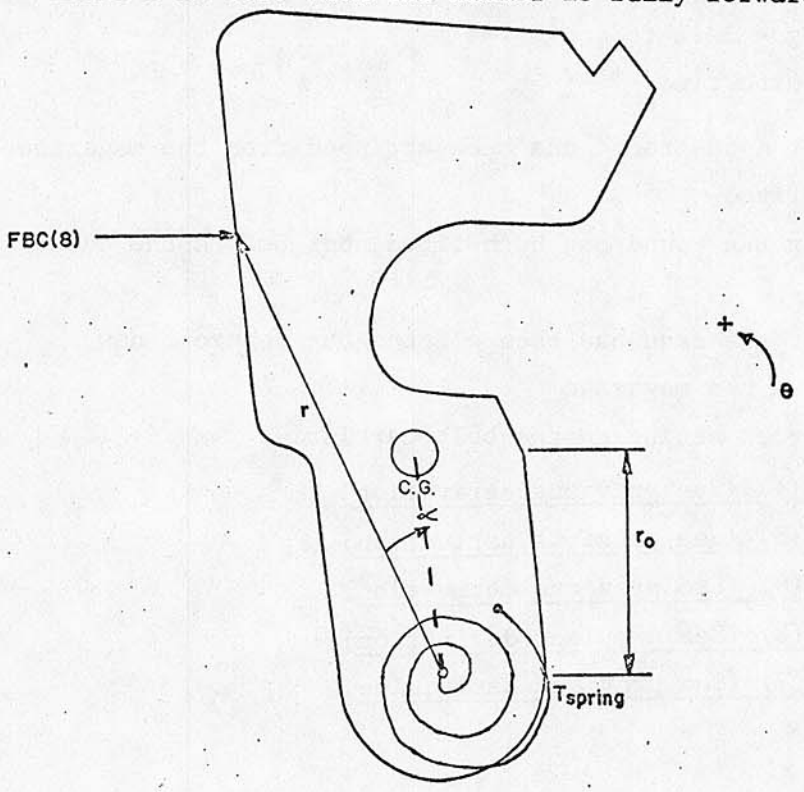

Equating rate of change of angular momentum with the sum of the moments, one finds:

$$I_H \ddot{\theta} = T_{SPRING} - r\ FBC(8) \cos(\theta + \alpha) - M_H[r_o \cos\theta]\ \ddot{X}_{MG} \qquad \text{(A-46)}$$

Ordinarily, in equating rate of change of angular momentum with the sum of moments, one must refer these quantities with respect to a fixed point on the hammer or to the center of mass of the hammer. Although the pivot point on the hammer is not fixed with respect to the ground because the main gun is in motion, reference of angular momentum and moments to this point would be convenient. This can be done if a correction factor is added to account for the motion of the pivot point. This term is $M_H [r_o \cos\theta] \ddot{X}_{MG}$, which is the last term in Equation (A-46). In general, the sum of the moments about an arbitrary point is equal to the vector cross product of the vector from the point to the C.G. and the vector from the body mass times the acceleration of the C.G. with respect to an inertial frame.

That is.

$$\Sigma \vec{M}_P - \dot{\vec{L}}_P = \vec{r}_{\substack{P \\ to \\ CG}} \times m\ddot{\vec{r}}_{CG} \cdot \qquad \text{(A-47)}$$

The truth is that all results derived from Newton's laws of motion relative to an inertial frame can be extended to an accelerating nonrotating frame if inertial forces associated with acceleration of the frame are treated as additional external forces on the system. (See Pg 146 of Ref[8])

NOTE: In Equation (A-46), M_H is the mass of the hammer, and r_o is the distance from the pivot point to the C.G.

I_H is the moment of inertia of the hammer about an axis through the pivot point. T_{SPRING} is the constant torque exerted by the hammer spring.

The constraint equation is given by the functional relation

$$\theta = f\ (X_{MG} - X_{BC}) \qquad \text{(A-48)}$$

whenever the hammer and bolt-carrier are in contact.

---

[8]Greenwood, D.T., Principles of Dynamics, Prentice-Hall, 1965

$$FBC(8) = \frac{T_{SPRING} - I_H\left[\frac{d^2 f}{d(X_{MG}-X_{BC})}(\dot{X}_{MG}-\dot{X}_{BC})^2 + \frac{d f}{d(X_{MG}-X_{BC})}(\ddot{X}_{MG}-\ddot{X}_{BC})\right]}{r \cos (f + \alpha)} \quad \text{(A-49)}$$

Derivations for $f(X_{MG} - X_{BC})$, r, and α will now be given. These are all functions of the angle of rotation of the hammer. First make the following definitions:

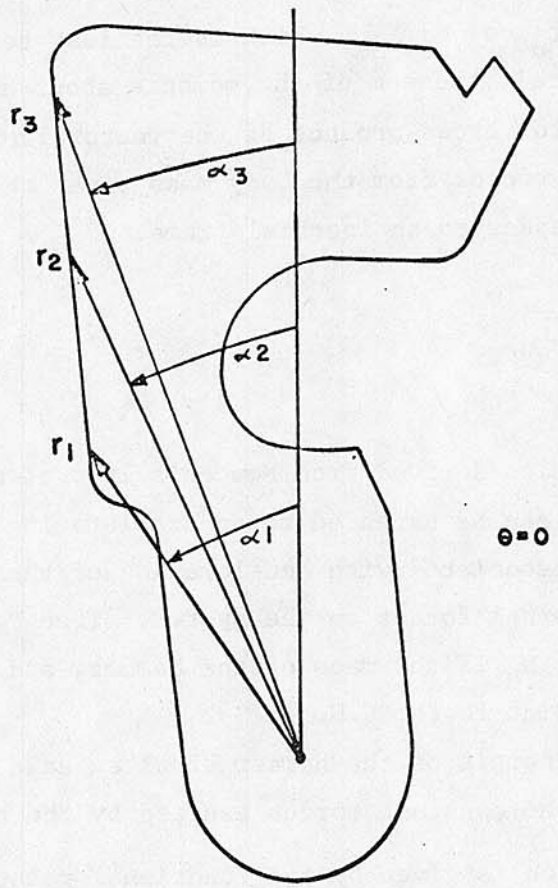

r_1 = radial distance from the pivot point to the point on the hammer that contacts the bolt-carrier when the hammer is in the firing position($\theta = 0$)

r_2 = radial distance from the pivot point to the point on the hammer that contacts the firing pin when $\theta = 0$.

r_3 = radial distance from the pivot point to the highest point on the hammer that ever contacts the bolt-carrier (occurs when $\theta = 77°$)

α_1, α_2, and α_3 are the corresponding angles $\theta = 0$.

r = radial distance from the pivot point to the point on the hammer in contact with the bolt-carrier for any position of the bolt-carrier

α = angle between r and a line imbedded in the hammer that passes through the pivot point and is perpendicular to the bore axis when $\theta = 0$.

Note that the line joining points on the hammer that contact the bolt-carrier lie in a straight vertical line when $\theta = 0$. Using this fact, one can solve for θ as a function of $X_{MG} - X_{BC}$. Consider the following diagram:

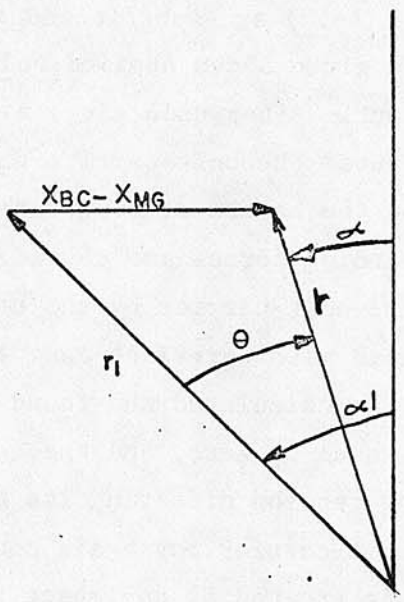

$$X_{BC} - X_{MG} = -r_1 \sin \alpha_1 + \tan (\alpha_1 + \theta) \, r_1 \cos \alpha_1 \qquad \text{(A-50)}$$

$$\theta = -\alpha_1 + \tan^{-1} \left[\frac{r_1 \sin \alpha_1 + (X_{BC} - X_{MG})}{r_1 \cos \alpha_1} \right] \qquad \text{(A-51)}$$

$$\therefore \; f\,(X_{MG} - X_{BC}) = -\alpha_1 + \tan^{-1} \left[\frac{r_1 \sin \alpha_1 + (X_{BC} - X_{MG})}{r_1 \cos \alpha_1} \right] \qquad \text{(A-52)}$$

This relationship applies only if $\theta \geq -70°$ because, after a 70° rotation, the hammer motion is determined by the geometry of the underside of the bolt-carrier.

From the previous diagram, one can also find r.

$$r = [(r_1 \cos \alpha_1)^2 + (r_1 \sin \alpha_1 + X_{BC} - X_{MG})^2]^{\frac{1}{2}} \qquad \text{(A-53)}$$

One can solve for α using the fact that the distance is constant from any point on the hammer contacting the bolt-carrier to the line through the pivot point imbedded in the hammer.

Thus, $r_1 \sin \alpha_1 = r \sin \alpha.$ (A-54)

$$\alpha = \sin^{-1} \left(\frac{r_1 \sin \alpha_1}{r} \right) \qquad \text{(A-55)}$$

Equations (A-51),(A-53), and (A-55) are substituted in Equation (A-49).

Note that the derivation given above applied only while the hammer and bolt-carrier are in contact. After unlocking, a series of forces acting on the bolt-carrier causes the bolt-carrier velocity to fall below that of the hammer, and the hammer continues rearward apart from the bolt-carrier. These retarding forces are caused by the strike of the end of the cam path in the bolt-carrier by the bolt pin, and they are caused by forces associated with cartridge case extraction. This situation occurs when FBC(8) is calculated and found to be a negative number. Then FBC(8) is set equal to zero, and the hammer continues rearward with only the spring tension affecting its motion. At a later time, the hammer and bolt-carrier may again come in contact with each other. This encounter is treated as an impact problem where a hypothetical spring and damper are assumed to come between the two bodies. Thus, $FBC(8) = K_H \cos \theta \, [\theta - f(X_{MG} - X_{BC})]$

$$+ C_H \cos \theta \, [\dot{\theta} - f\,(X_{MG} - X_{BC})(\dot{X}_{BC} - \dot{X}_{MG})] \qquad \text{(A-56)}$$

if

$$\theta > f\ (X_{MG} - X_{BC}).$$

Once the hammer reaches 77° or if f $(X_{MG} - X_{BC}) < 70°$ and $\dot{\theta} > 0$, the hammer angular velocity and acceleration are set to zero. Thus, constrained motion from 70° to 77° is not treated in detail. To do so requires accounting for the slope cut in the underside of the bolt-carrier. This small distance is of little consequence to the model and the effort required for accurate treatment would not be worthwhile. Note that the full 77° rotation is fully treated if the hammer is not in contact with the bolt-carrier after 70°. Very little interaction occurs between the bolt-carrier and the hammer after 70°. Most of this interaction is due to friction, and this force is included in the model.

Nominal values are:

$r_1 = 1.08$ in
$r_2 = 1.33$ in
$r_3 = 1.58$ in
$r_o = .75$ in
$M_H = .0683$ lb
$\alpha_1 = 22°$
$\alpha_2 = 17.5°$
$\alpha_3 = 15°$
$K_H = 4500$ lb/rad
$C_H = .086$ lb-sec/rad
$I_H = .00002$ slug-ft^2
$T_{SPRING} = 6$ in-lb

FBC(8) becomes nonzero when the bolt-carrier cavity pressure is nonzero, $\dot{X}_{MG} - \dot{X}_{BC} \geq 0$, and $X_{MG} - X_{BC} \geq 0$.

A.2.20 FBC(9) = -FB(10) (See previous derivation)

A.2.21 FBC(10) Friction between bolt-carrier and cartridge case

This force is caused by friction between the bolt-carrier and the uppermost cartridge in the magazine. The bolt-carrier depresses the cartridge a small amount. The situation is depicted schematically in the following diagram:

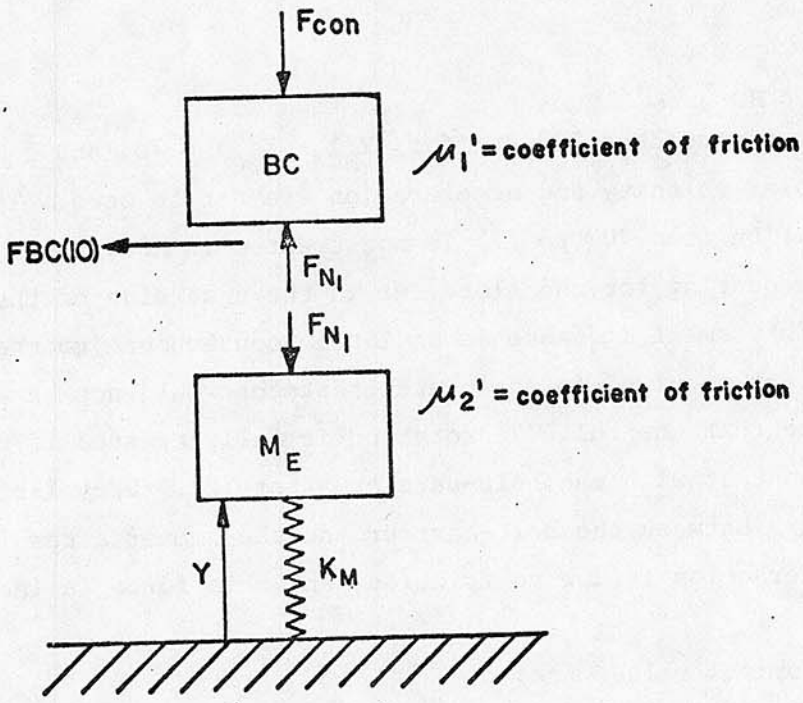

F_{CON} is the constraint force that ensures vertical equilibrium of the bolt-carrier. $M_E = kM_R + M_F + M_S/3$ (A-57)

where

k is the number of rounds in the magazine

M_F is the mass of the magazine follower

and M_S is the mass of the magazine spring.

For vertical equilibrium of the bolt-carrier,

$$F_{CON} = F_{N_1} \tag{A-58}$$

$$FBC(10) = -2\mu_1 F_{N_1} \operatorname{sgn}(\dot{X}_{BC} - \dot{X}_{MG}) \tag{A-59}$$

where

$2\mu_1 \equiv \mu_1^1 + \mu_2^1$ = twice the average coefficient of friction.

Now F_{N_1} must be determined. For vertical equilibrium of the ammunition,

$$-F_{N_1} - M_E g - K_M (Y - Y_o) = 0. \tag{A-60}$$

Y_o is the free length of the magazine spring. Y is the length of the magazine spring at any time.

$$\therefore \quad FBC(10) = 2\mu_1 \left[M_E g + k_M (Y - Y_o)\right] \operatorname{sgn} (\dot{X}_{BC} - \dot{X}_{MG}) \qquad \text{(A-61)}$$

One can determine exactly when the ammunition is in contact with the bolt-carrier. A number of milliseconds are required for the round just below the one being stripped to move upward into position. A derivation of the proper expression is on pg 7-5 of the "Engineering Design Handbook," Guns Series, Automatic Weapons, AMCP 706-260.

This expression is: $$t_{DELAY} = \sqrt{\frac{M_E}{\varepsilon K_M}} \cos^{-1}\left(\frac{F_o}{F_M}\right). \qquad \text{(A-62)}$$

F_M is the maximum spring force (preceding one cartridge displacement), and F_o is the minimum spring force (following one cartridge displacement). The efficiency of the system is ε and is assumed to be 1.0. If k is the number of rounds in the magazine, Δ is the displacement per round, and Y_o is the length of the magazine spring when the magazine is empty, then

$$F_o = -K_M(Y_e - k\,\Delta - Y_o) \quad \text{where } Y_e = \text{current length} \qquad \text{(A-63)}$$

and

$$F_M = -K_M(Y_e - (k+1)\,\Delta - Y_o). \qquad \text{(A-64)}$$

In summary, FBC(10) is nonzero when $X_{MG} - X_{BC} \geq 2.34$ inches and $t - t_{PICK} \geq t_{DELAY}$ where t_{PICK} is the time at which the topmost round is completely stripped from the magazine.

NOTE: An equal and opposite force FMG(12) acts on the main gun.

A.2.22 FBC(11) Friction between bolt-carrier and hammer

The bolt-carrier slides over the hammer after the hammer is fully cocked. Consider Figure 39 :

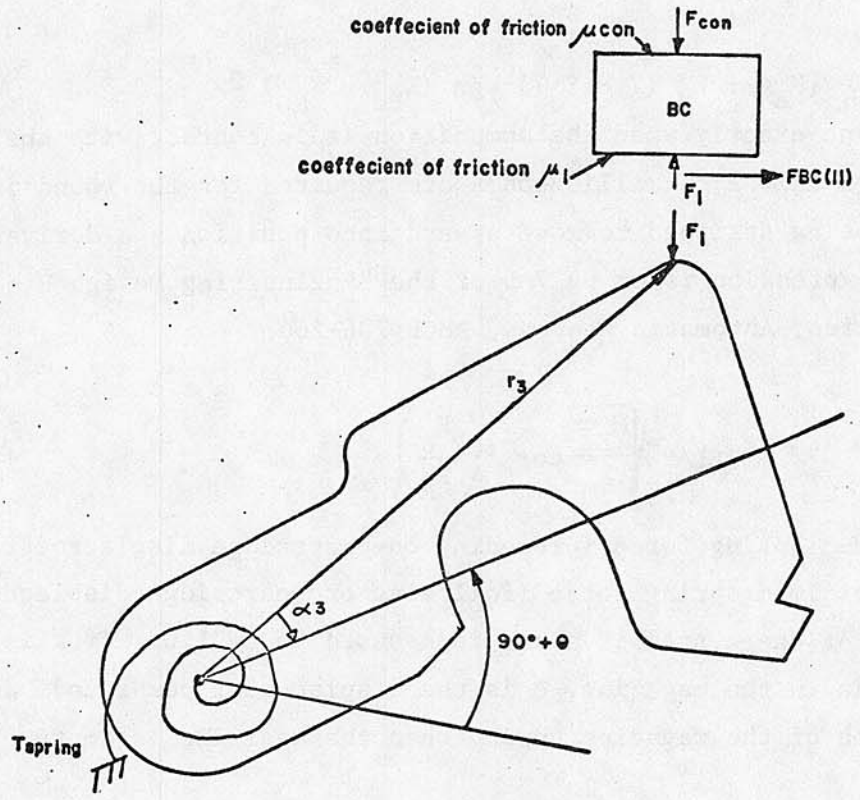

Figure 39 Schematic of Hammer - Bolt-Carrier Interaction

The constraint force F_1 that acts between the hammer and the bolt-carrier can be computed based on the assumption of rotational equilibrium. Equating moments, one finds that

$$T_{SPRING} = -F_1 \, r_3 \cos \alpha_3 \sin \theta \qquad \text{(A-65)}$$

$$\therefore \quad F_1 = - \frac{T_{SPRING}}{r_3 \cos\alpha_3 \sin\theta} \qquad \text{(A-66)}$$

$$FBC(11) = - [\mu_{CON} F_{CON} + \mu_1 F_1] \operatorname{sgn} (\dot{X}_{BC} - \dot{X}_{MG}) \qquad \text{(A-67)}$$

$$\text{Let } \mu_{eff} \equiv \frac{\mu_{CON}+\mu_1}{2}$$

Vertical equilibrium of the bolt-carrier requires that $F_{CON} = F_1$

$$FBC(11) = + 2 \, \mu_{eff} \frac{T_{SPRING}}{r_3 \cos\alpha_3 \sin\theta} \operatorname{sgn} (\dot{X}_{BC} - \dot{X}_{MG}) \qquad \text{(A-68)}$$

This force is nonzero only if the hammer is in rotational equilibrium, that is: $X_{MG} - X_{BC} \geq 1.36$ inches, and $\dot{\theta} = \ddot{\theta} = 0$. $\mu_{eff} = .15$.

NOTE: An equal and opposite force FMG(13) acts on the main gun.

A.2.23 FBC(12) Gravity force acting on the bolt-carrier

This force acts continuously. The angle of elevation is θ_E.

$$FBC(12) = -M_{BC} g \sin \theta_E \qquad \text{(A-69)}$$

$$M_{BC} = .0182 \text{ slug}$$

$$g = 32.2 \text{ ft/sec}^2$$

Forces Acting on Main Gun

A.2.24 FMG(1) Mount force

This is the force exerted by the shooter's shoulder acting on the butt of the weapon. Efforts are in progress to join the M16 Rifle mechanism model with a mechanical model of the shooter. Meanwhile, a simple spring-dashpot system will be used. Another approach by which FMG(1) is represented as a function of position, velocity, and acceleration, is detailed on Pg 44 of Ref[7].

$$FMG(1) = - K_{MOUNT} X_{MG} - C_{MOUNT} \dot{X}_{MG} \qquad \text{(A-70)}$$

where nominal values are:

$$K_{MOUNT} = 300 \text{ lb/ft}$$

$$C_{MOUNT} = 9.53 \text{ lb-sec/ft}$$

A.2.25 FMG(2) = -FB(2) (See previous derivation)

A.2.26 FMG(3) = -FB(3) (See previous derivation)

A.2.27 FMG(4) = -FBC(7) (See previous derivation)

A.2.28 FMG(5) = Drive spring force

This force acts continuously. It serves to retard the bolt-carrier on the recoil stroke and to provide energy for stripping and locking on the counterrecoil stroke.

The simplest model is based on the assumption that the drive spring is a massless, linear spring through which elastic waves travel with infinite velocity. One step higher in sophistication is the treatment of

---

[7]Ehle, P.E. and Rahe, A.E., "Development of a Finite Element Approach for Approximate Analysis of Unsteady Compressible Fluid Flow," WECOM Technical Report, SWERR-TR-72-36, AD 746234, Rock Island, Ill (Jun 1972)

mass effects by the addition of one-third the spring mass to the buffer tube. The reasoning behind this approach is discussed at the end of Appendix C. Further sophistication can be achieved by either continuum or finite-element approaches. Incorporated in the M16 Rifle model is a finite-element approach by which the spring is divided into a series of point masses and ideal springs. The program allows for a maximum of ten elements, and as few as two elements can be used to obtain reasonable results. A further step in sophistication can be taken by the division of the spring into a large number of elements and by the detailed treatment of coil clashing. This approach is discussed in Appendix C. However, since running time is significantly increased, this model is not used unless a special study of the spring itself is desired. The analysis for the small number of masses normally used in the model closely follows the analysis for the large number of masses given in Appendix C.

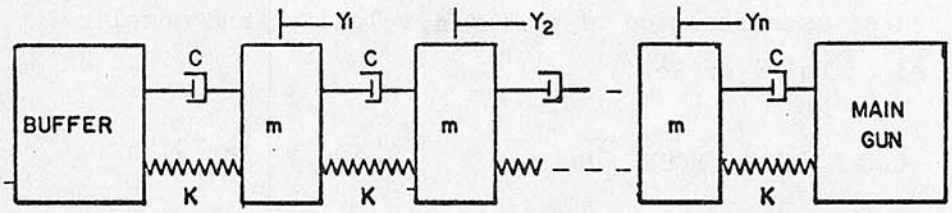

Figure 40 Finite-Element Model of Drive Spring

$$FMG(5) = -K(X_{MG} - Y_n) - C(\dot{X}_{MG} - \dot{Y}_n) - \beta K_5 \qquad \text{(A-71)}$$

where

β = preload distance = .337 ft

K = element spring constant = K_5 (n+1)

$m = m_s/n$

K_5 = drive spring constant = 19.2 lb/ft

m_s = mass of drive spring = .1336 lb

n = number of elements into which the drive spring is divided, n = 5 normally, but can be up to 10

C = .01 lb-sec/ft

NOTE: Under static conditions, an equal and opposite force FBUFF(3) acts on the buffer.

A.2.29 FMG(6) Bore Friction

This force is caused by friction between the bullet and the bore as the projectile travels along the length of the barrel. To experimentally obtain values for this force, a bullet was pushed down the barrel at about two inches per second. A steel rod actually pushed the bullet, and the rod was pushed by a machine normally used to obtain load versus deflection curves for springs. Certainly, numbers obtained at such a low speed are questionable. However, the impulse represented by the force obtained is in good agreement with values obtained at BRL. This impulse is roughly 17 percent of the impulse of the breech pressure curve. Thus, for small caliber weapons, this force appears to be rather important; and efforts should be made to obtain more accurate numbers. The values used are:

TABLE 10 BORE FRICTION vs TIME

Time (sec)	FMG(6) (lb)
0	210
.0001	325
.0002	295
.0003	265
.0004	240
.0005	210
.0006	180
.0007	155
.0008	125
.0009	100
.0010	70
.0011	40
.0012	20
.0013	0

A.2.30 FMG(7) Impact between hammer and main gun

This is the force that the hammer exerts on the main gun at the time of firing. It includes the strike of the firing pin, the impact of the firing pin with a spring-like primer, and the final strike of the hammer on the main gun itself. This final strike causes all rotational motion to cease. The entire force is treated as an effective inelastic collision between the hammer and the main gun. If, just after impact, the hammer tends to bounce back and to rotate rearward, its velocity and acceleration are set to zero until the bolt-carrier begins to move rearward.

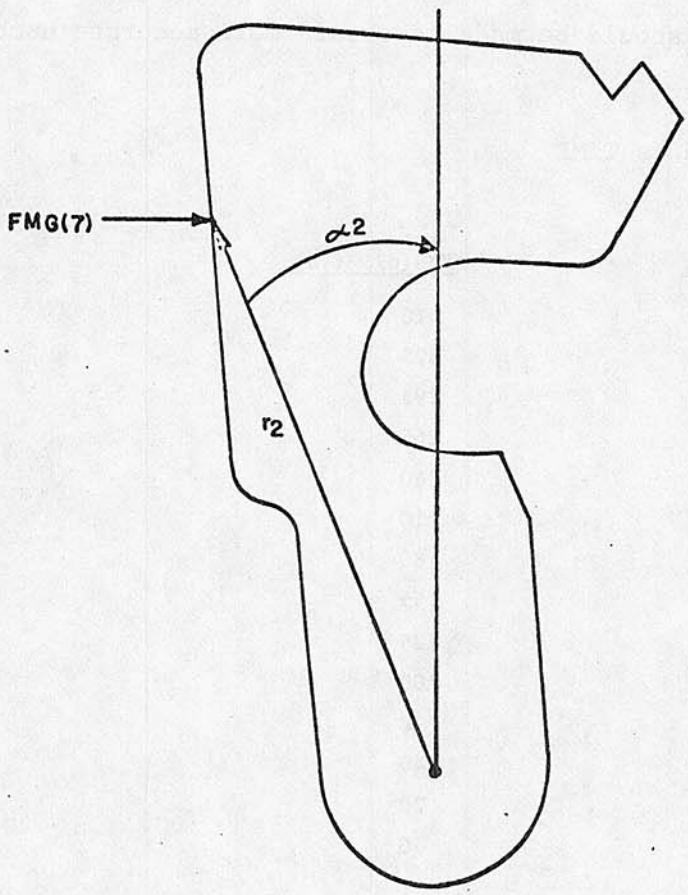

$$FMG(7) = K_H r_2 \sin\theta + C_H r_2 \dot{\theta} \cos\theta \qquad \text{(A-72)}$$

Nominal values are : $K_H = 50000$ lb/ft

$C_H = .278$ lb-sec/ft

This force is nonzero only if $\theta > 0$ and $\dot{\theta} > 0$.

NOTE: An equal and opposite force FHAM(2) acts on the hammer.

A.2.31 FMG(8) Constraint force between hammer and main gun

This force acts at the pivot point of the hammer. Consider the following diagram and write the equation of motion of the hammer in the horizontal direction.

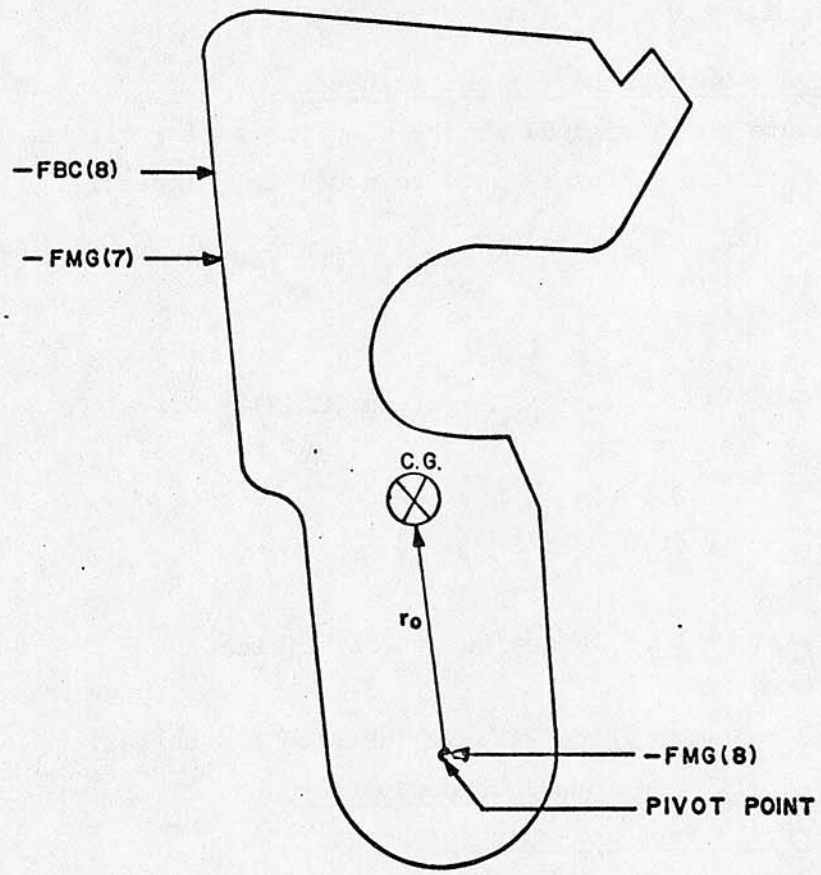

$$M_H \ddot{X}_H = -FMG(7) - FBC(8) - FMG(8) \quad \text{(A-73)}$$

$$\therefore FMG(8) = -[M_H \ddot{X}_H + FMG(7) + FBC(8)] \quad \text{(A-74)}$$

M_H = mass of hammer

$\ddot{X}_H$ = acceleration of the center of gravity of the hammer

The following constraint condition exists between the main gun and the hammer.

$$X_H = r_o \sin\theta + X_{MG} + \gamma \quad \text{where } \gamma \text{ is some constant} \quad \text{(A-75)}$$

$$\therefore \ddot{X}_H = r_o [\ddot{\theta} \cos\theta - \dot{\theta}^2 \sin\theta] + \ddot{X}_{MG} \quad \text{(A-76)}$$

$$\therefore FMG(8) = -M_H [r_o(\ddot{\theta} \cos\theta - \dot{\theta}^2 \sin\theta) + \ddot{X}_{MG}] - FMG(7) - FBC(8) \quad \text{(A-77)}$$

FMG(7) and FBC(8) are defined elsewhere in this report.

Nominal values are M_H = .0683 lb and r_o = .75 in

A.2.32 FMG(9) Impact between buffer and main gun

This force occurs on the recoil stroke when the buffer strikes the backplate. A hypothetical spring is used to model this impact.

$$FMG(9) = -K_{\substack{BACK \\ PLATE}} (X_{MG} - X_{BUFF} - \alpha) - C_{\substack{BACK \\ PLATE}} (\dot{X}_{MG} - \dot{X}_{BUFF}) \quad \text{(A-78)}$$

This force is nonzero if: $X_{MG} - X_{BUFF} \geq \alpha$ and $FMG(9) < 0$.

Nominal values are:

α = 3.80 in

$K_{\substack{BACK \\ PLATE}}$ = 60,000 lb/ft

$C_{\substack{BACK \\ PLATE}}$ = 10.8 lb-sec/ft = 40% critical

NOTE: An equal and opposite force FBUFF(2) acts on the buffer.

A.2.33 FMG(10) = -FB(11) (See previous derivation)

A.2.34 FMG(11) Gravity force on main gun

$$FMG(11) = -M_{MG} g \sin\theta_E \quad \text{(A-79)}$$

θ_E = angle of elevation of the gun

M_{MG} is a function of the number of rounds in the magazine. With no ammunition, M_{MG} = 5.84 lb

A.2.35 FMG(12) = -FBC(10) (See previous derivation)

A.2.36 FMG(13) = -FBC(11) (See previous derivation)

A.2.37 FMG(14) Friction between buffer and main gun

A combination of Coulomb friction and viscous damping was assumed.

$$FMG(14) = -\mu_{BUFF}\,(M_{BUFF} + M_{TOTAL})\cos\theta_E\ \text{sgn}\ (\dot{X}_{MG}-\dot{X}_{BUFF}) - C_{BUFF}(\dot{X}_{MG}-\dot{X}_{BUFF}) \quad \text{(A-80)}$$

M_{TOTAL} = mass of buffer weights = .224 lb

M_{BUFF} = effective mass of buffer tube = .146 lb (Includes $\frac{1}{3}$ mass of drive spring)

μ_{BUFF} = .2

C_{BUFF} = .01 lb-sec/ft

Forces Acting on the Buffer

A.2.38 FBUFF(1) = -FBC(6) (See previous derivation)

A.2.39 FBUFF(2) = -FMG(9) (See previous derivation)

A.2.40 FBUFF(3) Force from drive spring acting on buffer

$$FBUFF(3) = -K(X_{BUFF} - Y_1) - C(\dot{X}_{BUFF} - \dot{Y}_1) + \beta K_5 \quad \text{(A-81)}$$

See derivation of FMG(5)

A.2.41 FBUFF(4) Gravity force on buffer tube

This force acts continuously.

$$FBUFF(4) = -M_{BUFF} g \sin\theta_E \quad \text{(A-82)}$$

θ_E is the angle of elevation of the rifle

M_{BUFF} is the mass of the buffer tube.

A.2.42 FBUFF(5) Total buffer tube interaction with buffer weights.

This force arises from friction and from impact between the buffer tube and the end weights. Two methods of treating this force are presented. The first assumes that all the buffer weights are lumped together as a single mass. The second provides each mass with a separate degree of freedom.

LUMPED MASSES:

Consider the following idealization in Figure 41.

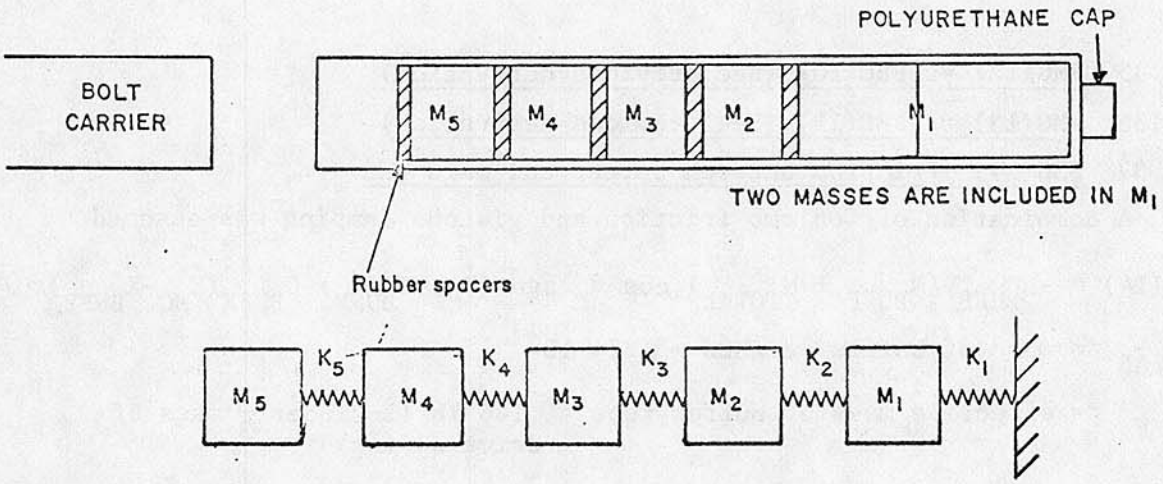

Figure 41 Schematic of Buffer Assembly

The equations of motion are:

$$M_1 \ddot{X}_1 = -K_1 X_1 + K_2 (X_2 - X_1)$$
$$M_2 \ddot{X}_2 = -K_2 (X_2 - X_1) + K_3 (X_3 - X_2)$$
$$M_3 \ddot{X}_3 = -K_3 (X_3 - X_2) + K_4 (X_4 - X_3)$$
$$M_4 \ddot{X}_4 = -K_4 (X_4 - X_3) + K_5 (X_5 - X_4)$$
$$M_5 \ddot{X}_5 = -K_5 (X_5 - X_4)$$

What is now sought is an effective spring constant for the following lumped system:

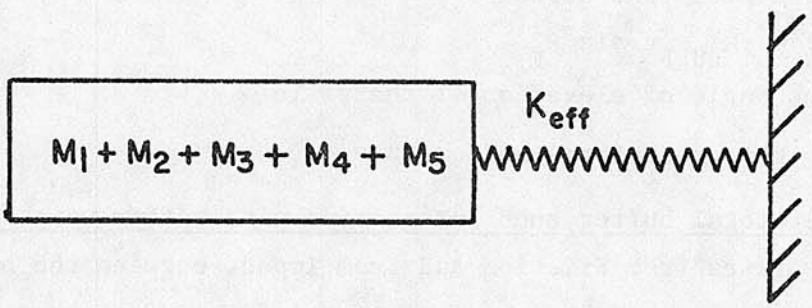

This effective spring constant will be chosen first by computation of lowest natural frequency of the five-mass system, and then by calculation of $K_{eff} = M_{TOTAL}\, \omega^2_{MIN}$. M_{TOTAL} is the total mass of the weights and spacers. ω_{MIN} is the lowest natural frequency, and K_{eff} is the effective spring constant of the system.

Now compute the lowest natural frequency. The equations of motion given above can be rewritten in matrix form as: $M\ddot{X} + KX = 0.$ (A-83)

$$M = \begin{bmatrix} M & 0 & 0 & 0 & 0 \\ 0^1 & M & 0 & 0 & 0 \\ 0 & 0^2 & M & 0 & 0 \\ 0 & 0 & 0^3 & M & 0 \\ 0 & 0 & 0 & 0^4 & M_5 \end{bmatrix} \quad \text{(A-84)}$$

$$K = \begin{bmatrix} K_1+K_2 & -K_2 & 0 & 0 & 0 \\ -K_2 & K_2+K_3 & -K_3 & 0 & 0 \\ 0 & -K_3 & K_3+K_4 & -K_4 & 0 \\ 0 & 0 & -K_4 & K_4+K_5 & -K_5 \\ 0 & 0 & 0 & -K_4 & K_5 \end{bmatrix} \quad \text{(A-85)}$$

$$X = (X_1, X_2, X_3, X_4, X_5)^T \quad \text{(A-86)}$$

Assume the following solution to the matrix equations: $X = X_o \sin \omega t$
Substitution into the equation then yields $\omega^2 MX_o = KX_o$

Let $\lambda \equiv \frac{1}{\omega^2}$. Then $\lambda X_o = K^{-1} M X_o$. The solution of this matrix equation is an eigenvalue problem. The largest eigenvalue λ_{MAX}, which corresponds to ω_{MIN}, is obtained by a standard numerical technique known as the power method. Then $K_{eff} = \frac{M_{TOTAL}}{\lambda_{MAX}}$. For purposes of calculation, all springs are assumed to act simultaneously. When the masses strike the forward end of the buffer body, $m_1 = m_2 = m_3 = m_4 = .0406$ lb, $m_5 = .0615$ lb, $K_1 = K_2 = K_3 = K_4 = K_5 = K_6 = 60{,}000$ lb/ft

Then

$\omega_{MIN} = 1801$ cps, and $K_{eff}^{(F)} = 22{,}567$ lb/ft.

When the masses strike the rearward end of the buffer tube, $m_1 = .0615$ lb, $m_2 = m_3 = m_4 = m_5 = .0406$ lb, $K_1 = K_2 = K_3 = K_4 = K_5 = 60{,}000$ lb/ft.

Then

$\omega_{MIN} = 1944$ cps, and $K_{eff}^{(R)} = 26{,}405$ lb/ft

Let X_{WTS} denote the position of the center of mass of the buffer masses. X_{WTS} is zero when the weights are fully forward. The following friction force exists between the buffer masses and the buffer tube:

$$F_{FRICTION} = -\mu_{WTS} M_{TOTAL} g \cos \theta_E \text{ sgn } (\dot{X}_{WTS} - \dot{X}_{BUFF})$$

μ_{WTS} is the coefficient of friction and θ_E is the angle of elevation of the rifle.

Let superscripts (R) and (F) denote rearward and forward impact, respectively.

Let X_s denote the total amount of play between the buffer weights and the ends of the buffer tube.

Then

$$FBUFF(5) = F_{FRICTION} + K_{eff}^{(F)} (X_{WTS} - X_{BUFF}) + C_{eff}^{(F)} (\dot{X}_{WTS} - \dot{X}_{BUFF}) \quad \text{(A-87)}$$

If $X_{WTS} - X_{BUFF} \geq 0$

$$FBUFF(5) = F_{FRICTION} + K_{eff}^{(R)} (X_{WTS} - X_{BUFF} + X_s) + C_{eff}^{(R)} (\dot{X}_{WTS} - \dot{X}_{BUFF}) \quad \text{(A-88)}$$

If $X_{WTS} - X_{BUFF} \leq -X_s$

$X_s = .13$ in

Nominal values are: $\mu_{WTS} = .2$

$C_{eff}^{(F)} = 6.44$ lb-sec/ft = 33% critical

$C_{eff}^{(R)} = 7.56$ lb-sec/ft = 33% critical

In the solution of the equations of motion involving X_{WTS}, the force acting on the lumped mass is then

$$F_{WTS} = -FBUFF(5) - M_{TOTAL} g \sin \theta_E$$

This lumped mass approach appears as an option in the computer program.

Individual Masses

In this approach, the motion of each mass must be considered to predict the motions of the end masses, by which the force input to the buffer body is controlled. Five systems, each consisting of a mass and a rubber spacer, are assumed to be free to move within the buffer body. These systems are not joined to each other as in the case of the lumped-mass analysis. Schematically, each system is idealized as:

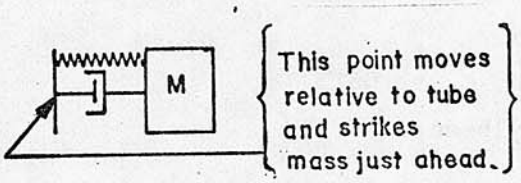

and appears in the buffer body as shown in Figure 42.

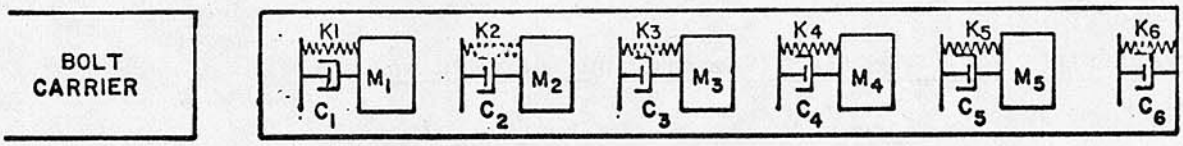

Figure 42 Schematic of Buffer Model

In this idealization, the metal spacer in the body is assumed to be joined to one of the buffer weights. Six masses could be used if a very stiff spring were assumed to act between this metal spacer and the adjacent buffer weight. However, the stiff spring would require the use of a very small integration interval, and the slight increase in realism would not be worth the increase in computation time.

The buffer weights also exert force on the buffer tube through friction. The total force on the tube from the weights is then:

$$FBUFF(5) = + \sum_{i=1}^{5} \mu_i M_i g \, sgn(\dot{X}_i - \dot{X}_{BUFF}) \cos \theta_E + K_1 (X_1 - X_{BUFF}) + C_1 (\dot{X}_1 - \dot{X}_{BUFF}) \quad \text{(A-89)}$$

If $X_1 - X_{BUFF} \geq 0$

$$FBUFF(5) = - \sum_{i=1}^{5} \mu_i M_i g \, sgn(\dot{X}_i - \dot{X}_{BUFF}) \cos \theta_E + K_6 (X_5 - X_{BUFF} + X_s) + C_6 (\dot{X}_5 - \dot{X}_{BUFF}) \quad \text{(A-90)}$$

If $X_5 - X_{BUFF} + X_s \leq 0$

X_{BUFF} is the position of the center of mass of the buffer tube,

μ_i is the coefficient of friction between the ith mass and the buffer tube,

θ_E is the angle of elevation of the rifle, and

g is the acceleration of gravity.

Nominal values for spring constants, masses, and damping coefficients are:

$M_1 = M_2 = M_3 = M_4 = .0406$ lb, $M_5 = .0615$ lb,

$C_1 = C_2 = C_3 = C_4 = C_5 = 12$ lb-sec/ft

$K_1 = K_2 = K_3 = K_4 = K_5 = K_6 = 60{,}000$ lb/ft

This individual-mass formulation is the one normally used in the computer program.

A.2.43 FBUFF(6) = -FMG(14) (See previous derivation)

Forces Acting on the Buffer Weights

A.2.44 F_{WTS} force acting on the lumped mass

This force is not used in the individual mass approach. Therefore, it is used only as an option. Part of this force is caused by friction, and part is due to impact of the lumped mass with the buffer body. The remainder is caused by gravity. $F_{WTS} = -FBUFF(5)' - M_{TOTAL}\, g \sin \theta_E$

A.2.45 $FM_{i,1}$ (i = 1,---5) force acting on individual buffer mass due to spring just forward of a mass

These forces do not occur when the lumped-mass approach is used. These spring forces act only when adjacent masses are in contact. In writing the equations, use of the following asymmetrical unit-step function is helpful:

$$U_+(X) = \begin{cases} 0 \text{ for } X \leq 0 \\ 1 \text{ for } X > 0 \end{cases}$$

Then define:

$$F_i \equiv [K_{i+1}(X_{i+1} - X_i) + C_{i+1}(\dot{X}_{i+1} - \dot{X}_i)]\, U_+(X_{i+1} - X_i) \qquad \text{(A-91)}$$

$$i = 1,2,3,4$$

$$F_o \equiv [K_1(X_1 - X_{BUFF}) + C_1(\dot{X}_1 - \dot{X}_{BUFF})]\, U_+(X_1 - X_{BUFF}) \qquad \text{(A-92)}$$

$$F_5 \equiv [K_6(X_{BUFF} - X_5 - X_s) + C_6(\dot{X}_{BUFF} - \dot{X}_5)]\, U_+(X_{BUFF} - X_5 - X_s) \qquad \text{(A-93)}$$

$$FM_{i,1} = -F_{i-1} \qquad i, 1,2,\ldots 5$$

X_s = "play" between buffer weights and tube in longitudinal direction

X_{BUFF} = position of C.G. of buffer tube.

A.2.46 $FM_{i,2}$ Force acting on individual buffer mass due to spring just rearward of mass

This force does not occur in the lumped mass approach.

$FM_{i,2} = F_i \quad i = 1,2,...5$ See A.2.45 for definition of F_i. (A-94)

(The subscript "i" refers to the ith mass.)

A.2.47 $FM_{i,3}$ Friction between buffer tube and buffer weight

This force does not occur in the lumped-mass approach.

$$FM_{i,3} = -\mu_i M_i g \cos \theta_E \text{ sgn } (\dot{X}_i - \dot{X}_{BUFF}) \quad \text{(A-95)}$$

$$i = 1,2,3,4,5$$

μ_i is the coefficient of friction between the ith mass and the buffer tube.

θ_E is the angle of elevation of the rifle.

A.2.48 $FM_{i,4}$ Gravity force

This force does not occur in the lumped-mass approach.

$$FM_{i,4} = -M_i g \sin \theta_E \quad \text{(A-96)}$$

$$i = 1,2,3,4,5$$

Torques That Affect Rifle Rotation

A.2.49 $T_{SHOULDER}$, T_{BODY}: Shooter's body applies torques that both increase and decrease rifle rotation

The model developed to account for rotational motion allows only one-way coupling between axial and rotational motion. That is, the forces acting parallel to the bore axis are allowed to affect the rotation of the rifle, but rotational motion is not allowed to affect axial motion. When the present M16 Rifle math model is joined with the man model under development, complete coupling will occur between axial and rotational motions.

In this model, the effect of the shooter's body is described by torsional and linear springs, and dashpots as shown in Figure 43.

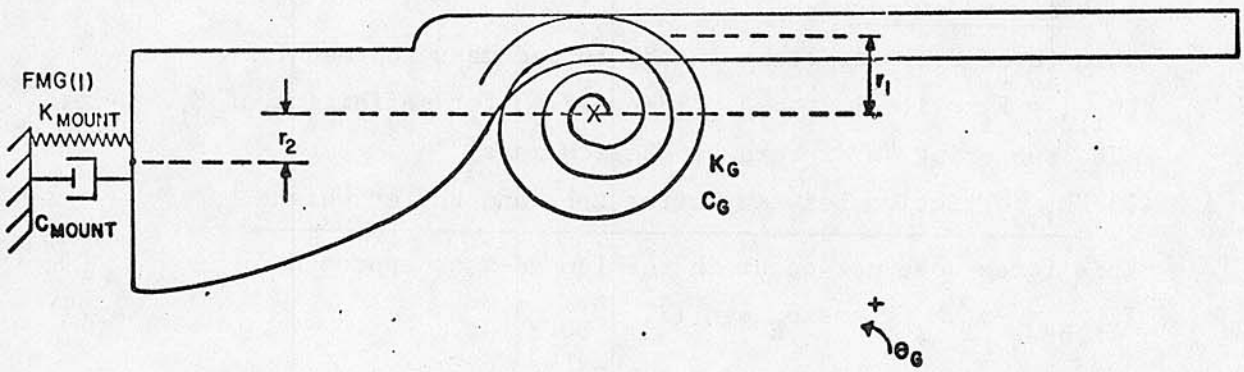

Figure 43 Schematic of Simple Man-Weapon Interaction Model

r_1 = distance from centerline of barrel to center

r_2 = distance from butt plate center to center of gravity of rifle

K_θ = effective torsional spring constant

C_θ = effective torsional damping constant

I_G = moment of inertia of rifle about a transverse axis through the center of gravity

θ_G = angle of elevation of barrel

The spring and dashpot at the butt are designed to approximate resistance from the shooter's shoulder. This resistance tends to cause rotation. The force acting through moment arm r_2 is identical to FMG(1). $T_{SHOULDER} = -r_2$ FMG(1).

The torsional spring and dashpot approximate the restoring moment exerted by the shooter's body in response to pitch motion. It includes the effects of his hands, arms, and upper torso. The values for K_G and C_G were selected as the same used for the XM19 Rifle model. These values lead to dispersion in bullet impact that accurately reflects what is found by experimental firings. That these values work well for two such diverse weapons is an indication that they constitute a valid approximation. They are not necessarily the only values that will give the proper dispersion, but they are physically reasonable.

$$T_{BODY} = K_G \theta_G - C_G \dot{\theta}_G \qquad \text{(A-97)}$$

Nominal values are: $r_2 = .34$ in

$K_G = 50$ ft-lb/rad

$C_G = 2.83$ ft-lb-sec/rad

$I_G = .135$ slug-ft^2

$K_{MOUNT} = 300$ lb/ft

$C_{MOUNT} = 9.53$ lb-sec/ft

A.2.50 $T_{INTERNAL\ GUN\ MOTION}$: Motion of internal operating parts tends to increase rifle rotation

These forces are assumed to act along the centerline of the barrel. They consist of all forces on the main gun except the mount force FMG(1). The force names are: FMG(2), FMG(3), FMG(4), FMG(5), FMG(6), FMG(7), FMG(8), FMG(9), FMG(10), FMG(11), FMG(12), FMG(13), FMG(14). The moment arm through which they act is $r_1 = .78$ inch. From Newton's Second Law, the sum of these forces is $\ddot{X}_{MG}\ (M_{MG}) - FMG(1)$.

$$T_{INTERNAL\ GUN\ MOTION} = r_1 [M_{MG} \ddot{X}_{MG} - FMG(1)] \qquad \text{(A-98)}$$

M_{MG} = mass of main gun = 6.2 -.0252 (N -19) lb

N = number of rounds of ammo in rifle at any given time

The following page is blank

APPENDIX B

SOLUTION OF EQUATIONS OF MOTION

In solving the equations of motion by the Runge-Kutta technique, one must put the equations in the form $\ddot{X} = f(y,x,\dot{x})$. Thus, second derivatives must be found explicitly. When constraint forces act, the equations for these second derivatives are coupled, and algebraic simultaneous equations must be solved. Otherwise, the second derivatives can be found explicitly by the simple rearrangement of terms in the equations. Cases where simultaneous equations must be solved to find second derivatives are described below. Cases in which no coupling of second derivatives exists, and in which second derivatives can be found by equation rearrangement will not be discussed.

B.1 Coupling between $\ddot{X}_{MG}$ and $\ddot{\theta}$ due to constraint force FMG(8) between hammer and gun

This force acts at all times.

$$\begin{cases} M_{MG}\,\ddot{X}_{MG} = \sum_{\substack{i=1 \\ (i\neq 8)}}^{15} FMG(i) + \left\{-M_H\,[\,r_o\,(\ddot{\theta}\cos\theta - \dot{\theta}^2 \sin\theta)] - FMG(7) - FBC(8)\right\} & \text{(B-1)} \\ I_H\,\ddot{\theta} = T_{SPRING} - r_2 \cos(\alpha_2 + \theta)\,FMG(7) - M_H\,\ddot{X}_{MG}\,(\cos\theta)\,r_o - r\cos(\theta+\alpha)\,FBC(8) & \text{(B-2)} \end{cases}$$

$$\ddot{X}_{MG} = \left[M_{MG} + M_H - \frac{M_H^2\, r_o^2 \cos^2\theta}{I_H}\right]^{-1} \left\{ \sum_{\substack{i=1 \\ (i\neq 7 \text{or} 8)}}^{15} FMG(i) \right. \qquad \text{(B-3)}$$

$$\left. -M_H\,[\,r_o\,((\,T_{SPRING} - r_2 \cos(\theta + \alpha_2)\,FMG(7) - r\cos(\alpha+\theta)\,FBC(8))\cos\theta\, I_H^{-1} - \dot{\theta}^2 \sin\theta)] - FBC(8) \right\}$$

$\ddot{\theta}$ can be found by substituting $\ddot{X}_{MG}$ into (B-2) and rearranging terms.

B.2 Interaction among $\ddot{X}_B$, $\ddot{X}_{BC}$, and $\ddot{X}_{MG}$ while bolt and main gun are locked together after locking

$$\begin{cases} \ddot{X}_B = \ddot{X}_{MG} \\ M_{MG}\ddot{X}_B = \sum_{i=1}^{15} FMG(i) + F_{con} \\ M_{B(E)}\ddot{X}_B = \sum_{i=1}^{12} FB(i) - F_{con} \end{cases}$$

$$\ddot{X}_B = \ddot{X}_{MG} = \left\{ \sum_{i=1}^{12} FB(i) + \sum_{\substack{i=1 \\ (i\neq 7 \text{or} 8)}}^{15} FMG(i) - FBC(8) - M_H [r_o(\theta_T \cos\theta - \dot{\theta}^2 \sin\theta)] \right\} \times \left[M_H + M_{MG} - \frac{M_H^2 r_o^2 \cos^2\theta}{I_H} \right]^{-1} \quad \text{(B-4)}$$

where $\theta_T \equiv [T_{SPRING} - r_2 \cos(\alpha_2 + \theta)\, FMG(7) - r \cos(\alpha+\theta)\, FBC(8)] I_H^{-1}$ (B-5)

B.3 Coupling between $\ddot{X}_B$ and $\ddot{X}_{BC}$ during the process of locking

$$\begin{cases} M_{B(E)}\ddot{X}_B = \sum_{\substack{i=1 \\ i\neq 7}}^{12} FB(i) + \left[\frac{d\theta_B}{d(X_B - X_{BC})} \right]^2 I_B(\ddot{X}_{BC} - \ddot{X}_B) & \text{(B-6)} \\ M_{BC}\ddot{X}_{BC} = \sum_{\substack{i=1 \\ i\neq 5}}^{12} FBC(i) - \left[\frac{d\theta_B}{d(X_B - X_{BC})} \right]^2 I_B(\ddot{X}_{BC} - \ddot{X}_B) & \text{(B-7)} \end{cases}$$

$$\ddot{X}_B = \left\{ M_{BC} \sum_{\substack{i=1 \\ i\neq 7}}^{12} FB(i) + \left[\frac{d\theta_B}{d(X_B - X_{BC})} \right]^2 I_B \left(\sum_{\substack{i=1 \\ i\neq 7}}^{12} FB(i) + \sum_{\substack{i=1 \\ i\neq 5}}^{12} FBC(i) \right) \right\} \left\{ M_{B(E)} M_{BC} + \left[\frac{d\theta_B}{d(X_B - X_{BC})} \right]^2 I_B (M_{B(E)} + M_{BC}) \right\}^{-1} \quad \text{(B-8)}$$

$$\ddot{X}_{BC} = \left\{ M_{B(E)} \sum_{\substack{i=1 \\ 1\neq 5}}^{12} FBC(i) + \left[\frac{d\theta_B}{d(X_B - X_{BC})} \right]^2 I_B \left(\sum_{\substack{i=1 \\ i\neq 7}}^{12} FB(i) + \sum_{\substack{i=1 \\ i\neq 5}}^{12} FBC(i) \right) \right\} \left\{ M_{B(E)} M_{BC} + \left[\frac{d\theta_B}{d(X_B - X_{BC})} \right]^2 I_B (M_{B(E)} + M_{BC}) \right\}^{-1} \quad \text{(B-9)}$$

B.4 Coupling between $\ddot{X}_B$ and $\ddot{X}_{MG}$ while the bolt is locked into the main gun, but before the locking process is completed

$$\ddot{X}_B = \ddot{X}_{MG} \tag{B-10}$$

$$\left[M_{MG} + M_H - \frac{M_H^2 r_o^2 \cos^2\theta}{I_H}\right] \ddot{X}_{MG} = \sum_{\substack{i=1 \\ i\neq 7 \text{or} 8}}^{15} FMG(i) - M_H r_o(\theta_T \cos\theta - \dot{\theta}^2 \sin\theta) - FBC(8) + F_{con} \tag{B-11}$$

$$M_{B(E)} \ddot{X}_B = \sum_{\substack{i=1 \\ i\neq 7}}^{12} FB(i) + \left[\frac{d\theta_B}{d(X_B - X_{BC})}\right]^2 I_B(\ddot{X}_{BC} - \ddot{X}_B) - F_{con} \tag{B-12}$$

$$M_{BC} \ddot{X}_{BC} = \sum_{i=1}^{12} FBC(i) - \left[\frac{d\theta_B}{d(X_B - X_{BC})}\right]^2 I_B(\ddot{X}_{BC} - \ddot{X}_B) \tag{B-13}$$

$$\ddot{X}_{MG} = \ddot{X}_B \tag{B-14}$$

The equation resulting from the addition of (B-11), (B-12) and (B-14) have the same form as (B-6) and (B-7) if M_B is replaced by

$$\left(M_{MG} + M_{B(E)} + M_H - \frac{M_H^2 r_o^2 \cos^2\theta}{I_H}\right) \text{ and } \sum_{\substack{i=1 \\ i\neq 7}}^{12} FB(i) \text{ is replaced by}$$

$$\sum_{\substack{i=1 \\ (i\neq 7 \text{or} 8)}}^{15} FMG(i) - M_H r_o (\theta_T \cos\theta - \dot{\theta}^2 \sin\theta) - FBC(8) + \sum_{\substack{i=1 \\ i\neq 7}}^{12} FB(i)$$

Hence, $\ddot{X}_B$ and $\ddot{X}_{BC}$ can be found.

B.5 Interaction among $\ddot{\theta}$, $\ddot{X}_{BC}$, $\ddot{X}_{MG}$ during cocking while the hammer and bolt-carrier are constrained to move together

$$M_{BC} \ddot{X}_{BC} = \sum_{\substack{i=1 \\ i\neq 8}}^{12} FBC(i) + FBC(8) \tag{B-15}$$

$$M_{MG} \ddot{X}_{MG} = \sum_{\substack{i=1 \\ (i\neq 7 \text{or} 8)}}^{15} FMG(i) - M_H [r_o (\ddot{\theta} \cos\theta - \dot{\theta}^2 \sin\theta) + \ddot{X}_{MG}] - FBC(8) \tag{B-16}$$

$$I_H \ddot{\theta} = T_{SPRING} - r\, FBC(8) \cos(\theta + \alpha) - M_H \ddot{X}_{MG} (\cos\theta)\, r_o \qquad \text{(B-17)}$$

The constraint equation and its derivatives are:

$$\theta = f(X_{MG} - X_{BC}) = -\alpha_1 + \tan^{-1}\left[\frac{r_1 \sin\alpha_1 + (X_{BC}-X_{MG})}{r_1 \cos\alpha_1}\right] \qquad \text{(B-18)}$$

$$\dot{\theta} = f'(X_{MG}-X_{BC})(\dot{X}_{MG}-\dot{X}_{BC}) \qquad \text{(B-19)}$$

$$\ddot{\theta} = f''(X_{MG}-X_{BC})(\dot{X}_{MG}-\dot{X}_{BC})^2 + f'(X_{MG}-X_{BC})(\ddot{X}_{MG}-\ddot{X}_{BC}) \qquad \text{(B-20)}$$

where $$f'(X_{MG}-X_{BC}) = -\left\{\left[1 + \left(\frac{r_1 \sin\alpha_1 + X_{BC}-X_{MG}}{r_1 \cos\alpha_1}\right)^2\right] r_1 \cos\alpha_1\right\}^{-1}$$

$$f''(X_{MG}-X_{BC}) = -2(r_1 \sin\alpha_1 + X_{BC}-X_{MG})\left\{\left[1 + \left(\frac{r_1 \sin\alpha_1 + X_{BC}-X_{MG}}{r_1 \cos\alpha_1}\right)^2\right]^2 r_1^3 \cos\alpha_1^3\right\}^{-1}$$

From (12) $$FBC(8) = [T_{SPRING} - I_H \ddot{\theta} - M_H r_o (\cos\theta) \ddot{X}_{MG}][r\cos(\theta+\alpha)]^{-1} \qquad \text{(B-21)}$$

Substitution of (B-20) into (B-21) and the result into (B-15) yields:

$$\left[M_{BC} - \frac{I_H f'(X_{MG}-X_{BC})}{r\cos(\alpha+\theta)}\right]\ddot{X}_{BC} + \left[\frac{I_H f'(X_{MG}-X_{BC}) + M_H r_o \cos\theta}{r\cos(\alpha+\theta)}\right]\ddot{X}_{MG} \qquad \text{(B-22)}$$

$$= \sum_{\substack{i=1 \\ i\neq 8}}^{12} FBC(i) + \frac{T_{SPRING}}{r\cos(\theta+\alpha)} - \frac{I_H f''(X_{MG}-X_{BC})(\dot{X}_{MG}-\dot{X}_{BC})^2}{r\cos(\alpha+\theta)}$$

Substitution of (B-21) into (B-16) yields:

$$\left[\frac{I_H f'(X_{MG}-X_{BC})}{r\cos(\alpha+\theta)} - M_H f'(X_{MG}-X_{BC})\, r_o \cos\theta\right]\ddot{X}_{BC} \qquad \text{(B-23)}$$

$$+\left[-\frac{M_H^2 r_o^2 \cos^2\theta}{I_H} + M_{MG} + f'(X_{MG}-X_{BC}) M_H r_o \cos\theta + M_H - \frac{I_H f'(X_{MG}-X_{BC}) - M_H r_o \cos\theta}{r\cos(\alpha+\theta)}\right]\ddot{X}_{MG}$$

$$= \sum_{\substack{i=1 \\ i\neq 7 \text{or} 8}}^{15} FMG(i) + M_H r_o \dot{\theta}^2 \sin\theta - \frac{T_{SPRING}}{r\cos(\alpha+\theta)} + \frac{I_H f''(X_{MG}-X_{BC})(\dot{X}_{MG}-\dot{X}_{BC})^2}{r\cos(\alpha+\theta)}$$

$$- M_H r_o \cos\theta\, f''(X_{MG}-X_{BC})(\dot{X}_{MG}-\dot{X}_{BC})^2$$

Thus, there are two equations (B-22) and (B-23), and two unknowns $\ddot{X}_{BC}$ and $\ddot{X}_{MG}$.

The equations are linear and of the form:

$$\begin{cases} T_1 \ddot{X}_{BC} + T_2 \ddot{X}_{MG} = T_3 & \text{(B-24)} \\ U_1 \ddot{X}_{BC} + U_2 \ddot{X}_{MG} = U_3 & \text{(B-25)} \end{cases}$$

$$\therefore \quad \ddot{X}_{BC} = \frac{T_3 U_2 - T_2 U_3}{T_1 U_2 - U_1 T_2} \qquad \text{(B-26)}$$

$$\ddot{X}_{MG} = \frac{T_1 U_3 - U_1 T_3}{T_1 U_2 - U_1 T_2} \qquad \text{(B-27)}$$

B.6 Interaction among $\ddot{\theta}$, $\ddot{X}_{BC}$, $\ddot{X}_{MG}$, $\ddot{X}_B$ during cocking while the bolt is locked into the main gun and the hammer is constrained to move with the bolt-carrier

$$\begin{cases} M_{B(E)} \ddot{X}_B = \sum_{i=1}^{12} FB(i) + F_{CON} & \text{(B-28)} \\ \ddot{X}_B = \ddot{X}_{MG} & \text{(B-29)} \\ T_1 \ddot{X}_{BC} + T_2 \ddot{X}_{MG} = T_3 & \text{(B-30)} \\ U_1 \ddot{X}_{BC} + U_2 \ddot{X}_{MG} = U_3 - F_{CON} & \text{(B-31)} \end{cases}$$

F_{CON} is a constraint force that acts between the bolt and main gun to prevent relative motion between them.

Add (B-30) and (B-24) to eliminate F_{CON}, then the equations to be solved are:

$$\begin{cases} U_1 \ddot{X}_{BC} + (U_2 + M_{B(E)}) \ddot{X}_{MG} = U_3 + \sum_{i=1}^{12} FB(i) & \text{(B-32)} \\ T_1 \ddot{X}_{BC} + T_2 \ddot{X}_{MG} = T_3 & \text{(B-33)} \\ \ddot{X}_B = \ddot{X}_{MG} & \text{(B-34)} \end{cases}$$

The first two equations are of the form (B-24) and thus have similar solutions. The third equation establishes $\ddot{X}_B$.

B.7 Interaction among $\ddot{X}_{MG}$, $\ddot{X}_{BC}$, $\ddot{X}_{B}$, $\ddot{\theta}$ while the hammer is cocking; the hammer and bolt-carrier are constrained to move together; unlocking is taking place, but the bolt is still locked into the main gun

This case is a combination of cases B.5 and B.6.

The equation for the bolt is:

$$M_B \ddot{X}_B = \sum_{\substack{i=1 \\ i\neq 6}}^{12} FB(i) + \left[\frac{d\theta_B}{d(X_B-X_{BC})}\right]^2 I_B(\ddot{X}_{BC}-\ddot{X}_B) + \frac{d\theta_B}{d(X_B-X_{BC}} \frac{2}{3} \mu_c \frac{r_2^3-r_1^3}{r_2^2-r_1^2} F_N+F_N \quad \text{(B-35)}$$

where M_B is the mass of the bolt alone.

The negative of FB(6) must now appear in the equation for the bolt-carrier

$$T_1 \ddot{X}_{BC} + T_2 \ddot{X}_{MG} = T_3 - \left[\frac{d\theta_B}{d(X_B-X_{BC})}\right]^2 I_B(\ddot{X}_{BC}-\ddot{X}_B) - \frac{d\theta_B}{d(X_B-X_{BC})}\frac{2}{3} \mu_c \frac{r_2^3-r_1^3}{r_2^2-r_1^2} F_N \quad \text{(B-36)}$$

NOTE: $\ddot{\theta}$ has already been eliminated in this equation.

For convenience in eliminating F_N, one can consider that the cartridge case is now part of the main gun rather than the bolt. The equation for the main gun becomes:

$$U_1 \ddot{X}_{BC} + (U_2 + M_c) \ddot{X}_{MG} = U_3 - F_N. \quad \text{(B-37)}$$

NOTE: $\ddot{\theta}$ has already been eliminated in this equation.

The equations can be summarized as follows:

$$\left\{M_B + \left[\frac{d\theta_B}{d(X_B-X_{BC})}\right]^2 I_B\right\}\ddot{X}_B - \left\{\left[\frac{d\theta_B}{d(X_B-X_{BC})}\right]^2 I_B\right\}\ddot{X}_{BC} = \sum_{\substack{i=1 \\ i\neq 6}}^{12} + \frac{d\theta_B}{d(X_B-X_{BC})}\frac{2}{3}\mu_c \frac{r_2^3-r_1^3}{r_2^2-r_1^2} F_N+F_N$$

$$-\left\{\left[\frac{d\theta_B}{d(X_B-X_{BC})}\right]^2 I_B\right\}\ddot{X}_B + \left\{T_1 + \left[\frac{d\theta_B}{d(X_B-X_{BC})}\right]^2 I_B\right\}\ddot{X}_{BC} + T_2\ddot{X}_{MG} = T_3 - \frac{d\theta_B}{d(X_B-X_{BC})}\frac{2}{3}\mu_c \frac{r_2^3-r_1^3}{r_2^2-r_1^2} F_N \quad \text{(B-38)}$$

$$U_1 \ddot{X}_{BC} + (U_2 + M_c) \ddot{X}_{MG} = U_3 - F_N \quad \text{(B-39)}$$

$$\ddot{X}_{MG} = \ddot{X}_B \quad \text{(B-40)}$$

To condense the equations, define the following:

$$K_1 \equiv \left[\frac{d\theta_B}{d(X_B - X_{BC})} \right] I_B$$

$$K_2 \equiv \frac{d\theta_B}{d(X_B - X_{BC})} \frac{2}{3} \mu_c \frac{r_2^3 - r_1^3}{r_2^2 - r_1^2}$$

The equations become:

$$[M_B + K_1] \ddot{X}_B - K_1 \ddot{X}_{BC} = \sum_{\substack{i=1 \\ i \neq 6}}^{12} FB(i) + K_2 F_N + F_N \qquad \text{(B-41)}$$

$$- K_1 \ddot{X}_B + [T_1 + K_1] \ddot{X}_{BC} + T_2 \ddot{X}_{MG} = T_3 - K_2 F_N \qquad \text{(B-42)}$$

$$U_1 \ddot{X}_{BC} + (U_2 + M_c) \ddot{X}_{MG} = U_3 - F_N \qquad \text{(B-43)}$$

$$\ddot{X}_{MG} = \ddot{X}_B \qquad \text{(B-44)}$$

Now eliminate F_N:

Multiply (B-43) by $(K_2 + 1)$ and add the result to (B-41).

$$[-K_1 + U_1 (K_2 + 1)] \ddot{X}_{BC} + [M_B + K_1 + (K_2 + 1)(U_2 + M_c)] \ddot{X}_{MG} \qquad \text{(B-45)}$$

$$= \sum_{\substack{i=1 \\ i \neq 6}}^{12} FB(i) + [1 + K_2] U_3$$

Next, multiply (B-43) by (K_2) and subtract the result from (B-42).

$$[T_1 + K_1 - U_1 K_2] \ddot{X}_{BC} + [T_2 - K_1 - K_2 (U_2 + M_c)] \ddot{X}_{MG} = T_3 - U_3 K_2 \qquad \text{(B-46)}$$

$\ddot{X}_{BC}$ and $\ddot{X}_{MG}$ can be found by solving (B-45) and (B-46) simultaneously.

$\ddot{X}_B = \ddot{X}_{MG}$ determines $\ddot{X}_B$.

$\ddot{\theta}$ can then be found from (B-17).

The following page is blank

APPENDIX C

SPRING-SURGING AND COIL-CLASHING ANALYSES

Many phenomena occur in weapon operation that can be modeled as a series of masses connected to ideal springs and dashpots in the following manner:

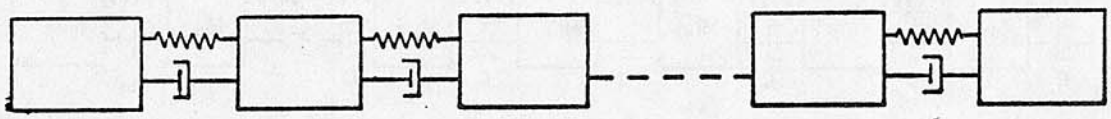

For example, instead of making the common assumption that one mass upon impact with another encounters an ideal stiff spring, one can account for the wave-like propagation of stresses by assuming that the body encounters the spring system shown above. The body being impacted is thus assumed to be composed of many masses separated by springs with stiffness based on Young's modulus. With proper selection of masses, springs, and dampers, one could better approximate impact and include higher modes of oscillation.

As an alternative to using linear springs for physical simulation of helicopters and other vehicles as firing platforms, one could include higher modes of oscillation and possibly more closely duplicate the response of the actual system to firing loads. For a helicopter simulation, one would need one set of springs for each mode of vehicle flight such as hovering, diving, etc.

One can also use this spring-mass system to represent the action of rapidly compressed springs in the philosophy of the finite-element or lumped-mass concept. Each point mass could be considered to be one coil mass, although several coils could be combined and considered, in a rough approximation, as one point mass. Spring constants could be set so as to force the overall system to have the same spring rate under static conditions as that of the actual spring. Damping coefficients could be set so as to make the overall damping equivalent to the best estimate for the actual spring.

For all the above-listed applications, including the spring, the governing equation for the ith mass, where "i" denotes neither the first or last mass is:

$$M\ddot{X}_i + 2C\dot{X}_i + 2K X_i = K(X_{i-1} + X_{i+1}) + C(\dot{X}_{i-1} + X_{i+1}) . \qquad \text{(C-1)}$$

In this formulation, mass, spring, and damping values do not change along the spring.

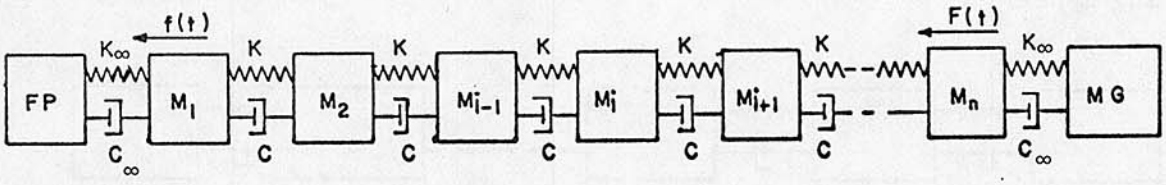

Figure 44 Drive Spring Model

Consider the following drive spring. The main gun is on one end, and the firing pin is on the other. The equations are:

$$M\ddot{X}_1 = -[X_1 - X_2 - (\Delta-\delta)]\,K - (\dot{X}_1 - \dot{X}_2)\,C + f(t) \qquad \text{(C-2)}$$

$$M\ddot{X}_i = -(X_i - X_{i+1})\,K - (\dot{X}_i - \dot{X}_{i+1})\,C - (X_i - X_{i-1})\,K - C\,(\dot{X}_i - \dot{X}_{i-1}) \qquad \text{(C-3)}$$

$$M\ddot{X}_n = [X_{n-1} - X_n - (\Delta-\delta)]\,K + C\,(\dot{X}_{n-1} - \dot{X}_n) + F(t) \qquad \text{(C-4)}$$

X's are measured with respect to ground at t = 0 for a preloaded spring.

The free length of each spring is Δ = (Free length of total spring)/(Number of coils + 1).

The length of each spring at t = 0 is δ = (Initial length of total spring)/(Number of coils + 1).

The length at any t is $\delta + X_j - X_{j+1}$ for a spring located between mass j and mass j+1.

The force exerted on masses j and j+1 by the spring located between them is $[\Delta - \delta - X_i + X_{i+1}]\,K_{TOT}(n+1)$ where K_{TOT} is constant for the entire spring and n is the number of coils.

Now

$$f(t) = K_\infty [X_{FP} - X_{FP_o} - X_1 - (\Delta_\infty - \delta_\infty)] + C_\infty (\dot{X}_{FP} - \dot{X}_1).$$

Set $(\Delta_\infty - \delta_\infty)$ such that the net force on M_1 is zero at t = 0.

Then

$$K_\infty [-\Delta_\infty + \delta_\infty] = (\Delta-\delta) K$$

$$-\Delta_\infty + \delta_\infty = \frac{K}{K_\infty} (\Delta-\delta)$$

$$f(t) = K_\infty [X_{FP} - X_{FP_o} - X_1 - \frac{K}{K_\infty} (\Delta-\delta)] + C_\infty [\dot{X}_{FP} - \dot{X}_1] \qquad \text{(C-5)}$$

Now $F(t) = K_\infty [X_{MG}-X_{MG_o}-X_n + (\Delta'_\infty \delta'_\infty)] + C_\infty [\dot{X}_{MG}-\dot{X}_n]$

Set $[\Delta'_\infty - \delta'_\infty]$ such that the net force on M_n is zero at t=o.

$$K(\Delta-\delta) = K_\infty [\Delta'_\infty - \delta'_\infty]$$

$$\Delta'_\infty - \delta'_\infty = \frac{K}{K_\infty} [\Delta-\delta]$$

$$F(t) = K_\infty [X_{MG}-X_{MG_o}-X_n + \frac{K}{K_\infty} (\Delta-\delta)] + C_\infty [\dot{X}_{MG}-\dot{X}_n] \qquad \text{(C-6)}$$

NOTE: f(t) is the force exerted by FP on M_1, and F(t) is the force exerted by MG on M_n.

In many instances, one is not interested in the details of the motions for each mass, but rather in how the first and last masses respond to input signals. Thus, for many applications, it would be very useful and economical to use a transfer function for the system, if such a ratio of output to input could be found. Laplace transforms were applied to the equations, but no inverse was found. Because this approach still seems potentially profitable, the preliminary work is now presented.

First substitute (C-5) and (C-6) into (C-2) and (C-4), respectively. The term $K(\Delta -\delta)$ is cancelled, and the result is:

$$M\ddot{X}_1 + (K+K_\infty) X_1 + (C+C_\infty) \dot{X}_1 - KX_2 - C\dot{X}_2 = K_\infty [X_{FP}-X_{FP_o}] + C_\infty \dot{X}_{FP} \qquad \text{(C-7)}$$

$$\vdots$$

$$M\ddot{X}_i + 2KX_i + 2C\dot{X}_i - KX_{i+1} - C\dot{X}_{i+1} - KX_{i-1} - C\dot{X}_{i-1} = 0 \qquad \text{(C-8)}$$

$$\vdots$$

$$M\ddot{X}_n + (K+K_\infty) X_n + (C+C_\infty) \dot{X}_n - KX_{n-1} - C\dot{X}_{n-1} = K_\infty (X_{MG}-X_{MG_o}) + C_\infty \dot{X}_{MG} \qquad \text{(C-9)}$$